Investigations on Modelling of Hybrid Renewable Energy Sources for Power System Network: Case Studies

Thesis Submitted in Partial Fulfilment of the Requirements of the Degree of

Doctor of Philosophy

Submitted by

Negasa Muleta

(Reg. no. 719126)

Supervisor:

Dr. Altaf Q.H. Badar

Department of Electrical Engineering

National Institute of Technology Warangal

2022

Approval Sheet

This Thesis entitled **"Investigations on Modelling of Hybrid Renewable Energy Sources for Power System Network"** by **Mr. Negasa Muleta** is approved for the degree of Doctor of Philosophy

Examiners

_____

_____

_____

Supervisor

Dr. Altaf Q. H. Badar

Assistant Professor,

EED, NIT Warangal

Chairman

Dr. D. V. S. S. Siva Sarma

Professor,

EED, NIT Warangal

Date:_____

Department of Electrical Engineering

National Institute of Technology, Warangal-506004

Department of Electrical Engineering

National Institute of Technology Warangal-506004

Certificate

This is to certify that the thesis entitled '**"Investigations on Modelling of Hybrid Renewable Energy Sources for Power System Network"** being submitted by **Negasa Muleta (719126)** is a bonafide research work carried out under my supervision and guidance in fulfillment of the requirement for the award of the degree of **Doctor of Philosophy** in the Department of Electrical Engineering, National Institute of Technology Warangal-506004, Telangana, India. The matter embodied in this thesis is original and has not been submitted to any other University or Institute for the award of any other degree.

Place: Warangal
Date:

Dr. Altaf Q. H. Badar
Assistant Professor
(EED, NIT Warangal)

Declaration

This is to certify that the work presented in the thesis entitled **"Investigations on Modelling of Hybrid Renewable Energy Sources for Power System Network"** is a bonafide work done by me under the supervision of **Dr. Altaf Q. H. Badar** and was not submitted elsewhere for the award of any degree. I declare that this written submission represents my ideas in my own words and where others' ideas or words have been included, I have adequately cited and referenced the original sources. I also declare that I have adhered to all principles of academic honesty and integrity and have not misrepresented or fabricated or falsified any idea / data / fact / source in my submission. I understand that any violation of the above will be a cause for disciplinary action by the Institute and can also evoke penal action from the sources which have thus not been properly cited or from whom proper permission has not been taken when needed.

_____

Negasa Muleta

(Reg. no. 719126)

Date:

Memorial to my Father Muleta Feyisa

Acknowledgments

First and foremost, I would like to express my gratitude to God Almighty for providing me with the opportunity and guidance to achieve my goal and be successful in this part.

It is a great pleasure for me to express my respect and a deep sense of gratitude to my Ph.D. supervisor **Dr. Altaf Q. H. Badar**, Assistant Professor, Department of Electrical Engineering, National Institute of Technology, Warangal, for his wisdom, vision, expertise, guidance, enthusiastic involvement and persistent encouragement during the planning and development of this research work. I also want to thank him for his hard work in thoroughly reviewing and improving the manuscripts, without which this work would not have been possible.

I am also thankful to the anonymous reviewers of my research publications. Their comments and suggestions were very helpful in shaping my research work. I would also like to thank the DSC members for their constructive suggestions, support and encouragement.

I am highly obliged to **Dr. N.V. Ramana Rao**, Professor and Director, NIT Warangal and **Dr. Sailaja Kumari M**, Professor and Head of Electrical Engineering Department, for providing all the facilities, help and encouragement for carrying out the research work. I would also like to express my gratitude to the entire NIT Warangal community for their humbleness efforts in serving me on any given occasion.

I'd like to thank my country, Ethiopia, the Dire Dawa University community and the Ethiopian Embassy in India for all of their help and encouragement. I also have a thankful full for Dire dawa University Institute of Technology, School of Electrical and Computer Engineering staffs and managements to their

support and encouragements.

I am obliged to my parents: my father **Muleta Feyisa**, my mother **Asefu Roba**, brothers and sisters for their moral support, love, encouragement and blessings to complete this task.

I am especially thankful to my spouse and beloved **Genet Bekele** for her patience, love and encouragement during this journey. I'm also grateful to my son **Hundaol** and daughter **Koket** for their love and joy.

I wish to express my appreciation to my friends and grateful thanks to research fellows at the department for their help and motivation throughout my research work. I also would like to express my deep and sincere thanks to my friends and all other people whose names do not appear here, for helping me either directly or indirectly in all times.

Negasa Muleta

Abstract

Electricity is the most desired resource in this world and it is crucial for the development of any sector. The electric power system network consists of generation, transmission and distribution. Generation is categorized according to the kind of resource as non-renewable or renewable. Non-renewable energy sources are expected to be substituted by Renewable Energy Sources (RES) due to high operating costs and greater emissions of Green House Gas (GHG). RES, on the other hand, has a low operating cost, is environmentally friendly, plentiful and easily accessible. RES suffers from intermittent generation and is not reliable. These issues of RES can be reduced through Hybrid Renewable Energy Sources (HRES). HRES is a combination of renewable energy generating plants and energy storage technologies that address the limitations of a single energy source.

HRES can be implemented as a part of standalone Microgrid (MG) or can be integrated into the grid. The main goal of HRES integration to power network is to improve the system performance. The parameters such as economic cost, reliability, GHG emissions, power loss and voltage profile are considered in this study, to evaluate the power system network performance. These parameters are applied to systems with different modes of operations (standalone or grid connected), locations and objectives. The following locations are considered for case studies: i) Jarre village, Ethiopia, ii) Eastern Region of Ethiopian Electric Power (EEP), Ethiopia and iii) cluster of Baheya, Ulatu and Karmadhippa villages, India.

Jarre village is a remote area that is yet to be electrified. It has an abundance of RES like solar and wind. The case study is intended to model a cost

efficient power system for the village. The cost feasibility of grid extension or installing stand-alone system is compared. The analysis of the investigation reveals that standalone MG is economically effective than grid extension. A standalone HRES MG with solar PV, WT and BS is proposed. Other tasks involved in this case study include determining the optimal combination of HRES components. Minimization of economic costs and GHG emissions are considered as objectives. Reliability index is considered as a constraint for stand alone MG modelling.

Metaheuristic techniques such as Particle Swarm Optimization (PSO), Differential Evolution (DE), Manta Ray Foraging Optimization (MRFO), Shuffled Frog-Leaping Algorithm (SFLA), Reptile Search Algorithm (RSA) and RUNge Kutta Optimizer (RUN) are employed to determine the optimal size of HRES components. According to the analysis, the modelled standalone HRES MG system is cost effective, reliable and emits less GHG.

To investigate the advantages of HRES integration as DG, Eastern Region EEP system is considered. This region has low voltage profile, high power loss and unreliable power supply. Optimal DG placement and sizing is proposed to address these problems. Standard IEEE 33 bus system is initially optimized for DG placement and sizing through MRFO. The output is compared with other optimization techniques to select the better performing optimization technique. This optimization technique is then applied to solve the placement and sizing problem of DG in Eastern Region EEP network. The optimal size of solar PV and WT as part of the proposed DG is determined using the same optimization technique. The economic benefit due HRES integration as DG is also investigated.

The impact of subsidy on the economic costs of HRES MG is investigated

for the clustered villages of Baheya, Ulatu and Karmadhippa, Jharkhand, India. These villages are powered by an unreliable and conventional grid. Grid connected MG consisting of solar PV, micro hydropower and biogas is proposed for these villages. The MG is supposed to provide the villages with reliable and cost effective electric supply having a high ratio of RES. The economic cost analysis is performed considering the effect of subsidies. Subsidies are given on component installation costs in order to reduce system costs and promote renewable energy technologies.

Contents

Approval Sheet ii

Certificate iii

Declaration iv

Dedication vi

Acknowledgments vii

Abstract x

List of Figures xv

List of Tables xvii

List of Acronyms and Abbreviations xx

List of Symbols xxi

1 Introduction 1

1.1 Background 1

1.2 Motivation of Research 6

1.3 Aim and Objectives 6

1.4 Significance of the Study 7

1.5 Work Plan 7

1.6 Organization of the Thesis 8

2 Literature Review **10**

2.1 Introduction 10

2.2 Hybrid Renewable Energy Sources 10

2.3 Research Gap 16

3 Modelling of HRES and Methodology **18**

3.1 Modelling of HRES MG Components 18

3.1.1 Solar Energy 18

3.1.2 Wind Energy 20

3.1.3 Hydro Power 21

3.1.4 Biogas Energy 21

3.1.5 Energy Storage System 22

3.2 HRES Performance Evaluation Parameters 25

3.2.1 Reliability Analysis 25

3.2.2 Economic Analysis 26

3.2.3 Analysis of Environmental Effects 28

3.3 **Optimization Methods to Optimize HRES** 29

4 Standalone MG with HRES **45**

4.1 Grid Extension for Remote Area Electrification 45

4.2 Standalone HRES MG : Jarre Village (Part I) 47

4.2.1 Load Profile and Resource Potential of Jarre Village 49

4.2.2 Problem Formulation : Standalone MG 51

4.2.3 Methodology 52

4.2.4 Result and Discussion 54

4.3 Standalone HRES MG : Jarre Village (Part II) 57

4.3.1 Problem Formulation 57
4.3.2 Result and Discussion 58
4.4 Summary 60

5 Grid Performance Improvement with HRES 62

5.1 Power System Performance Assessment with DG Integration . . . 62
5.1.1 Problem Formulation for DG Placement and Sizing 64
5.1.2 Methodology 66
5.1.3 Optimal DG Placement and Sizing for IEEE 33 Bus System 66
5.1.4 Optimal DG Placement and Sizing for EEP 68
5.1.5 Determination of HRES Constituent Ratings 75
5.1.6 Economic Benefit of HRES Integration to Grid 81
5.2 Analysis of Subsidy on HRES MG 82
5.2.1 Problem Formulation 83
5.2.2 Load Profile and Resource Potential for Clustered Indian Villages 83
5.2.3 Result and Discussion 87
5.3 Summary 89

6 Conclusions and Future Scopes 90

6.1 Conclusions 90
6.2 Future Scope 93

Appendix 94

References 96

List of Publications 114

List of Figures

1.1 World RES Installed Capacity @ 2021 [5] 3

1.2 Workflow of the Study 8

3.1 Energy Storage Technology 24

3.2 Flowchart for PSO and DE Algorithms 34

3.3 Flowchart of MRFO and SFLA Algorithms 36

3.4 Flowchart of RSA Algorithm 43

3.5 Flowchart of RUN Algorithm 44

4.1 Geographical Location of Jarre Village 47

4.2 Grid Extension Feasibility Result for BED Analysis 48

4.3 Standalone HRES MG Model for Jarre Village 48

4.4 Daily Load Profile of Jarre Village 49

4.5 Average Monthly Wind and Solar Profile, @ 2020-2021 [93] . . . 50

4.6 Daily Solar and Wind Pattern of Jarre Village 50

4.7 Daily Power Generation per unit of Wind and Solar: Jarre Village 51

4.8 Methodology for HRES Optimization 53

4.9 Battery Status for Ideal and Practical Cases 56

4.10 Daily Power Generation from Solar PV and WT plants 56

4.11 Daily Power Supply and Demand Profile 57

4.12 Economic Cost Comparison for Different Optimization Methods . 59

4.13 Excess Energy Comparison for Different Optimization Methods . 60

4.14 Daily Energy Pattern of RES for Optimal Solution 60
4.15 Daily Power Supply and Demand for Optimal HRES MG 61
4.16 Demand and Supply Pattern for Optimal HRES MG 61

5.1 Minimum and Maximum Voltage Profile of Eastern Region of EEP [99] 64
5.2 Methodology for Optimal Placement and Sizing of DG 67
5.3 Eastern Region EEP Network Layout 69
5.4 Optimal DG Integration in Eastern Region of EEP Network . . . 75
5.5 Voltage Magnitude Variation due to DG Integration 76
5.6 Proposed RES Model for Eastern Region of EEP 78
5.7 Daily Power Generation per unit of Wind and Solar: Eastern Region EEP 79
5.8 Daily Energy Profile for Optimal Combination of RES 79
5.9 Daily Power Supply and Demand for Eastern Region of EEP . . . 79
5.10 Daily Power Losses Before and After HRES Integration 80
5.11 HRES MG Model for Grid Connected System 84
5.12 Geographical Location of Clustered Indian Villages 85
5.13 Seasonal Load Variation of Clustered Indian Villages 86
5.14 Monthly Average Solar Energy of Clustered Indian Villages [93] 86

List of Tables

1.1 Cost Trends of RES, from 2010 to 2020 [3] 2

2.1 Collection of Reviewed Literature on HRES MG Optimization . . 16

3.1 Solar Energy Characteristics [53] 19
3.2 Wind Energy Characteristics [53] 21
3.3 Hydropower Characteristics [56] 22
3.4 Biogas Energy Characteristics [57] 23
3.5 Reliability Assessment Indices 26
3.6 Economic Performance Evaluation Indices 27
3.7 Performance Evaluation Indices of Environmental Effects [77] . 28

4.1 Costing for Grid Extension [91] 46
4.2 Costs of Standalone HRES MG Components 51
4.3 Specifications of Standalone HRES MG 54
4.4 Feasibility of Solutions within a Random Population 55
4.5 Comparison of Ideal and Practical HRES Combinations 56
4.6 Life Cycle CO_2 Emission of HRES Components [17, 94, 95] . . . 58
4.7 Comparison of Various Optimization Techniques 59

5.1 Power Outages Data for EEP @2021 [98] 63
5.2 Comparison of Optimal DG Placement and Sizing for IEEE 33 Bus System 70
5.3 Network Power Loss Before DG Integration 71

5.4 Voltage Profile Before DG Integration 72
5.5 Sample Solutions and their Analysis for DG Sizing and Placement 73
5.6 Network Power Loss after DG Integration 74
5.7 Voltage Profile After DG Integration 77
5.8 Component Costs of Renewable Energy Sources 80
5.9 Summary of Energy Distribution before and after HRES Integration 80
5.10 Results of Economic Cost Analysis for HRES Integration to Grid 82
5.11 Specifications of Solar PV Panels 87
5.12 Specifications of Converter 87
5.13 Specifications of Micro Hydro Power Plant 88
5.14 Biogas Potential of Clustered Indian Villages [107] 88
5.15 Specifications of Biogas Plant 89
5.16 Total Energy Generation per unit of RES. 89
5.17 Economic Analysis Without and With Subsidy 89

List of Acronyms and Abbreviations

ASAI	Average Service Availability Index
BS	Battery Storage
BED	Break Even Distance
CAIDI	Customer Average Interruption Duration Index
CAIFI	Customer Average Interruption Frequency Index
CIII	Customer Interrupted per Interruption Index
CO_2	Carbon Dioxide
COE	Cost of Energy
C_{tf}	Grid tariff Cost
DCE	Daily Carbon-Dioxide Emission
DE	Differential Evolution
DG	Distributed Generation
DoD	Depth of Discharge
DPSP	Deficiency in Power Supply Probability
DR	Demand Response
DSM	Demand Side Management
EE	Energy Efficiency
Een	Embodied Energy
EENS	Expected Energy Not Supplied
EIR	Energy Index of Reliability
EMS	Energy Management System

EPBT	Energy Pay Back Time
ESS	Energy Storage System
FC	Fuel Cell
FE	Fuel Emissions
GHG	Green House Gas
HRES	Hybrid Renewable Energy Sources
HOMER	Hybrid Optimization of Multiple Energy Resources
LCA	Life Cycle Assessment
LCC	Life Cycle Cost
LCOE	Levilezed Cost of Energy
LFF	Load Fill Factor
LLRI	Line Loss Reduction Index
LOLE	Loss of Load Expectation
LOLP	Loss of Load Probability
LPSP	Loss of Power Supply Probability
MAIFI	Momentary Average Interruption Frequency Index
MG	Micro Grid
MRFO	Manta Ray Foraging Optimization
NPC	Net Present Cost
NOCT	Nominal Operating Cell Temperature
P_L	Power Loss
PSO	Particle Swarm Optimization
PV	Photo-Voltaic

REP	Renewable Energy Penetration
RES	Renewable Energy Sources
RSA	Reptile Search Algorithm
RUN	RUNge Kutta Optimizer
SAC	System Annualized Cost
SAIDI	System Average Interruption Duration Index
SAIFI	System Average Interruption Frequency Index
SFLA	Shuffled Frog-Leaping Algorithm
SoC	State of Charge
SPB	Simple Pay Back
S_p	Annual profit
SSM	Supply Side Management
TAC	Total Annual cost
T & D	Transmission and Distribution
$TCEP_C$	Total Carbon Dioxide Emission Cost
VPII	Voltage Profile Improvement Index
WT	Wind Turbine

List of Symbols

A	Cross section area	m^2
C_c	Capital cost	$/kW
C_{OM}	Operation and Maintenance cost	$/kW/yr
C_p	Wind power coefficient	%
C_r	Replacement cost	$/kW
CV	Calorific value	$kcal/m^3$
E	Electrical Energy	kWh
G	Solar irradiance	W/m^2
g	Gravitational acceleration	m/s^2
H	Water head	m
I	Current	A
P	Power	W
q	Charge of electron	C
Q	Water flow rate	m^3/s
R	Resistance	Ω
T	Temperature	^oC
T_g	Total biogas availability	m^3/day
V	Voltage	V
v	Velocity	m/s
X	Reactance	Ω
η	Power plant efficiency	%
ρ	Water /air density	kg/m^3
σ	Self-discharge rate of battery	%

Chapter 1

Introduction

This chapter focuses on various types of electrical energy resources and their characteristics. The modes of operation of HRES MG in power system networks are also highlighted. The parameters used to evaluate the performance of power system network are thoroughly discussed.

1.1 Background

An electric power system is a network of electrical components that generate, transmit and distribute energy from sources to the loads. Based on the source and its ability to regenerate, electric power generation sources are classified as non-renewable and renewable. Non-renewable sources are limited and take a long time to replenish. They regenerate more slowly, which causes them to become depleted. Natural gas, coal, petroleum, etc. are categorized under non-renewable energy sources. Renewable Energy Sources (RES) are generated from natural resources and are replenished at a faster rate than they are consumed. RES includes geothermal, biomass, tidal, solar, wind energy, etc.

RES energy production is growing faster than conventional (coal-fired) energy production. The global share of electricity generation from RES is expected to increase from 27% in 2019 to 85% by 2050 [1]. Solar and wind have a significant contribution in the expected growth of RES. They are abundant

and easily accessible everywhere, as well as a widely deployed, cost-effective and use adaptable technology [2]. The total installation costs of solar PV and WT are gradually decreasing, as shown in Table 1.1. Comparing 2020 to 2010, the installation cost of a solar PV plant decreased by 81% and WT decreased by 32% for offshore and 31% for onshore. On the other hand, the cost of installing hydro and geothermal systems has increased by 47% and 71%, respectively [3]. According to this data, the total installation cost of solar PV and WT will no longer be considered a significant disadvantage in the near future. The

Table 1.1: Cost Trends of RES, from 2010 to 2020 [3]

	Total Installed Costs ($/kW)			**Levelised Cost ($/kWh)**		
RES	**2010**	**2020**	**% Change**	**2010**	**2020**	**% Change**
Bio-energy	2619	2543	-3%	0.076	0.076	0%
Geothermal	2620	4468	71%	0.049	0.071	45%
Hydropower	1269	1870	47%	0.038	0.044	18%
Solar PV	4731	883	-81%	0.381	0.057	-85%
Onshore wind	1971	1355	-31%	0.089	0.039	-56%
Offshore wind	4706	3185	-32%	0.162	0.084	-48%

global exploitable potential of solar, wind and hydroelectric energy is estimated to be 4.44×10^8 GWh, 1.67×10^8 GWh and 1.39×10^7 GWh, respectively [4]. In 2021, the total installed capacity of RES is expected to be 3064 GW. Hydropower, solar and wind energy account for 1230 GW, 849 GW and 825 GW, respectively. The rest of the energy contribution, i.e., 160 GW, is from other renewable sources [5]. Figure 1.1 depicts the global share of installed RES.

According to the statistics presented above, solar and wind energy resources are abundant but underutilized. As a result, the use of RES will help to alleviate the global energy crisis and mitigate climate change.

The depth of RE Penetration (REP) in the grid is a topic of contention. RES suffers from intermittent and stochastic nature [6], which makes it an unreli-

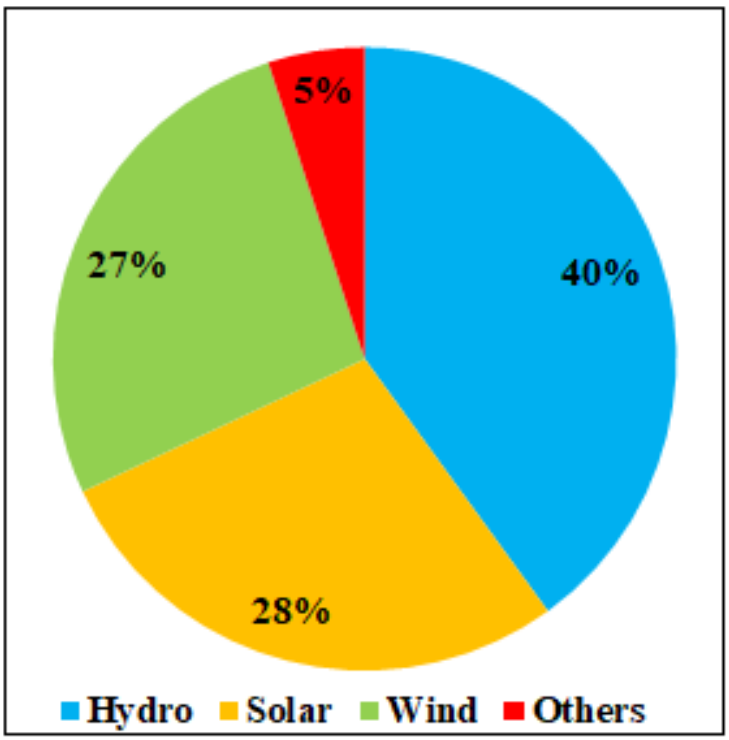

Figure 1.1: World RES Installed Capacity @ 2021 [5]

able source of energy. On the other hand, by using Hybrid Renewable Energy Sources (HRES) along with proper storage and control techniques a 100% RES based grid can be realised. Some countries have achieved this feat or are on their way to achieving 100% REP in their grid. For example - Paraguay: 100%, Ethiopia: 98%, Norway: 97%, Iceland: 97%, Costa Rica: 87 %, and Brazil: 83% of RE penetration in 2020 [3, 7].

HRES is a combination of renewable energy-generating plants and energy storage technologies that address the limitations of a single energy source. HRES increases power system reliability by diversifying energy sources and increasing robustness [8]. HRES can be utilized as a part of a standalone Microgrid (MG) or can be integrated into the grid to improve the performance of the power system network. A standalone MG is a local energy system with control capability and can operate independently. A grid-connected MG is an entity that is electrically connected to the grid and is part of a vast interconnected system.

The utilization of HRES MG in the power network promotes decarbonization, decentralization and democratization. Decarbonization is the process of replacing the fossil fuel energy sources currently being used with energy sources that emit less Green House Gas (GHG). Decentralization is a significant step in the electricity sector for the spread of RES and reduces dependence on fossil fuels. A concept developed within the environmental justice movement to make energy accessible to everyone is termed as democratization [9].

The integration of HRES into the power systems is intended to enhance reliability, reduce economic cost, lower environmental effects and improve power quality by reducing power loss and improving voltage profile. The power system network performance is improved through Demand Side Management (DSM) and Supply Side Management (SSM) methods. DSM includes utility actions to adjust the amount and timing of energy usage by customers. It includes changing energy usage patterns and using efficient energy-consuming devices [10].

SSM control strategies include planning and scheduling the power generation plants to operate at optimal levels, adjusting power generation with load variation, using FACTS devices and including distributed generators. Distributed Generation (DG) refers to a variety of technologies that generate electricity at or near the load. It may consist of diesel generators, storage systems and RES [11]. DG is an alternative generation that improves reliability, power quality and flexibility of the power system [12]. Solar and wind energy are the most potential RES used as DG to improve power system network performance [13–15].

The economic performance of the power system can be improved by introducing lower-cost energy generation plants and subsidizing the components. Subsidies, also known as government incentives, are financial aids provided to electric power producers. Its purpose is to offset capital costs to promote green

energy (renewable energy) policy. So, subsidization is proposed as an alternative strategy for operating RES more economically.

The combination of HRES components is determined by performance evaluation parameters such as reliability, economic cost, environmental effects, etc. The optimal size and placement of HRES components are obtained through optimization techniques while considering the objectives and constraints. The optimization techniques are classified as classical and meta-heuristic algorithms. The applications of these methods varies according to performance, flexibility and objective function. Meta-heuristic methods are more accurate, efficient and capable of obtaining optimal solutions for hybrid systems [16, 17]. Due of the benefits listed above, the metaheuristic methods are being considered for optimizing the objective problems in this research work.

1.2 Motivation of Research

- Population in remote areas lack access to electricity since they are far away from the grid.
- The existing power system in underdeveloped countries is characterized by high power loss, low voltage profile and poor reliability.
- RES in such locations is available but not utilized.

1.3 Aim and Objectives

The aim of the research work is to model the optimal combination of HRES components that are to be integrated into the power system network for improving its performance.

The objective in this research is to operate the power system at the lowest possible cost while maintaining reliability, lowering GHG emissions and improving power quality. The investigations are applied to real-world power systems as case studies. The following are the specific objectives of the research.

- To evaluate a feasible economic solution for non-electrified remote region, by comparing grid extension and standalone HRES MG.
- To optimize size and location of HRES components considering performance evaluation parameters such as reliability, economic cost, GHG emission (CO_2), power loss and voltage profile, as applicable to the case studies.
- To investigate the integration of DG into the power system network to reduce power loss and to improve voltage profile.
- To determine optimal combination of HRES components used as DG.

- To evaluate the cost-effectiveness of HRES integration to power system network.
- To ascertain the impact of subsidy on the total cost of HRES in the grid-connected framework.

1.4 Significance of the Study

- Encourage the community to get access to electricity at a lower cost with lesser GHG emissions and better reliability.
- Reduce a utility's burden by proposing optimal usage of RES.
- Quantify the utility's economic benefits by reducing power losses through the introduction HRES to the power system network.

1.5 Work Plan

The steps taken to complete the study are as follows: (i) the research area is shortlisted by identifying the existing problems in the power system of developing countries. (ii) remote regions are marked which do not have electric supply or suffer from irregular supply, (iii) economic analysis is considered for all the proposed models, (iv) constraints are formulated based on different factors, (v) evaluation parameters are selected based on the requirements of the case study (vi) optimal combination of available HRES components are obtained through different evolutionary optimization techniques, (vii) the optimal solution is checked for feasibility before being recommended for the site under consideration. The work plan flow chart used in this study is summarized in Figure 1.2.

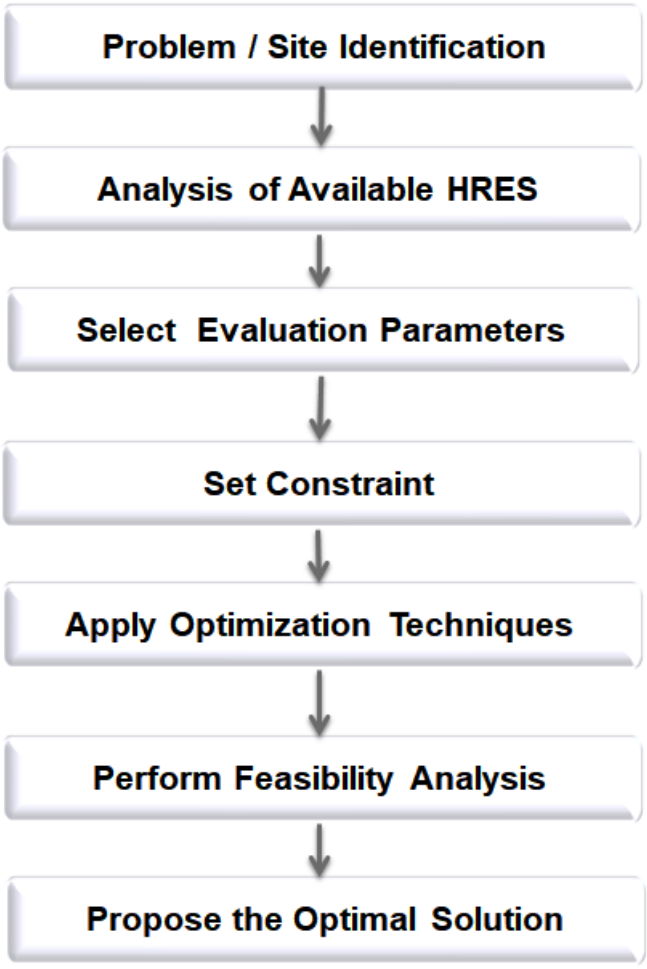

Figure 1.2: Workflow of the Study

1.6 Organization of the Thesis

The research work presented in the thesis is organized and structured in the form of six chapters, which are briefly described as follows:

i) **Chapter 1** focuses on various types of electrical energy resources and their characteristics. The modes of operation of HRES MG in power system networks are also highlighted. The parameters used to evaluate the performance of power system network are thoroughly discussed

ii) **Chapter 2** provides literature review of HRES utilization for electrification of remote region and improvement of power system performance. The per-

formance evaluation parameters considered as objectives for HRES modeling / integration are thoroughly discussed. Finally, the research gaps identified in the studied literature are listed.

iii) **Chapter 3** discusses the mathematical modelling of HRES components and performance evaluation parameters. The optimization methods used to determine the best solution with respect to the objective are also thoroughly discussed.

iv) **Chapter 4** compares the feasibility of grid extension and a standalone system for remote area electrification. The optimization of HRES components is analyzed and compared using meta-heuristic techniques.

v) **Chapter 5** discusses the techno-economical advantage of HRES DG integration into power system network. The economic benefit of subsidized grid-connected HRES MG is also evaluated in this chapter.

vi) **Chapter 6** concludes the overall findings of the case studies. The scope of future work is also presented.

Chapter 2

Literature Review

This chapter provides overviews of different researchers' work related to HRES utilization and their optimization. The publications related to the HRES application in improving power system network performance are reviewed. The performance evaluation parameters and optimization techniques used to find the best solution for the given objectives are thoroughly discussed. Finally, the research gaps are identified in the studied literature.

2.1 Introduction

The literature review was conducted to include publications which considered HRES applications. The objective of these publications is to improve the power system performance evaluated through different parameters. Application of meta-heuristic optimization techniques is also discussed for optimal economic applications of HRES. The published papers selected in review the process based on their objectives that are relevant to our research work, accessible and recently published in scientific journals.

2.2 Hybrid Renewable Energy Sources

Increased studies are being conducted with HRES to improve the power system performances while taking into account various factors which are presented

in later in the chapter.

Techno-economic feasibility and flexibility of HRES are evaluated under both standalone and grid-connected MG in [18]. The objective of this work is to reduce the total Net Present Cost (NPC) and Cost of Energy (COE). The result indicates that grid connection is more cost-effective and reduces CO_2 emissions for the case study under consideration. In [19], a standalone system with solar and wind energy is analyzed to supply electricity to small loads, community or households. The investigation shows that the suggested MG emits fewer GHGs and has lower operation costs.

A standalone hybrid system with solar, wind, biogas and Battery Storage (BS) is studied in [17]. The evaluation parameters such as COE, life cycle gas emissions and Loss of Power Supply Probability (LPSP) are considered as objectives. A multi-objective genetic algorithm is applied to find the optimal size of components. The results show that the unit electricity cost of the proposed hybrid system configuration is better than the grid electricity supply. In [20], reliability enhancement and System Annualized Cost (SAC) of standalone HRES are considered as optimization problems. Bonobo Optimizer (BO) is applied to determine the optimal solution. The economic impact of solar PV on the grid-connected system is analyzed in [21]. To lower the energy deficit: peak load and the least amount of solar irradiation are considered. According to the analysis in this paper, the COE from solar PV is lower than grid costs and emits less GHG.

In [22], the optimal sizing of a hybrid MG system is investigated. The MG consists of solar PV panels, diesel generator (dg) and Fuel Cell (FC). The objective of the study is to minimize NPC. Renewable Energy Penetration (REP) and LPSP are considered as constraints. A Crow Search Algorithm (CSA) is used to optimize the objective problem. The results show that the proposed system

established a reliable and cost-effective MG. Sizing of HRES with geothermal, PV, WT and dg systems are analyzed for both standalone and grid-connected MG in [23]. Reducing the total system cost and GHG emissions are considered as the objectives. The Harmony Search Algorithm (HSA) is used to determine the best configuration of components.

Integration of HRES with the grid system as a backup in the case of a power outage is examined in [24]. RES components sizing is performed through Hybrid Firefly Algorithm (HFA) and Harmony Search (HS) algorithms. According to the study's findings, HFA / HS outperforms Particle Swarm Optimization (PSO) in terms of execution time and energy cost. In [25], MG consists of PV, WT and BS with a dump load for a standalone system. The objectives of the study is to improve the reliability and economic cost with LPSP and COE as indices, respectively. The optimal MG component size is determined according to saturation values by varying PV and WT units.

The concept of a zero-carbon emission strategy is analyzed in [26]. The main goal of the study is to achieve a reliable and affordable solution. This study proposed a combination of PV, WT and energy storage to obtain the best solution. A scalable planning framework that increases the REP rate is proposed in [27]. The analysis is carried out by contrasting the previously stated system with the system supplied with dg. Minimization of SAC is the objective of the study. CO_2 emission and LPSP are considered as constraints. The result shows that using MG consisting of solar PV, WT, BS and dg is cost-effective and reduces CO_2 emissions.

The benefits of RES MG integration to the power system is analyzed in [28]. The system consists of PV, WT, dg and storage systems. Minimizing the COE, lifecycle GHG emission costs and the annual cost of load loss is set as the ob-

jectives in this paper. The findings indicate that incorporating green technology into the MG system improves the specified requirements. The feasibility of off-grid MG from a techno-economic perspective is studied in [29]. The system consists of WT, solar PV, BS and dg. The objective of the study is to minimize NPC. Economic profitability parameters like net present value and pay-back period are also examined. As a result, offering subsidies to RES capital costs is proposed as a solution to lower energy prices and make it more profitable. Techno-economic and environmental investigation of off-grid HRES is analyzed in [30]. The objectives are determined by factors such as economic cost, reliability and sustainability. According to the findings, MG with solar PV, dg and BS is the most cost-effective model for the selected area. Economic cost and GHG emissions reduction of solar PV MG is analyzed in [31]. Genetic Algorithm (GA) and General Algebraic Modeling System (GAMS) are compared by their computation time and accuracy to get the optimal solutions. The results show that GA performed better in the modelling of the MG system. In [32], the surplus energy from RES is stored in FC and reused during high demand or when all other sources of power are exhausted. This approach decreases energy waste, improves system reliability and increases producer income.

The optimal siting and sizing of DG in the distribution system are analyzed in [33]. Standard IEEE bus systems are used to evaluate power loss and voltage profile improvement. Opposition-based Tuned-Chaotic Differential Evolution (OTCDE) technique is applied to find the solutions. The optimal location and sizing of solar PV and BS, used as DG, are assessed in [34]. The objective of the study is to minimize system power loss. A Whale Optimization Algorithm (WOA) is used as an optimization method in the study. According to the analysis, employing BS as DG is more cost-effective for networks with small loads.

In [35], sizing of HRES components used as DG is investigated. A standard IEEE 51-bus system is used to analyze the techno-economic parameters of DG integration. The PSO algorithm is used to obtain the optimal solution. The results show that the introduction of HRES as DG reduces power losses and enhances voltage profile. The optimal placement and sizing of HRES with PV, WT and FC-based DG units in distribution systems are discussed in [36]. The objective of the study is to minimize power losses, the cost of DG units and GHG emissions. The results of the analysis show that the integration of RES as DG improves the stated objective.

The optimal size and location of solar PV-based DG in the primary distribution system are investigated in [37]. Power loss reduction and voltage profile improvement, as well as economic benefits, are considered as objectives. The evaluation is performed on standard IEEE 33 and IEEE 69 bus systems. It is determined that multiple-site DG installations outperformed a single DG placement and thus also provided more economic benefits.

In [38], sizing and placement of PV, WT and BS systems as DGs in the distribution network are analyzed. The objectives of the study are to minimize power loss costs, enhance voltage profile and minimize power purchased. The Improved Whale Optimization Algorithm (IWOA) is used to determine the optimal location and size of DG components. The study is carried out using a standard IEEE 33-bus system. The results show that the application of HRES as DG improves system performance. Sizing and placement of BS and WT are analyzed in [39]. The objective of the study is to minimize total power loss and the costs of the power system network. BS is introduced to the network to flatten the output power injected into the grid by WT. GA is used to obtain an optimal combination of BS and WT. The analysis is performed on a standard IEEE 33-

bus system for validation purposes. The study's findings reveal that using BS as DG is used for peak shaving and improves load voltage profile.

Optimal size and location of DG and network reconfiguration are conducted in [40]. The objective of the study is to minimize total costs, power losses and voltage deviation. A multi-objective PSO algorithm is implemented to determine the objective of the study. The network performance is tested by re-configuring the standard IEEE-33 bus system. The results reveal that the combination of re-configuring the network and the optimal DG size and placement technique is efficient in achieving the objectives. Optimal DG size and location for the smart grid are investigated in [41]. The objective of the paper is to minimize line loss, improve voltage profile and reduce harmonic distortion. To find the best solution, a hybrid Interactive Autodidactic School (IAS) and Most Valuable Player Algorithm (MVPA) optimization techniques are used. The standard IEEE 33-bus system is considered for the analysis. The results show that the proposed strategy is more efficient in the power system planning stage.

Table 2.1 depicts the collection of literature dealing with HRES modelling to improve power system network performance.

Table 2.1: Collection of Reviewed Literature on HRES MG Optimization

Techniques	**HRES Components**	**Objective**	**Ref**
PSO	WT, CSP and energy storage	Reduce economic cost and CO_2 emission	[42]
PSO	PV-WT	Improve reliability and reduce economic cost	[43]
GA	PV, WT, BS, dg and FC	Reduce GHG emission and economic cost	[44]
GA, MOPSO	PV,WT and BS	Reduce economic costs and improve reliability	[45]
GA, MILP	WT and solar with TES	Improve reliability	[46]
FA	WT, PV and BS	Reducing economic costs and improve reliability	[47]
MILP	RES, energy storage and dg	Reduce economic cost and risk indices	[48]
PSO, FLC	FC, WT, PV and CHP	Reduce economic cost	[49]
PSO	Standard IEEE 33-bus radial distribution	Reduce power losses	[50]
HOMER	PV, WT, hydropower and BS	Reduce economic cost and GHG emission	[51]

2.3 Research Gap

- In several articles, a diesel generator is recommended for hybrid systems to improve reliability, however, it produces more CO_2 and has a high operating cost.
- The economic cost of HRES is determined by altering reliability indices, notably LPSP values, which are taken higher than the minimal value (LPSP=0), which affects system reliability.

- DG placement and sizing are analyzed with IEEE standard bus systems in the literature. This system is modeled for time-invariant load and supply (i.e., one set of values). However, in practice, load and supply (RES) vary over time (i.e, change over a time frame).
- The introduction of BS is recommended in the literature to improve the performance of large power systems, but it is not cost-effective.

Chapter 3

Modelling of HRES and Methodology

This chapter highlights the mathematical modelling of HRES components and performance evaluation parameters. The optimization methods used to determine the optimal solution with respect to the objectives are also thoroughly discussed.

3.1 Modelling of HRES MG Components

The mathematical modelling as well as the characteristics of HRES components are presented in detail in this section. Solar, wind, hydro, biomass and energy storage are HRES MG that are considered for analysis in different case studies. The RES are selected based on their abundant availability in the specific region.

3.1.1 Solar Energy

Sun is the primary source of the majority of energy on earth, including solar energy. Solar energy is the radiant light and heat received from the sun that is captured and used in a variety of technologies, including solar power to generate electricity and solar thermal energy. Solar power is the conversion of energy from sunlight into electricity, either directly by using photovoltaics (PV) or indirectly by using concentrated solar power or a combination.

The electric energy is harvested from solar energy via Photo Voltaic (PV) cells. A solar PV cell is a semiconductor material that converts the energy of light directly into electricity through the photovoltaic effect. The electric power (P_{pv}) (W) harvested from solar irradiation through a PV panel is computed as in Eq. (3.1.1) [52].

$$P_{PV} = \begin{cases} P_r(\frac{G^2}{G_{sr} \times G_{cr}}) & 0 \leq G < G_{cr} \\ P_r(\frac{G}{G_{sr}}) & Gcr \leq G < G_{sr} \\ P_r & otherwise \end{cases} \tag{3.1.1}$$

Where P_r: rated power of PV panel (W); G: instant solar radiation (W/m^2); G_{sr}: solar radiation at standard environment (1000 W/m^2); G_{cr}: certain radiation point (150 W/m^2) [52].

Solar PV panels are mainly classified as mono-crystalline or poly-crystalline based on their purity. Mono-crystalline solar panels have a higher purity of silicon and a better efficiency (17–23%). They are more expensive, more durable and require less installation area. Poly-crystalline solar panels are less efficient (<18%), occupy more space and have a shorter lifespan than mono-crystalline panels. The solar energy resource features are listed in Table 3.1.

Table 3.1: Solar Energy Characteristics [53]

Advantages	**Limitations**
Renewable and low GHG emissions	High investment costs
Reduces electricity bills	Intermittent and stochastic
Low maintenance costs	Requires large spaces

3.1.2 Wind Energy

Wind energy is derived from solar energy due to a combination of three concurrent events, the sun unevenly heating the atmosphere, irregularities in the earth's surface and rotation of the earth. Wind turbines use the wind's motion to rotate the turbine, which then drives the rotor of a generator to produce power. The electric power (P_{WT}) (W) converted from wind energy is calculated using Eq. (3.1.2).

$$P_{WT} = \begin{cases} 0, & 0 \leq v \leq v_C \quad or \quad v_f \leq v \\ P_r \frac{(v-v_c)}{v_r-v_c}), & v_c \leq v < v_r \\ P_r, & v_r \leq v \leq v_f \end{cases} \tag{3.1.2}$$

Where v: instantaneous wind speed (m/s); v_c: cut-in wind speed (m/s); v_r: rated wind speed (m/s); v_f: cut-off wind speed (m/s); P_r: rated power output of WT (W).

The wind speed used to generate electric power varies with tower height. The wind speed at the desired hub height is determined using Eq. (3.1.3).

$$v_{hub} = v_o \left(\frac{H_{hub}}{H_o} \right)^{\alpha} \tag{3.1.3}$$

where v_{hub} and v_o: the wind speed at hub height (H_{hub}) and wind speed at reference height (H_o), respectively; and α: power-law exponent (friction component), ranging from 1/7 to 1/4 [54].

The features of wind energy resources are summarized in Table 3.2.

Table 3.2: Wind Energy Characteristics [53]

Advantages	**Limitations**
Environment-friendly and pollution-free	Vulnerable to extreme weather conditions
Abundantly available	Influences system's stability
The total cost decreases with time	Low energy density
Land usage is limited	Available at selected locations
Low power losses in T & D lines	Intermittent and stochastic behavior
Enhances power quality and reliability	

3.1.3 Hydro Power

Hydropower is a renewable energy source that generates electricity from the natural flow of moving water or from reserve. It is categorized as micro, mini, small, large and ultra-large power with the power rating of $<$ 100 kW, 100 kW to 1 MW, 1 to 10 MW, 10 MW to 50 MW and $>$50 MW, respectively [55]. The power generated from hydropower (P_h) (W) is calculated using Eq. (3.1.4).

$$P_h = \eta Q H \rho g \tag{3.1.4}$$

Where Q: water flow rate (m^3/s); ρ: density of water (1000 kg/m^3); H: water head (m); g: gravitational acceleration (9.81 m/s^2); η: total power plant efficiency (%).

The hydropower resource properties are summarized in Table 3.3.

3.1.4 Biogas Energy

Biogas is a mixture of gases such as methane, carbon dioxide and hydrogen sulfide. It is produced from agricultural waste, dung, plant material, sewage

Table 3.3: Hydropower Characteristics [56]

Advantages	**Limitations**
Provides benefits for irrigation support	High investment cost with risks
Affordable and low-cost electricity	Susceptible to environmental degradation and climate change
Longer life span	More sensitive to environmental effects
Provides flood control	Relocates population and changes the ecosystem

and food waste. Biogas is used as a fuel for heating purposes or to generate electricity using a gas engine. The electric power that can be harvested from biogas (P_{bg}) (W) is calculated using Eq. (3.1.5).

$$P_{bg} = \frac{\eta_{obg} \times CV_{bg} \times T_g}{860} \tag{3.1.5}$$

where η_{obg}: total efficiency of plant (%); CV_{bg}: the calorific value of biogas (kcal/m^3); T_g: total gas yield for electricity generation (m^3/day), it is calculated using Eq. (3.1.6).

$$T_g = M_g T_s A_c B_g \tag{3.1.6}$$

Where M_g: gross cumulative manure from cattle (kg/day); T_s:total solids in manure (%); A_c: availability coefficient of animal manure for selected species (%); B_g: biogas yield of animal manure from a single kilogram of solids (m^3/kg). Biomass has advantages and limitations as explained in Table 3.4.

3.1.5 Energy Storage System

Energy storage systems are the set of methods and technologies used to store energy, which can be used later on. They are used for enhancing the system reliability through peak-shaving, providing spinning reserves, ancillary services,

Table 3.4: Biogas Energy Characteristics [57]

Advantages	**Limitations**
Available in abundance	Raw material transportation
Reduces over-reliance on fossil fuels	Complicated gasification process
Utilizes waste	Cost-intensive and complex in the removal of syngas
Produces a circular economy	Weather dependent (seasonal)

power quality improvement, etc. [58, 59]. Energy storage technologies are classified as chemical, electrical, electrochemical, thermal and mechanical [60] as illustrated in Figure 3.1.

A Battery Storage (BS) is an electrochemical device employed in electrical power systems to store energy. BS has a high energy density, operates at high efficiency, has low cost and compact storage. It has an adequate cycle life and significant service years. Due to these advantages, BS is preferred as energy storage in RES MG [60].

Capacity of BS in the analysis of HRES MG is determined through the State of Charge (SoC). SoC is the percentage of stored charge in the battery relative to its capacity. The BS status, SoC at a given time 't' is calculated using Eq. (3.1.7).

$$SoC_{(t)} = SoC_{(t-1)}(1-\sigma) + \left(E_{g(t)} - \frac{E_{l(t)}}{\eta_{inv}}\right)\eta_b \tag{3.1.7}$$

Where $SoC_{(t)}$: charge level of BS at a given time 't'; $SoC_{(t-1)}$: charge level of BS before time 't'; σ: self-discharge rate per time unit, 2×10^{-4} per hour (10-15% per month for lead acid BS) [61]; $E_{g(t)}$ and $E_{l(t)}$: generated energy and energy demand at time 't', respectively.

During the charging or discharging of BS, the SoC must be within the specified limits to increase the battery life and efficiency. The battery limit constraint

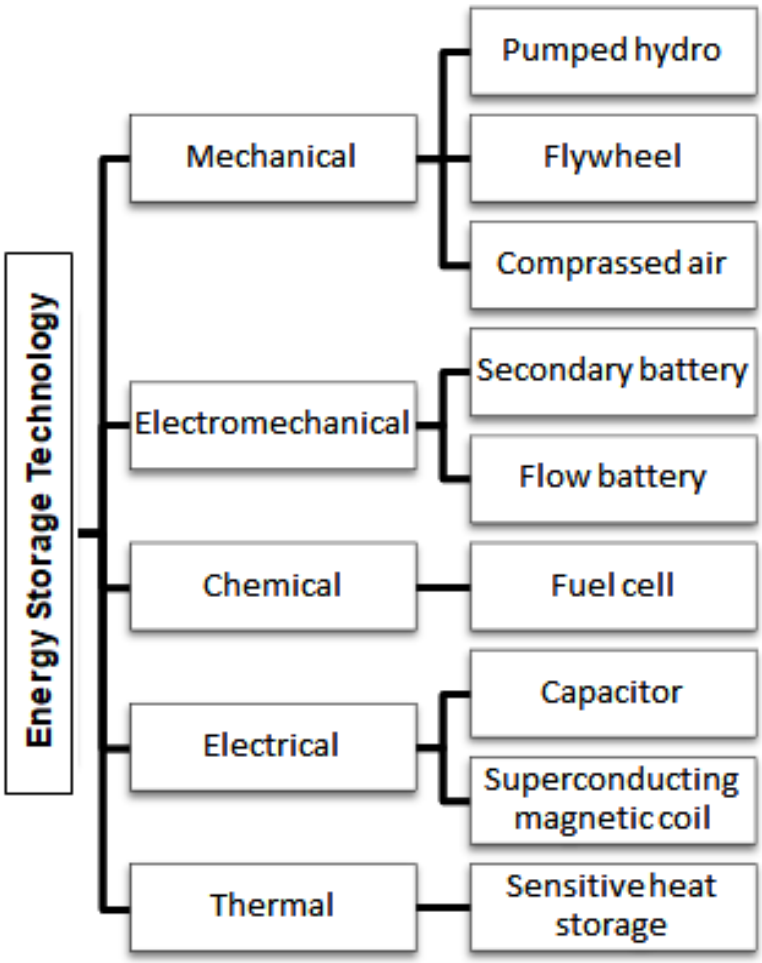

Figure 3.1: Energy Storage Technology

is represented through Eq. (3.1.8).

$$SoC_{(t)} = \begin{cases} SoC_{min}, & SoC_{(t)} \leq SoC_{min} \\ SoC_{(t)}, & SoC_{min} \leq SoC_{(t)} \leq SoC_{max}, \\ SoC_{max} & SoC_{(t)} \geq SoC_{max} \end{cases} \tag{3.1.8}$$

Where SoC_{max} and SoC_{min}: maximum and minimum allowable limit of charging and discharging BS, respectively.

The energy storage in a BS at a specific time 't' is determined by Eq. (3.1.9).

$$E_{(t)} = SoC_{(t)} - SoC_{(t-1)} \tag{3.1.9}$$

3.2 HRES Performance Evaluation Parameters

RES such as solar and wind are characterized by their intermittence and stochastic behavior. Hybridizing them with an optimal combination is a method used to overcome RES drawbacks. The performance of the HRES combination is evaluated through parameters such as economic cost, reliability, environmental effects (GHG emissions), etc. They are discussed in the following subsections.

3.2.1 Reliability Analysis

The reliability of a power system is its ability to deliver continuous and sufficient energy to the connected load. From the planning to the operating stages of power systems, reliability evaluation is a critical and significant parameter. The reliability of the power system network is measured through different indices as listed in Table 3.5.

LPSP is applied as a constraint to determine the HRES component size [69, 70]. LPSP represents the probability that the power supply may not be able to fulfill the load demand. The system LPSP is determined using Eq. (3.2.1) [71].

$$LPSP = \frac{\sum_1^T (P_{d(t)} - P_{g(t)})}{\sum_1^T P_{d(t)}} \tag{3.2.1}$$

where $P_{g(t)}$ and $P_{d(t)}$: total generated power and demand at time 't' (W), respectively.

Table 3.5: Reliability Assessment Indices

Indices	Description	Ref
LPSP	Expectation that load is not satisfied by the total energy produced	[28]
LOLP	Ratio of annual energy deficits to annual load demands in the overall system	[62]
DPSP	Amount of deficient power at specific hours	[63]
LOLE	Expected number of hours or days when loss of load occurs	[64]
EENS	Amount of energy demand not supplied during a specified period of time	[65]
SAIDI	Average outage duration for each customer served	[66]
SAIFI	Average frequency of sustained interruptions per customer during a year	[66]
CAIDI	Average time to restore service	[66]
CIII	Average number of customers interrupted during an outage	[67]
CAIFI	Average number of interruptions per customer interrupted in a year	[67]
ASAI	Ratio of total number of hours for which service is provided to the total hours demanded, in a specified period	[67]
MAIFI	Average number of momentary interruptions that a customer experiences during a given time period	[68]

3.2.2 Economic Analysis

The economic analysis performs economic viability analysis for a project, for better resource allocation. It is a cost-benefit analysis that is applied for planning, capacity enhancement and improving operation efficiency. The system cost performance is evaluated using different indices that are summarized in Table 3.6. The Cost of Energy (COE) ($/kWh) is one such index which is used to determine the techno-economic performance of the power system. The COE is calculated using Eq. (3.2.2) [73].

$$COE = \frac{TAC}{E_t} \tag{3.2.2}$$

Table 3.6: Economic Performance Evaluation Indices

Indices	Description	Ref
LCOE	Ratio of overall lifetime costs involved with a power plant to the lifetime energy production by that power plant.	[70]
COE	Proportion of the aggregate annual costs of a system to the annual power provided by the system	[70]
ACS	Represents maintenance cost, capital cost and replacement cost of a system in a specified year	[70]
NPC	Summation of initial cost, operational and maintenance cost and replacement cost of the system	[70]
LCC	Total cost of one-time and recurring costs for the lifetime duration of a system	[70]
SPB	Expected number of years it will take to recover the invested amount of the project	[72]
EPBT	Time required to generate as much energy as is consumed during production and lifetime operation of a system	[72]

Where E_t: annual energy produced (kWh/yr); TAC: total annualized cost ($/yr) that is calculated by using Eq. (3.2.3).

$$TAC = \sum_{k=1}^{K} N_{cop,k} \left(C_{ck} \left(\frac{i(1+i)^n}{(1+i)^n - 1} \right) + C_{OMk} + C_{rk} \left(\frac{i}{(1+i)^{LF} - 1} \right) \right) \tag{3.2.3}$$

Where C_c: total capital cost of component ($/kW); C_{OM}: annual operating and maintenance cost ($/kW/yr); C_r: total replacement cost ($/kW); N_{cop}: number of components used; n: project lifetime (yr); LF: Components lifetime (yr); i: interest rate per year (%); k: component type.

Simple Payback Period (PBP) is another index that is used to evaluate the economic cost of a power system and is formulated as Eq. (3.2.4).

$$PBP = \frac{C_c}{S_A} \tag{3.2.4}$$

Where C_{ct}: total investment cost ($); S_A: annual saving ($/yr).

3.2.3 Analysis of Environmental Effects

Environmental concerns are inextricably linked to energy production and consumption. The environmental impact of one component for its entire life cycle varies from another component, depending on the methods deployed from manufacturing process to disposal [74, 75]. In WT, environmental issues like sound, bird safety and visual pollution are frequent. Effects of solar power plants include habitat destruction, extensive land use, water use and use of hazardous materials during manufacturing. The establishment of hydroelectric power dams and reservoirs destroys forests and relocates populations and wildlife habitats. Burning of biomass emits GHG gases in abundance which leads to global warming. Relative to the other pollutant particles, the amount of CO_2 emitted from energy generation plants is higher in percentage [76]. Thus, in this study, the CO_2 emission through the life cycle of the components is considered as a parameter for considering environmental effects. Daily Carbon Dioxide Emission

Table 3.7: Performance Evaluation Indices of Environmental Effects [77]

Indices	**Description**
Een	Energy used during the activities related to a production process/ consumption of energy for components manufacturing
LCA	Evaluation of all life cycle stages of components for gas emissions
FE	Total gas emissions produced by generating units through a defined time duration

(DCE), (Kg/day) from HRES components is calculated in Eq. (3.2.5).

$$DCE = \sum_{k=1}^{K} C_k \times E_{T,k} \tag{3.2.5}$$

Where E_T: daily total energy produced from HRES unit 'k' (kWh/day); C_k: life cycle emission of CO_2 released from unit 'k' (kg/kWh).

To include the environmental effects in HRES modelling, GHG emissions are converted to cost by taking into account the emitted gas per unit time and the penalty cost. The Total CO_2 Emissions with Penalty cost ($TCEP_c$) ($/yr) from different components is calculated using Eq. (3.2.6) [78].

$$TCEP_c = PF \sum_{t=1}^{T} DCE \tag{3.2.6}$$

Where PF: penalty factor, cost imposed to reduce gas emission (0.075 $/kg), [79]; T: time period.

3.3 Optimization Methods to Optimize HRES

To improve system performance, HRES modelling requires an optimal combination of components to supply the load. Optimization is the process of determining the optimal solution for an objective function within its feasible space. The goal of optimization is to maximize the desired benefit or to minimize the required effort.

The performance parameters for HRES are either optimized individually as single objective or combined as multi-objective functions [80]. A single objective problem is the one that must be solved for only one output parameter. A multi-objective function combines various parameters to achieve the best optimal solution. Multi-objective functions are optimized through scalarization or Pareto approach [81]. The scalarization approach multiplies each solution by a predefined weight (w), which is then converted to a single-objective function as formulated in Eq. (3.3.1) and (3.3.2). It is usually applied for problems having

similar outcome, minimization or maximization.

$$Min/Max \sum_{i=1}^{I} w_i f_i(x) \tag{3.3.1}$$

where $f_i : i^{th}$ function definition; w_i : weight allocated to i^{th} function. For

$$\sum_{i=1}^{I} w_i = 1, \forall_i : w_i \geq 0 \tag{3.3.2}$$

If the issues contain opposing objectives, Eq. (3.3.3) is used to combine them into a single form and solve the issue simultaneously.

$$minF = \sum_i min(f_i) + \frac{1}{\sum_j max(h_j)} \quad or \quad maxH = \frac{1}{\sum_i min(f_i)} + \sum_j max(h_j) \tag{3.3.3}$$

where $h_j : j^{th}$ function definition;

The optimization methods that are applied to determine the size of HRES components are categorized as: classical and metaheuristic [16].

Classical Method

The classical method is a branch of numerical optimization that focuses on obtaining global solutions. They are based on iterative methods, numerical and analytical methods, probabilistic and graphical construction methods. Linear programming (LP), Mixed integer LP (MILP) and iterative schemes are categorized under the classical methods.

Meta-heuristic Methods

Meta-heuristic methods are stochastic optimization algorithms that maintain a population of candidate solutions that are used to sample, explore and close in on an optimal solution. They are intended for solving more complex objective problems that may have multiple global optima or are feasibility problems.

Meta-heuristic methods are more accurate, efficient and capable of getting optimal solutions for hybrid systems [16]. These optimization approaches are designed to improve the technical, economic and efficient operation of a hybrid system by determining the optimal system configuration [82]. Particle Swarm Optimization (PSO), Differential Evolution (DE), Manta Ray Foraging Optimization (MRFO), Shuffled Frog-Leaping Algorithm (SFLA), Reptile Search Algorithm (RSA) and RUNge Kutta optimizer (RUN) are used in this research work to obtain the optimal solution.

The population is randomly generated within the search space. To obtain the best solution, the candidate solutions are updated according to the meta-heuristic algorithm being implemented. The different optimization technique are presented below:

1. Particle Swarm Optimization (PSO): PSO imitates the social behavior of bird flocking or schools of fish to search for food [83]. Variables are updated through changes in particle velocity and position.

- **Particle velocity**

Particle velocity for the new iteration, $V_{i(t+1)}$ for i^{th} particle is calculated by using Eq. (3.3.4).

$$V(_{i(t+1)}=K \times [V_{i(t)} + c_1 rand(0,1)(pb - X_{i(t)}) + c_2 rand(0,1)(gb - X_{i(t)})] \tag{3.3.4a}$$

$$K = \frac{2}{|2 - \phi - \sqrt{\phi^2 - 4\phi}|} \tag{3.3.4b}$$

Where $V_{i(t)}$: current velocity of particle, i; pb: particle best position; gb: global best position; c_1: personal influence coefficient; c_2: social influence coefficient; $\phi = c_1 + c_2, \quad \phi > 4$; K : constriction factor; $X_{i(t)}$: particle current position

- **New Particle Position**

The new particle position, $X_{i(t+1)}$ for i^{th} particle is calculated by using Eq. (3.3.5).

$$X_{i(t+1)} = V_{i(t+1)} + X_{i(t)} \tag{3.3.5}$$

The flowchart of PSO is presented in Figure 3.2a.

2. Differential Evolution (DE): DE is inspired by Darwin's theory of evolution [84]. The population is generated randomly as in other meta-heuristic methods. The variations in parameters in each iteration happens through mutation, cross-over and selection processes.

- **Mutation**

In DE a vector termed as a mutant vector, V_i is obtained using Eq. (3.3.6).

$$V_i = X_{r_1} + F(X_{r_2} - X_{r_3}) \tag{3.3.6}$$

Where $r_1; r_2; r_3$: random indices $\in$ [1,NP]; i $\neq r_1 \neq r_2 \neq r_3$; F: real and constant factor $\in$ [0, 2]; NP: Population size

- **Crossover**

Crossover introduces increased diversity in parameter vectors. Trial vector u_i, for crossover update, is calculated in Eq. (3.3.7).

$$u_i = \begin{cases} v_i & if \quad rand(j) \leq CR \\ X_i & otherwise \end{cases} \tag{3.3.7}$$
$$j = 1, 2, \ldots, D$$

Where CR : crossover probability (or crossover control parameter), (0,1); D: Dimension.

A random number generated through 'rand' is used to decide the content of trial vector.

- **Selection**

In this step, the greedy criterion is used to compare the trial vector to the target vector. If the trial vector yields a better cost function value than the target vector, then X_i is set to u_i for the next iteration; otherwise, the old value X_i is retained as shown in Eq. (3.3.8).

$$X_{i+1} = \begin{cases} U_i & if \quad F(u_j) \leq F(X_i) \\ X_i & otherwise \end{cases} \tag{3.3.8}$$

Where F: Objective function value

The flowchart of DE algorithm is summarized in Figure 3.2b.

3. Manta Ray Foraging Optimization (MRFO): MRFO imitates the behavior of Manta rays while catching its prey [85]. MRFO is inspired by three foraging behaviors: chain foraging, cyclone foraging and somersault foraging. The mathematical models are described below.

- **Chain Foraging**

The mathematical model for chain foraging can be represented through Eq. (3.3.9) and (3.3.10.

$$X^d_{i(t+1)} = \begin{cases} X^d_{i(t)} + r(X^d_{b(t)} - X^d_{i(t)}) + \alpha(X^d_{b(t)} - X^d_{i(t)}) & i = 1 \\ X^d_{i(t)} + r(X^d_{(i-1)(t)} - X^d_{i(t)}) + \alpha(X^d_{b(t)} - X^d_{i(t)}) & i = 2, ...N \end{cases} \tag{3.3.9}$$

$$\alpha = 2r\sqrt{|log(r)|} \tag{3.3.10}$$

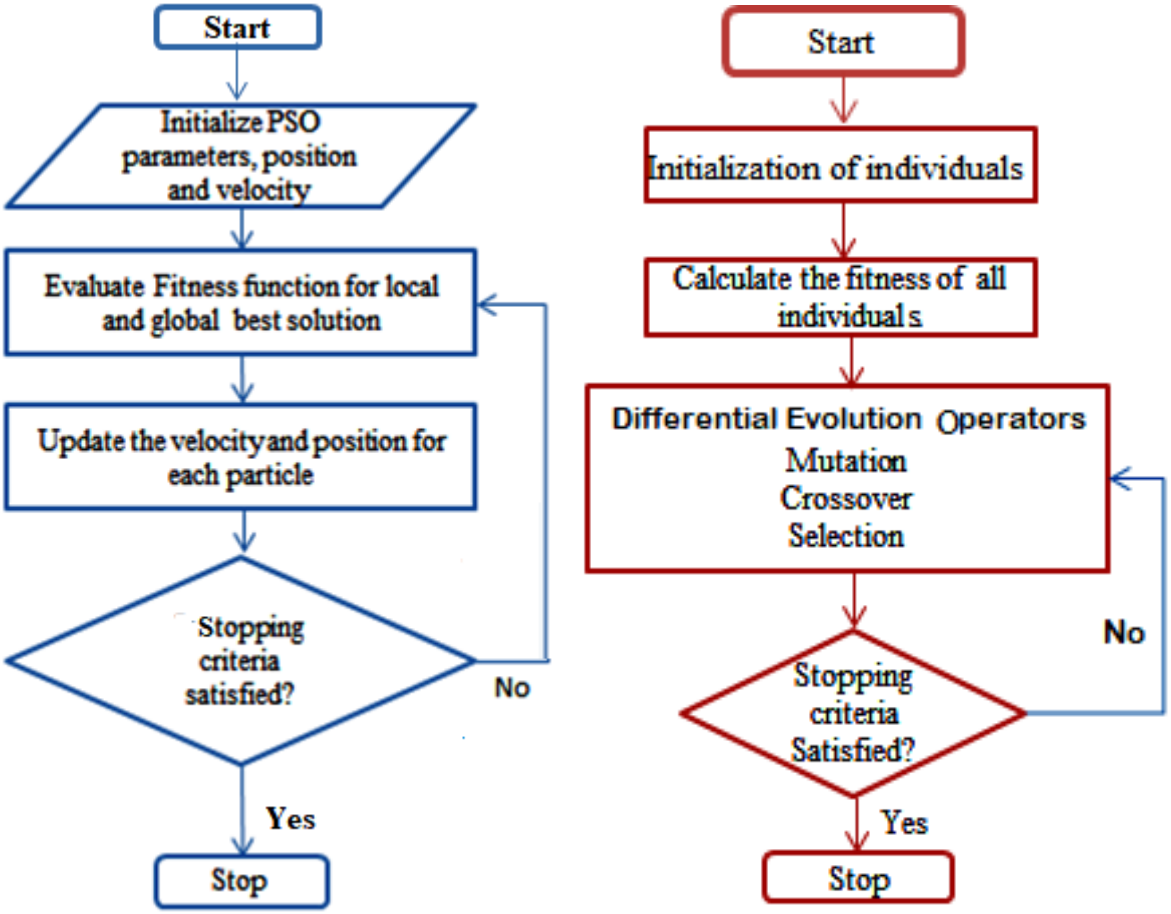

(a) Flowchart PSO Algorithm

(b) Flowchart of DE Algorithm

Figure 3.2: Flowchart for PSO and DE Algorithms

Where r: random number (0,1), d : dimension; t: current iteration; $X^d_{i(t)}$: position of manta ray for t^{th} iteration and i^{th} position; $X^d_{b(t)}$: region with a high concentration of plankton; α: a weight coefficient; N: Population size

- **Cyclone Foraging**

When a school of manta rays recognize a patch of plankton in deep water, they will form a long foraging chain and swim toward the food in a spiral formation. Mathematical model of cyclone foraging is formulated in Eq. (3.3.11) and

(3.3.12) to extend the motion to an n-D space.

$$X_i^d(t+1) = \begin{cases} X_{b(t)}^d + r(X_{b(t)}^d - X_{i(t)}^d) + \beta(X_{b(t)}^d - X_{i(t)}^d) & i = 1 \\ X_{b(t)}^d + r(X_{(i-1)(t)}^d - X_{i(t)}^d) + \beta(X_{b(t)}^d - X_{i(t)}^d) & i = 2, ...N \end{cases} \tag{3.3.11}$$

Where β: a weight coefficient and formulated as in Eq. (3.3.12).

$$\beta = 2e^{r1\left(\frac{T-(t+1)}{T}\right)} \times sin(2\pi r1) \tag{3.3.12}$$

Where T: maximum iterations; r1: the random number [0, 1].

- **Somersault Foraging**

The position of the food is viewed as a pivot at this stage. Each individual tends to swim to and from around the pivot and somersault to a new position. The Somersault foraging stage is updated according to Eq. (3.3.13).

$$X_i^d(t+1) = X_{i(t)}^d + S(r_2 X_{b(t)}^d - r_3 X_{i(t)}^d), \quad i = 1, ...N \tag{3.3.13}$$

Where r_2 and r_3 : random numbers [0 1]; S: the somersault factor, S=2.

The flowchart algorithm of MRFO is summarized in Figure 3.3a.

4. Shuffled Frog-Leaping Algorithm (SFLA): SFLA is conceptualized by observing, imitating and modelling the behavior of frogs searching for food [86]. SFLA creates subdivisions within the population which are termed memeplexes and submemeplexes. Some frogs from a memeplexe are selected to form a submemeplex. The frogs within the submemeplexes help each other to improve their positions. The population is again merged and the process is repeated. From the selected population, the worst and best position of the frog is determined. The step (S) and new position (X_N) are computed for the frog with the

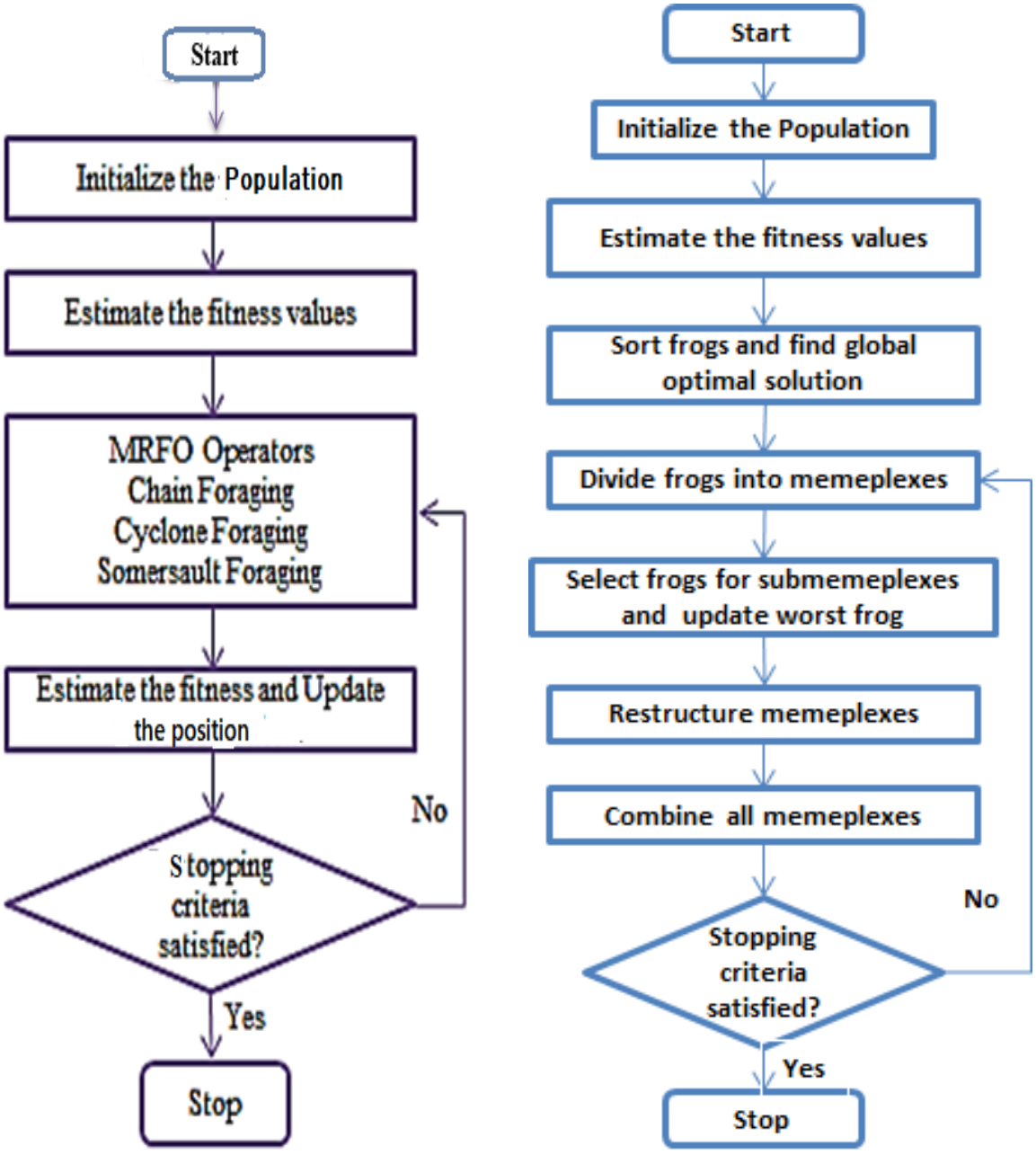

(a) Flowchart of MRFO algorithms

(b) Flowchart of SFLA Algorithm

Figure 3.3: Flowchart of MRFO and SFLA Algorithms

worst performance in the submemeplexes using Eq. (3.3.14) and (3.3.15).

$$S = r(X_b - X_w) \tag{3.3.14}$$

$$X_N = X_w + S \qquad for \quad S < S_{max} \tag{3.3.15}$$

Where r: random number (0,1); X_w: worst frog position; X_b: best frog position; S_{max}: maximum allowed distance in one jump.

If the new position is better than the old position, the new position replaces the old position; otherwise, the old position is discarded and a new solution is randomly determined using Eq. (3.3.16).

$$X'_N = \begin{cases} X_N & for \quad F(X_N) \\ r & otherwise \end{cases} \tag{3.3.16}$$

Where r: new random frog position.

The flowchart algorithm of SFLA is summarized in Figure 3.3b.

5. Reptile Search Algorithm (RSA): Reptile Search Algorithm (RSA) is motivated by the hunting behavior of crocodiles [87]. RSA is inspired by the encircling mechanisms, hunting mechanisms and the social behavior of crocodiles in nature. The mathematical model of RSA is explained below:

- **Encircling Phase (Exploration)**

Each solution updates its position using Eq. (3.3.17) as required in exploration

phase.

$$X_{i,j}(t+1) = \begin{cases} Best_j(t) \times -\eta_{(i,j)}(t)\beta - R_{(i,j)}(t) \times r, & t \leq \frac{T}{4} \\ Best_j(t) \times x_{(r1,j)} \times ES(t) \times r, & t \leq 2\frac{T}{4} \ \& \ t > \frac{T}{4} \end{cases} \tag{3.3.17}$$

Where Best$_j(t)$: best solution for jth position; r: random number (0,1); T: maximum iterations; t: current iteration; $\eta_{(i,j)}$: hunting operator for ith solution and jth position as calculated in Eq. (3.3.18); β: controls exploration accuracy (0.1); R$_{(i,j)}$: reduce function used to reduce search area as calculated in Eq. (3.3.19); x$_{(r1,j)}$: random position of ith solution; r1: random number [1, N]; N: population size; ES(t): probability ratio, has randomly decreasing values [-2, 2] throughout the process and is calculated using Eq. (3.3.20).

$$\eta_{(i,j)} = Best_j(t) \times P_{(i,j)} \tag{3.3.18}$$

$$R_{(i,j)} = \frac{Best_j(t) - X_{(r2,j)}}{Best_j(t) + \epsilon} \tag{3.3.19}$$

$$ES(t) = 2 \times r_3 \times (1 - \frac{1}{T}) \tag{3.3.20}$$

Where ϵ: small value; r$_2$: random number [1, N]; r$_3$: random integer [-1 1]; P$_{(i,j)}$: percentage difference between best solution and current solution of the jth position and calculated using Eq. (3.3.21).

$$P_{i,j} = \alpha + \frac{X_{i,j} - M(_{X_i})}{Best_j(t) \times (UB_j - UL_j) + \epsilon} \tag{3.3.21}$$

Where M($_{X_i}$): average position of ith solution calculated using Eq. (3.3.22); UB$_j$ and LB$_j$: upper and lower boundaries of the jth position, respectively; α:

constant (0.1).

$$M(_{X_i}) = \frac{1}{n}\sum_{j=1}^{n} X_{(i,j)} \tag{3.3.22}$$

Where n: number of positions

- **Hunting phase (exploitation)**

RSA exploitation mechanism locates the best solution by employing coordination and collaboration methods of the crocodiles during hunting. It is formulated in Eq. (3.3.23).

$$X_{i,j}(t+1) = \begin{cases} Best_j(t) \times P_{(i,j)}(t) \times r, & t \leq 3\frac{T}{4} \& t > 2\frac{T}{4} \\ Best_j(t) - \eta_{(i,j)}(t) \times \epsilon - R_{(i,j)}(t) \times r, & t \leq \frac{T}{4} \& t > 3\frac{T}{4} \end{cases} \tag{3.3.23}$$

The flowchart representing RSA is given in Figure 3.4.

6. RUNge Kutta Optimizer (RUN): RUN is a metaphor-free population-based optimization technique that is based on basic mathematics [88]. Its variables are updated using the following steps.

- **Root of Search Mechanism**

The Search Mechanism (SM) is formulated through Eq. (3.3.24).

$$SM = \frac{1}{6} X_{RK} \Delta X \tag{3.3.24}$$

Where

$$X_{RK} = k_1 + 2k_2 + 2k_3 + k_4 \tag{3.3.25}$$

ΔX: position increment; $k_1, k_2, k_3$and k_4: coefficient variables calculated in Eq. (3.3.26) to (3.3.30).

$$k_1 = \frac{r \times X_w - u \times X_B}{2\Delta X} \tag{3.3.26}$$

Where X_w: position of the worst solution; X_b: position best solution; u: random value calculated using Eq. (3.3.27).

$$u = round(1 + r) \times (1 - r) \tag{3.3.27}$$

$$k_2 = \frac{1}{2\Delta X}(r(X_w + r1 \times k_1 \times \Delta X) - (u \times X_b + r2 \times k_1 \times \Delta X)) \tag{3.3.28}$$

$$k_3 = \frac{1}{2\Delta X}(r(X_w + r1 \times \frac{k_2}{2} \times \Delta X) - (u \times X_b + r2 \times \frac{k_2}{2} \times \Delta X)) \tag{3.3.29}$$

$$k_4 = \frac{1}{2\Delta X}(r(X_w + r1 \times k_3 \times \Delta X) - (u \times X_b + r2 \times k_3 \times \Delta X)) \tag{3.3.30}$$

Where r, r1 and r2: random numbers [0, 1].

- **Position Update of Population**

Population position is updated through exploration and exploitation according to Eq. (3.3.31).

$$X_{n+1} = X_c + SF + SM + \mu + X_s \tag{3.3.31}$$

For

$$\mu = 0.5 + 0.1 \times rn \tag{3.3.32}$$

Where μ: a random number; rn: random number with a normal distribution; X_S

and X_c are derived from Eq. (3.3.33) to (3.3.35).

$$X_s = rn(X_m - X_c) \tag{3.3.33}$$

$$X_c = rX_n + (1 - r)X_r \tag{3.3.34}$$

$$X_m = rX_{best} + (1 - r)X_{besti} \tag{3.3.35}$$

SF: adaptive factor formulated as Eq. (3.3.36).

$$SF = 2(0.5 - r) \times f \tag{3.3.36}$$

In which

$$f = a^{(-b \times r\frac{t}{T})} \tag{3.3.37}$$

Where a and b: constant numbers; t: current iteration; T: total iterations.

- **Enhanced Solution Quality (ESQ)**

The application of ESQ is for upgrading the status of solutions along with the elimination of local optima. A better position of each solution is ensured by applying ESQ in RUN algorithm. It compares the fitness function values and selects the best from them. The following scheme is executed to create the solution (X_{new2}) by using the ESQ, that is presented as Eq. (3.3.38).

$$X_{new2} = X_{new1} + r.w|(X_{new1} - X_{avg}) + rn| \tag{3.3.38}$$

For,

$$w = rand(0, 2)^{(c\frac{t}{T})} \tag{3.3.39}$$

$$X_{avg} = \frac{X_{r1} + X_{r2} + X_{r3}}{3} \tag{3.3.40}$$

$$X_{new1} = \beta \times X_{avg} + (1 - \beta) \times X_{best} \tag{3.3.41}$$

Where β, r1, r2 and r3: random numbers [0, 1]; c: random number (5$\times$rand);

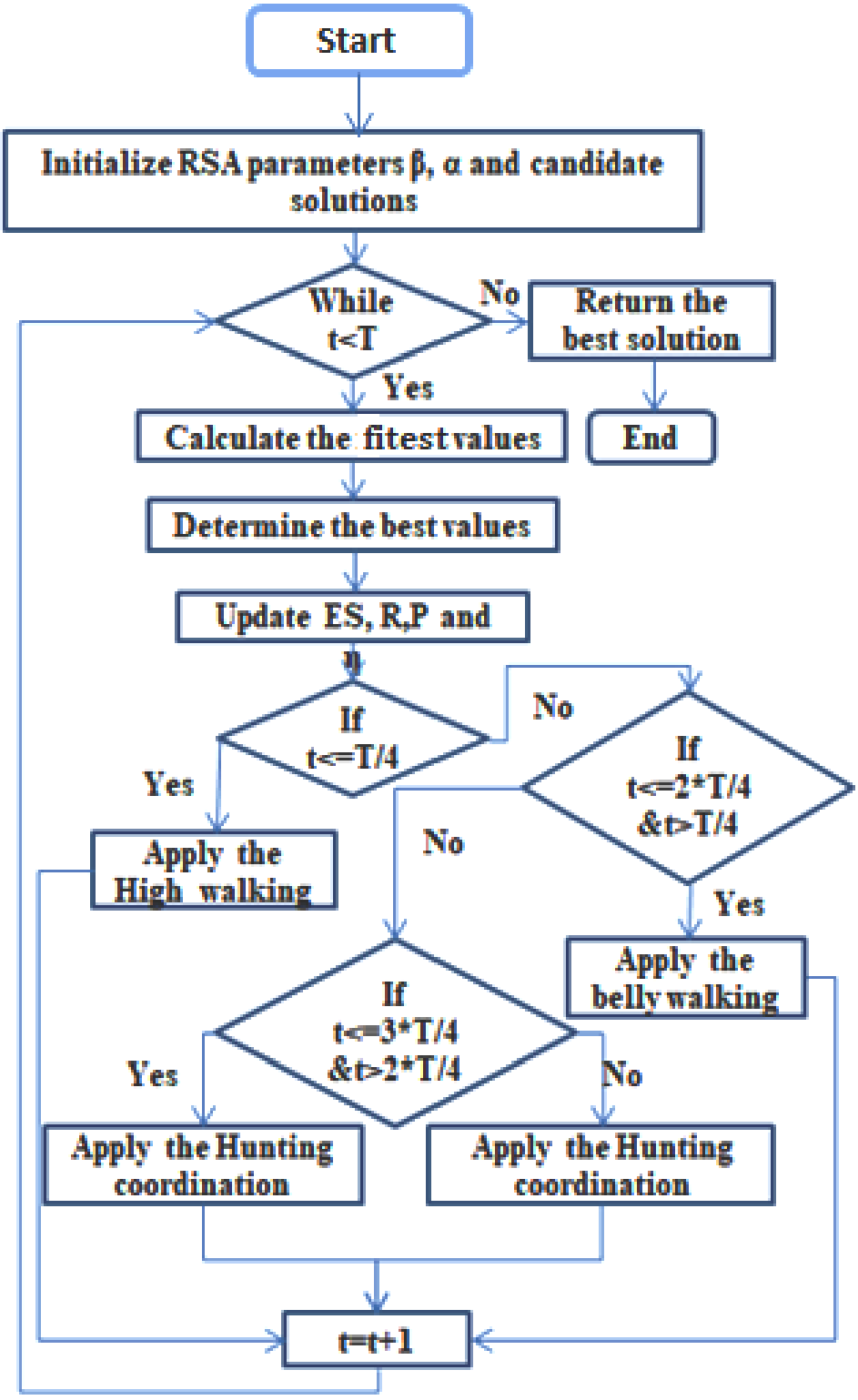

Figure 3.4: Flowchart of RSA Algorithm

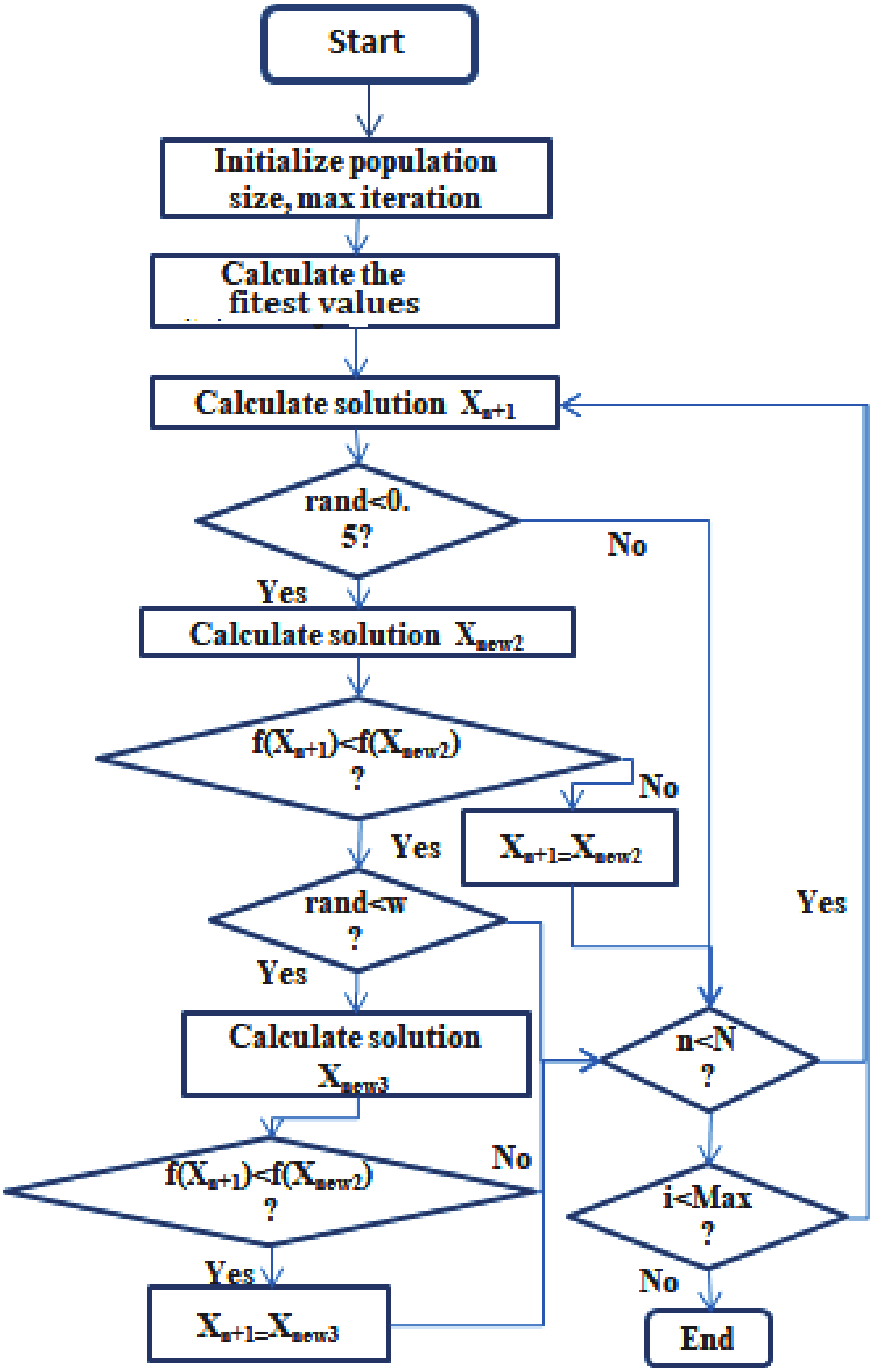

Figure 3.5: Flowchart of RUN Algorithm

Chapter 4

Standalone MG with HRES

The initial case study being presented in this research has the objective to determine an economic power supply for un-electrified remote region, Jarre Village. The economic analysis compares grid extension costs against the costs related to installation of a standalone system. The optimal combination of HRES components is determined through different meta-heuristic methods. The optimal solution is recommended considering economic cost, GHG emission and reliability as performance parameters.

4.1 Grid Extension for Remote Area Electrification

Electricity is inaccessible in rural areas, particularly for citizens of developing countries. Grid extensions or standalone systems are employed to supply power to such villages. Grid extension connects non-electrified regions to the existing grid network through the installation of transmission lines. The cost of line extension, geographical location or distance, political issues and load level determine the viability of grid extension. Grid extension for rural areas is determined by Break-Even Distance (BED). BED is the distance at which the total NPC of grid extension and installing a stand-alone system are equal [89]. BED gives the distance for which extending the grid would be economically feasible. For the remote regions that lie at a distance greater than BED, a standalone

system is preferable. BED is calculated using Eq. (4.1.1).

$$BED = \frac{C_{NPC} \times (\frac{i(1+i)^n}{(1+i)^n-1}) - C_p.E_l}{C_{cap_G} \times (\frac{i(1+i)^n}{(1+i)^n-1}) + C_{om_G}} \tag{4.1.1}$$

Where C_{NPC}: total NPC of power system ($); E_l: total annual electrical demand (kWh/yr); C_p: cost of power from the grid ($/kWh); C_{om_G}: O & M cost of grid extension ($/yr/km); C_{cap_G}: capital cost of grid extension ($/km); i: interest rate per year (%); n: project life time (yr).

The construction cost of a transmission line varies depending on the types of equipment and technology used for construction. In Sub-Saharan Africa, the average grid extension cost with medium-voltage line construction is estimated to be $20,000 to $25,000 /km [90]. The cost of grid extension for medium voltage is taken from the Ethiopian Electric Utility and is listed in Table 4.1.

Jarre village is located at 9.6908738° N, 42.7539328° E. The village site is shown in Figure 4.1. The Jarre village is 50 km away from the nearest substation located at Jigjiga. The village has approximately 3173 kWh of potential daily load.

Table 4.1: Costing for Grid Extension [91]

Types of Costs	**Costs** ($/km)
Material cost	16091.62
Labor cost	2237.14
Overhead cost	808.97
Total cost	19137.74
Reserve cost (20% of total cost)	3827.55
Grand total	**22,965.28**

To determine the economic feasibility of the modelled system, Hybrid Optimization of Multiple Energy Resources (HOMER) software is applied. HOMER software is used to design and evaluate cost-effective and reliable systems for

Figure 4.1: Geographical Location of Jarre Village

both off-grid and grid-connected power systems [92]. The analysis shows that the system's BED is achieved at a distance of 31.6 km, i.e., grid extension is economical up to this radius, whereas, Jarre Village is outside of this range. Figure 4.2 depicts the costs for extending the grid and installing a standalone system for Jarre village. So, a standalone MG is more economical than a grid extension.

4.2 Standalone HRES MG : Jarre Village (Part I)

The standalone MG is economically feasible for this case study, as stated in section 4.1. According to the geographical analysis, Jarre village has plenty of wind and solar potential. A standalone HRES MG consisting of solar PV, WT and BS is therefore considered to supply the required load. The proposed HRES MG model for electrifying Jarre village is shown in Figure 4.3. BS is used to improve the reliability of the modelled systems. Each component of

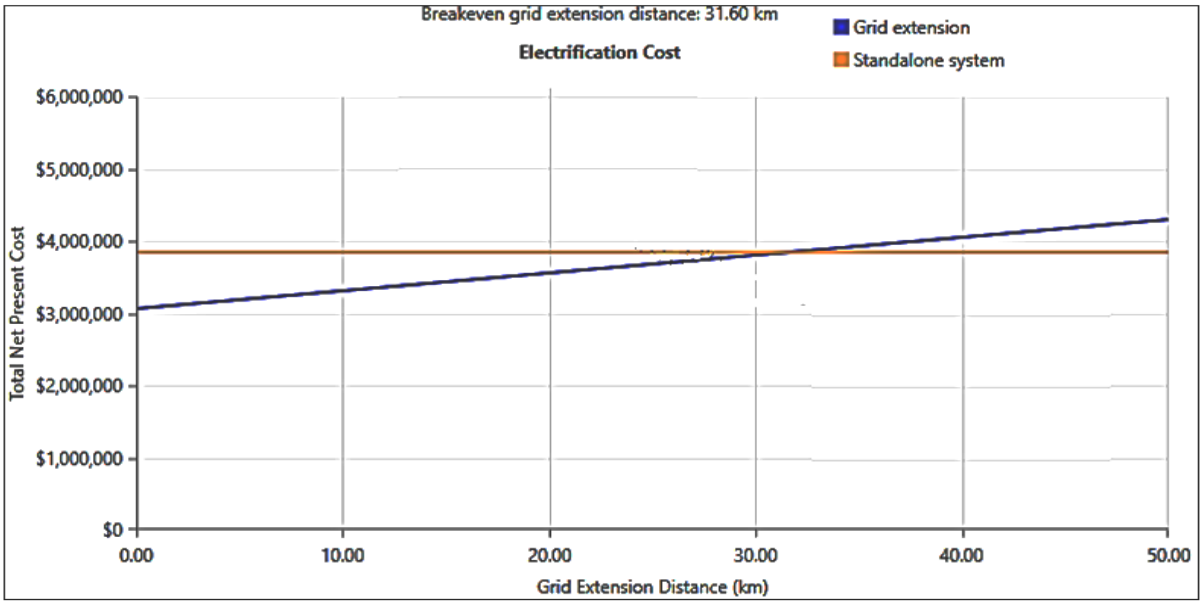

Figure 4.2: Grid Extension Feasibility Result for BED Analysis

standalone MG has different characteristics. Hybridizing these components reduces drawbacks that are present individually and helps improve power system performance.

The combination of HRES components is evaluated through different performance parameters. Economical cost and reliability are the parameters that are considered in this case study. To determine the optimal combination of HRES components, PSO is applied. The algorithm is implemented in MATLAB.

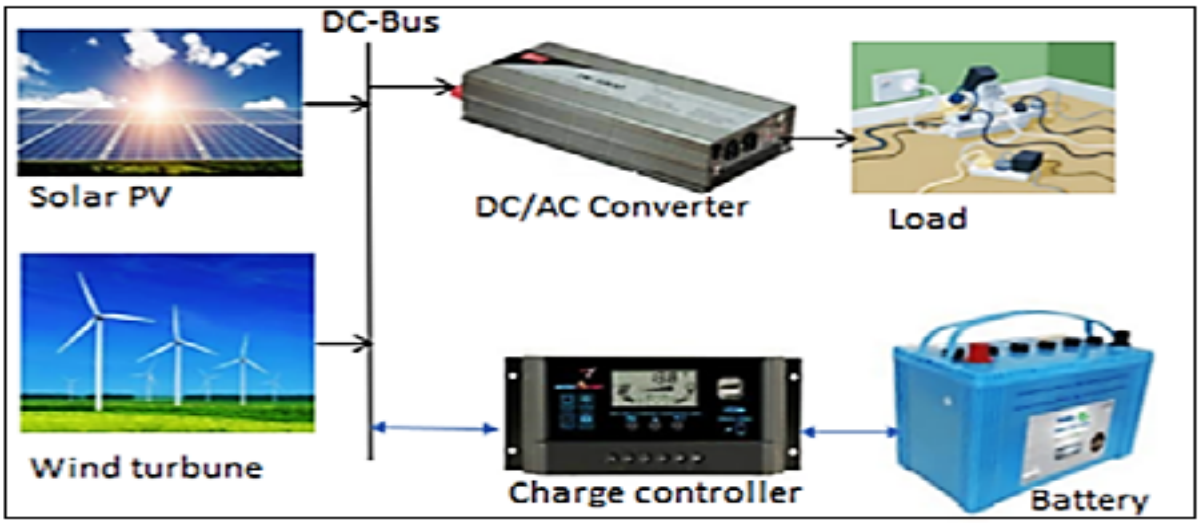

Figure 4.3: Standalone HRES MG Model for Jarre Village

4.2.1 Load Profile and Resource Potential of Jarre Village

Village Load Profile

The proposed research work is carried out to obtain an optimal solution to provide electricity to Jarre village. At this site, there are about 150 households. Lighting, television, radio, mobile chargers, refrigerators, ventilation, cooking stoves, etc., are the common loads that can be used by these households. Community loads, such as the school, health post, flour mill, water pump, etc., are taken into account when estimating the total load and its pattern. The Jarre daily average load is estimated to be 3173 kWh/day. The maximum and minimum demand is 285.5 kW and 8.25 kW, respectively. The estimated daily load curve of Jarre Village is shown in Figure 4.4.

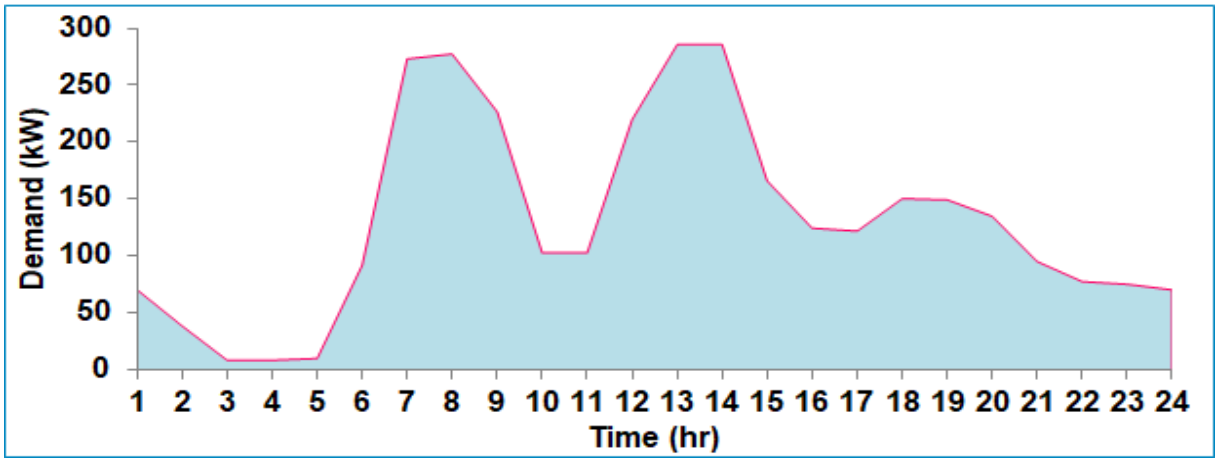

Figure 4.4: Daily Load Profile of Jarre Village

Renewable Energy Sources

Solar and Wind are considered as energy sources for the proposed standalone MG at Jarre. The months which have minimum generation capacity for these resources are considered. This selection is preferred to contemplate the worst case scenario for generation. April and July months have a minimum average wind

speed and solar irradiation, respectively, as seen in Figure 4.5. Wind and solar resource availability patterns are complementary to each other at the selected site. This further enhances the reliability of the proposed model. The daily av-

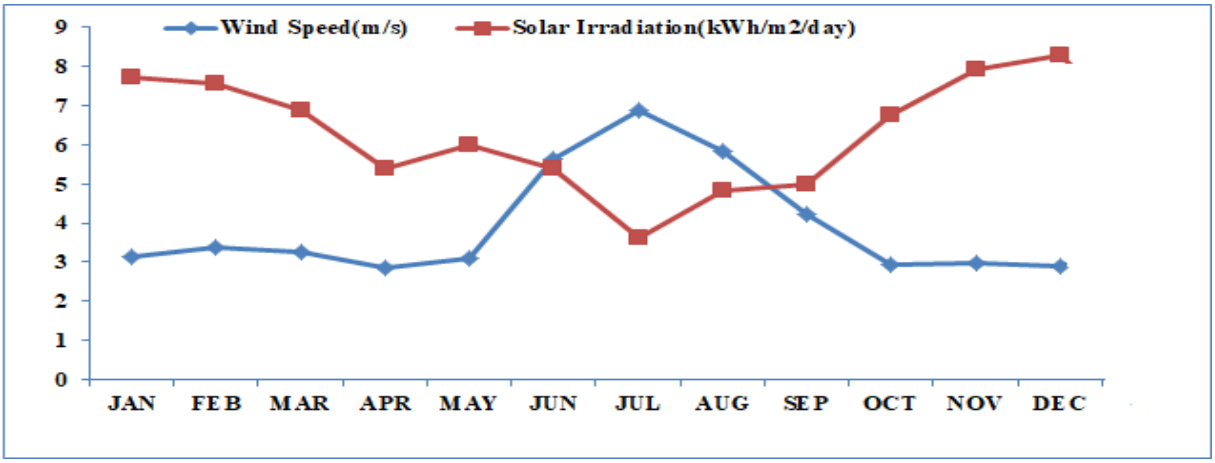

Figure 4.5: Average Monthly Wind and Solar Profile, @ 2020-2021 [93]

erage, wind speed and solar irradiation, of Jarre village are shown in Figure 4.6. The resource data is taken from the NASA database [93]. The generation potential of Solar PV and Wind for the input data is determined using Eq. (3.1.1) and (3.1.2), respectively. The daily electrical power generation pattern from a single unit of Solar PV and Wind is shown in Figure 4.7. The costs of HRES components used in MG are listed in Table 4.2.

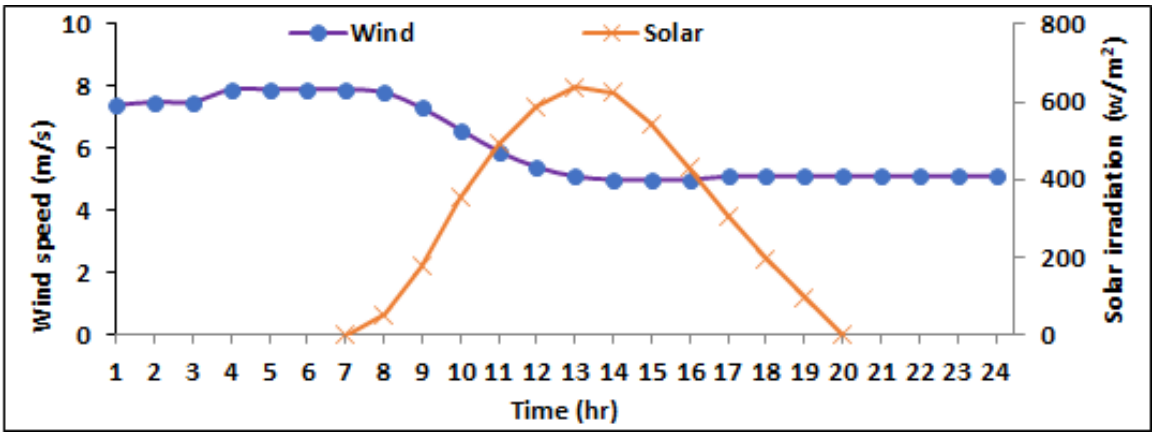

Figure 4.6: Daily Solar and Wind Pattern of Jarre Village

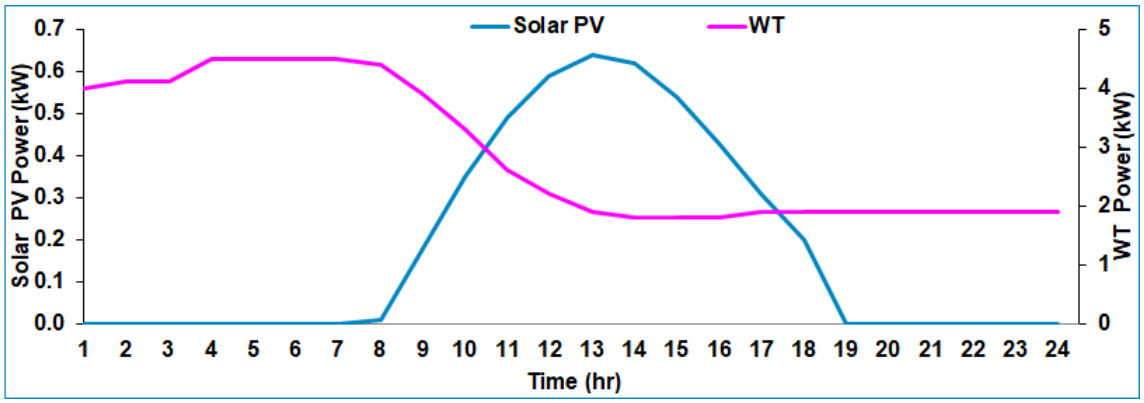

Figure 4.7: Daily Power Generation per unit of Wind and Solar: Jarre Village

Table 4.2: Costs of Standalone HRES MG Components

Component	**Rating**	**C$_c$ ($/kW)**	**C$_r$ ($/kW)**	**C$_{OM}$ ($/kW/yr)**	**Life Span (yr)**
Solar PV	1 kW	1000	0	5	20
Wind turbine	10 kW	1500	0	9	20
Battery	100 Ah	150	150	10	5
Converter	300 kW	250	250	2	10

4.2.2 Problem Formulation : Standalone MG

The objectives of modelling a standalone MG are economic cost and reliability. To minimize the system cost, TAC and COE are utilized as given in Eq. (4.2.1). The reliability is considered to be maximum for the proposed MG and is therefore considered as a constraint along with other constraints as listed in Eq. (4.2.2) to (4.2.6).

$$F = Minimize \quad (TAC, COE) \tag{4.2.1}$$

Subject to

$$LPSP = 0 \tag{4.2.2}$$

$$P_d \leq N_{PV} P_{PV} + N_{WT} P_{WT} \pm N_{BS} P_{BS} \tag{4.2.3}$$

$$0 \leq N_{PV} P_{PV} \leq P_{PV} max \tag{4.2.4}$$

$$0 \leq N_{WT} P_{WT} \leq P_{WT} max \tag{4.2.5}$$

$$SoC_{min} \leq SoC_t \leq SoC_{max} \tag{4.2.6}$$

where $P_{PV}max$, $P_{WT}max$ and P_{BS}: maximum power limit for solar PV (kW), wind turbines (kW) and battery, respectively; SoC_{min} and SoC_{max}: minimum and maximum allowable BS SoC, respectively; N_{PV}, N_{WT} and N_{BS}: number of solar PV panels, WT and BS packs, respectively.

In Eq. (4.2.2), LPSP is considered to be zero, i.e., the supply system should be 100% available. The $\pm$ sign in Eq. (4.2.3) is to show the battery is charging or discharging in accordance with the balance of the load and supply. The resources should be able to meet the load at all times, so the combination of supply from HRES should be greater than the demand.

4.2.3 Methodology

The methodology used to determine the size of HRES components is shown in Figure 4.8.

The resources and load data are collected and organized in accordance with the specifications. In this study, a daily, i.e., 24-hour, data set is evaluated for analysis. Initially, the population is produced at random within the search space. A meta-heuristic optimization method, to achieve the optimum solution, is applied. The feasibility of the generated random variables within the predefined constraints is tested. In these case studies, feasibility of a solution is important.

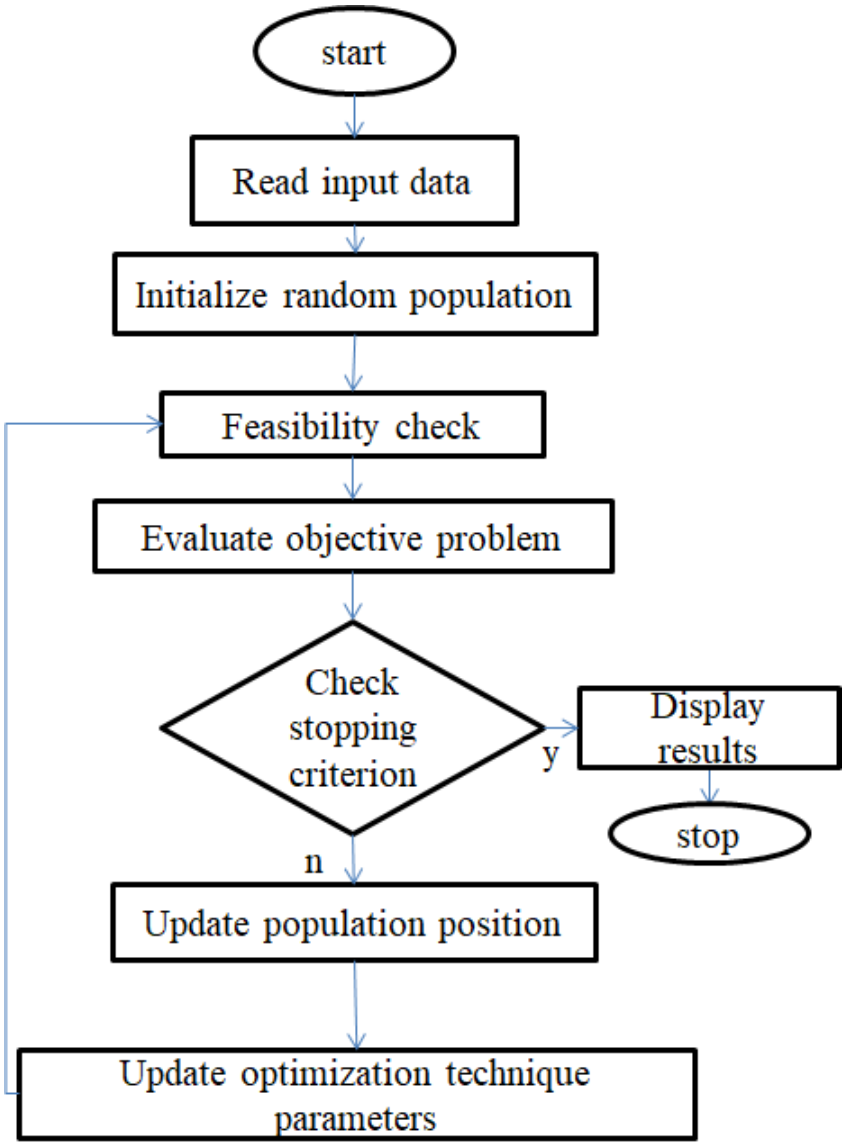

Figure 4.8: Methodology for HRES Optimization

The solution should satisfy all constraints to make it acceptable. In the optimization problems discussed, many of the candidate solutions may be present within the search space but are not feasible. Thus, the optimization problems are more of a feasibility problem rather than optimization problem. The analysis is carried on by updating the population until the stopping condition is reached. The best solution with optimal component size is taken as the output of the algorithm. The simulation is repeated several times and the best of the results is chosen as the solution. The component specifications used for standalone HRES

modelling are listed in Table 4.3.

Table 4.3: Specifications of Standalone HRES MG

Solar PV	
Solar Panel Rating	250 W
Operating Voltage	24 V
Maximum power voltage, V_{mp}	39.60 V
Open Circuit Voltage, V_{oc}	47.52 V
Short circuit current, I_{sc}	6.48 A
Maximum Power Current, I_{mp}	6.36 A
Cell efficiency	23.0 %
Wind Turbine	
Rated power	10 kW
Cut in speed	2 m/s
Rated wind speed	14 m/s
cut-out speed	25 m/s
Battery Storage	
Rated capacity	100 Ah
SoC_{min}	20 %
SoC_{max}	90 %
Charge and discharge efficiency	90%
Voltage	12V
Converter(DC/AC)	
Input Data(DC)	
Rated DC Voltage	600 V
Rated DC Current	500 A
Nominal AC Power	300 kW
Rated AC Voltage	380 V
Rated AC Current	454.5 A
Frequency	50 Hz
Max. Efficiency	93%

4.2.4 Result and Discussion

As illustrated in subsection 4.2.3, the optimization of HRES MG component sizing is calculated according to the objective and constraints. The maximum

limits of the components are determined by considering the daily peak load. The component size is taken into account as a variable for HRES analysis. The economic cost associated with TAC and COE is considered as an objective function.

The optimization method uses a population size of 300 and an iteration count of 500. The simulation is executed 40 times to obtain the best result. The feasibility of all solutions is checked in each execution. The randomly generated population and its solution are depicted in Table 4.4 to give an idea of the solutions being categorised as feasible or not feasible. It can be observed that about 40% of the solutions are not feasible. In this case study, a solution not satisfying LPSP=0 shall be categorised as ”Not Feasible”.

Table 4.4: Feasibility of Solutions within a Random Population

$\mathbf{N}_{PV}$	$\mathbf{N}_{WT}$	$\mathbf{N}_{BS}$	**TAC ($/yr)**	**Feasibility**
138	45	44	9673781	Not Feasible
328	66	92	149963	Feasible
175	116	237	218127	Feasible
353	66	186	157359	Feasible
29	94	138	16509424	Not Feasible
337	98	170	203442	Feasible
104	114	100	200881	Feasible
120	34	165	8459530	Not Feasible
284	37	18	9776323	Not Feasible
186	195	224	338297	Feasible

The analysis presents the results for battery characteristics as: ideal and practical. For case 1 (ideal), the system modelling is evaluated without considering SoC limits (SoC_{min} = 0, SoC_{max} = 100) and charging and discharging efficiency. Case 2 (practical) considers the BS, SoC_{min} and SoC_{max} as 20% and 90%, respectively. The charging and discharging BS efficiency is considered to be 90%. The optimal solution for ideal and practical cases is summarized in Table 4.5. The TAC for cases 1 and 2 is $103816.2 /yr and $119991.2 /yr, respectively.

Table 4.5: Comparison of Ideal and Practical HRES Combinations

System	N_{pv}	N_{WT}	N_{BS}	TAC ($/yr)	COE ($/kWh)	Excess Energy (kWh/day)
Ideal	260	35	235	103816.2	0.090	400
Practical	247	46	250	119991.2	0.104	677

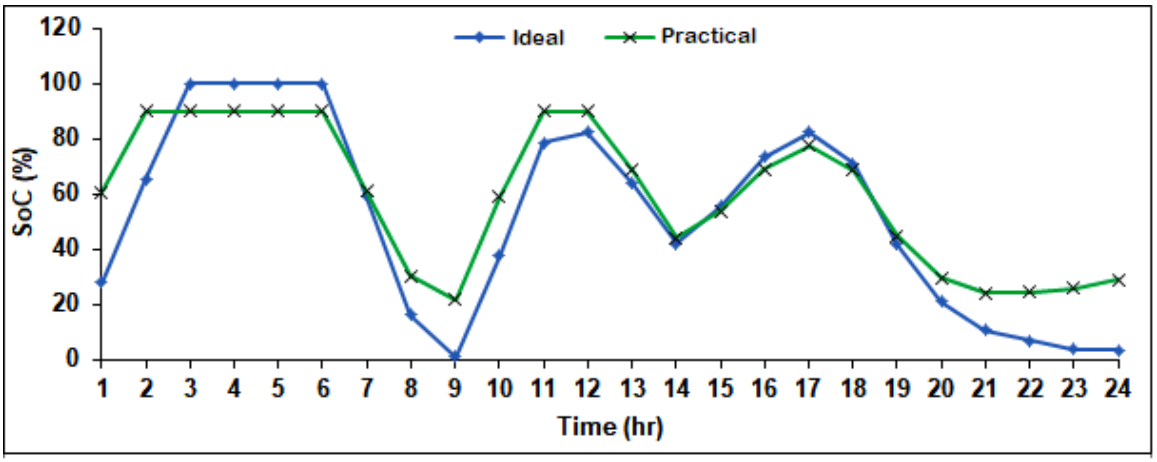

Figure 4.9: Battery Status for Ideal and Practical Cases

The numbers of PV, WT and BS are 260, 35 and 235 for case 1 and 247, 46 and 250 for case 2. The BS status for a day is plotted in Figure 4.9, for the optimal solution of ideal and practical case. The daily generation pattern of HRES components is plotted in Figure 4.10.

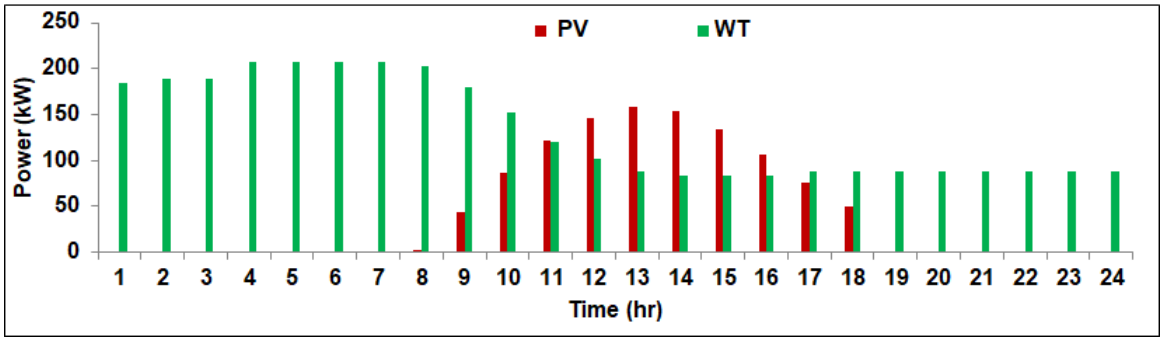

Figure 4.10: Daily Power Generation from Solar PV and WT plants

The daily power supply and demand profile are presented in Figure 4.11. The BS acts as a source or load as can be observed from the figure. The negative value of BS is to signify the charging state and the positive value is used to show

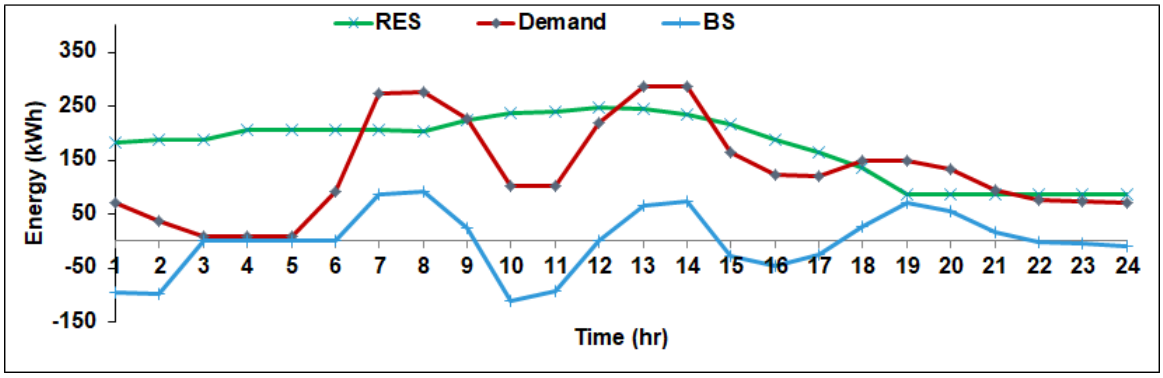

Figure 4.11: Daily Power Supply and Demand Profile

discharging. The state of BS varies considering the supply and demand balance at a given hour. The observation from the graph is that, for the specified time period, there is no instance where the load exceeds the supply (i.e., LPSP=0).

4.3 Standalone HRES MG : Jarre Village (Part II)

In this section, the optimal stand-alone MG modelling for Jarre village is analyzed through multiple meta-heuristic methods while including GHG Emissions in the objective function. The cost of GHG emissions (CO_2) is included along with TAC in the objective. This case study takes into account all of the input data provided in Section 4.2.

4.3.1 Problem Formulation

The new objective function is represented as TAC_T ($/yr), which includes component cost and penalty cost due to CO_2 emissions as formulated in Eq. (4.3.1). The constraints listed in the Section 4.2 are considered in this case as well.

$$F = Minimize(TAC_T) \tag{4.3.1}$$

$$For \qquad TAC_T = TAC_c + TCEP_c \tag{4.3.2}$$

Where TAC_c: total annual components cost of HRES ($/yr) (Eq. (3.2.3); $TCEP_c$: total annual penalty cost due to CO_2 emission ($/yr) (Eq. (3.2.6).

The life cycle emission of CO_2, (C_k=0.075 $/kg) produced from different HRES MG components is tabulated in Table 4.6.

Table 4.6: Life Cycle CO_2 Emission of HRES Components [17, 94, 95]

Component	**Life Cycle Emission (kg CO_2/kWh)**
Hydro Power	0.024-0.027
Wind Turbine	0.011
Solar PV	0.045
Biomass	0.6
Battery	0.0402
Converters	0.0047

4.3.2 Result and Discussion

Evolutionary Optimization Techniques of Particle Swarm Optimization (PSO), Differential Evolution (DE), Manta Ray Foraging Optimization (MRFO), Shuffled Frog-Leaping Algorithm (SFLA), Reptile Search Algorithms (RSA) and RUNge Kutta optimizer (RUN) are used to obtain the optimal solution. The reasons for selecting these methods are their flexibility and performance, as recommended in different publications. The population size and the number of iterations for all optimization methods are set to 300 and 500, respectively. All the optimization methods are implemented in MATLAB. The techniques are executed 40 times to find the best solution. The optimum solution of each method are compared with each other.

The TAC_T values for PSO, DE, MRFO, SFLA, RSA and RUN are $135293.1

/yr, $137981.9 /yr, $134275.8 /yr, $135029.2 /yr, $135358.8 /yr and $134275.8 /yr, respectively, as shown in Table 4.7. The daily excess energy is the energy that can be produced by HRES components but is curtailed due to the absence of demand. The daily excess energy obtained in MRFO and RUN is 677 kWh, which is the minimum as compared to others. Even though the TAC_T and Excess Energy results for MRFO and RUN are similar, MRFO requires lesser run time (MRFO - 42 sec and RUN - 67 sec). The optimal component units obtained from the analysis are: 247 of PV panels, 46 of WT and 249 of BS packs. The

Table 4.7: Comparison of Various Optimization Techniques

Methods	N_{PV}	N_{WT}	N_{BT}	**TAC ($/yr)**	**Excess Energy (kWh)**	**Run time (sec)**
PSO	242	47	249	135293.1	719	31
DE	227	52	204	137981.9	971	19
MRFO	247	46	249	134275.8	677	42
SFLA	243	48	224	135029.2	786	12
RSA	243	49	208	135358.8	837	33
RUN	247	46	249	134275.8	677	67

TAC and excess energy of different methods are compared in Figures 4.12 and 4.13. The daily energy share from WT, solar PV and BS is shown in Figure

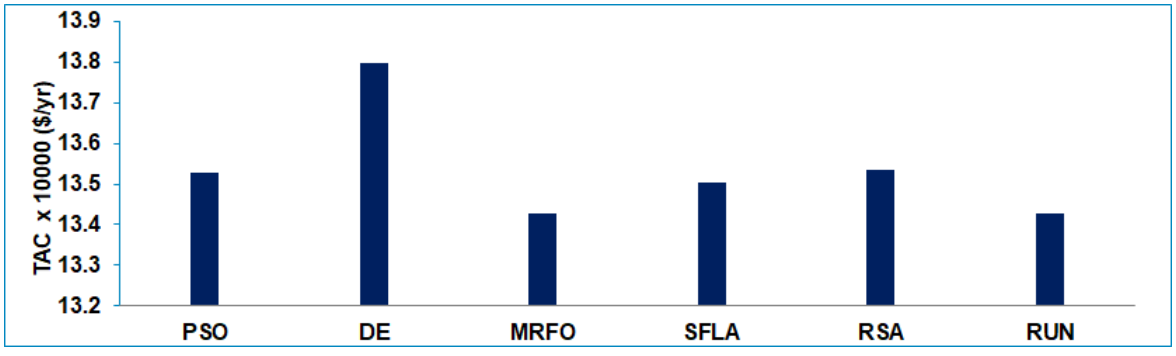

Figure 4.12: Economic Cost Comparison for Different Optimization Methods

4.14. The daily RES Generation, Demand and BS pattern is plotted in Figure 4.15. The daily supply and demand patterns are shown in Figure 4.16.

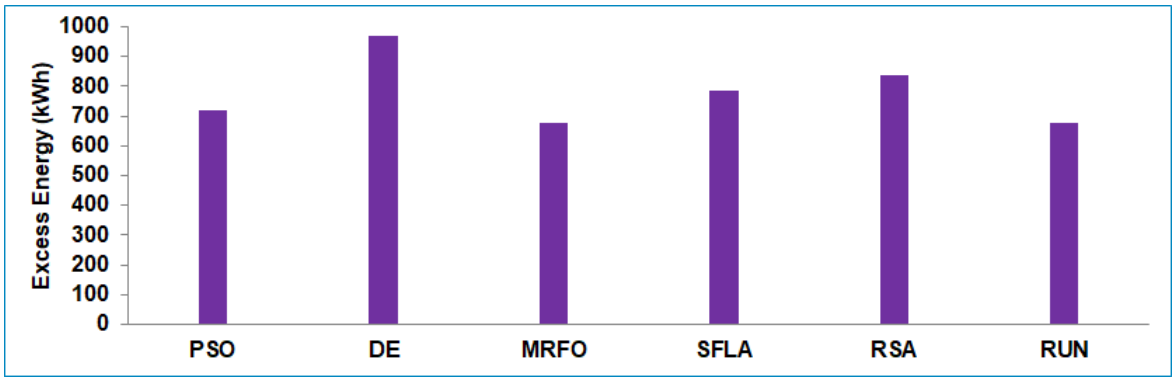

Figure 4.13: Excess Energy Comparison for Different Optimization Methods

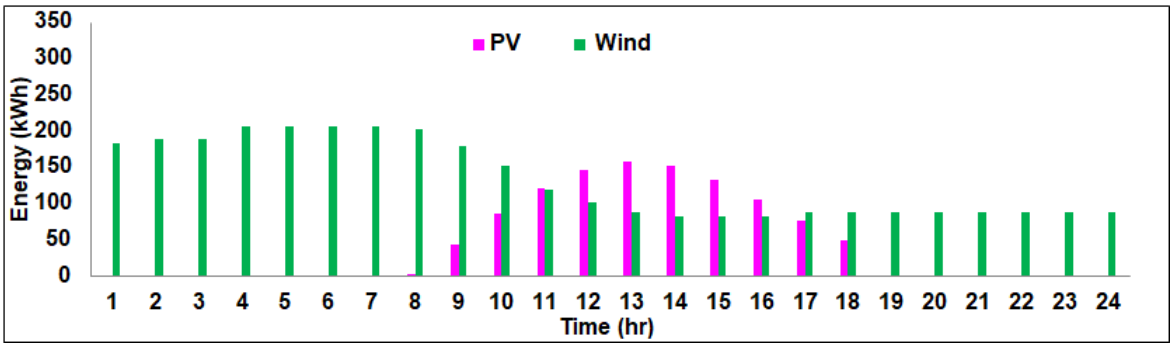

Figure 4.14: Daily Energy Pattern of RES for Optimal Solution

4.4 Summary

A comparison of grid extension and standalone MG systems was performed for Jarre village electrification. The analysis results confirm that, economically, the standalone HRES is more feasible than grid extension. An optimal combination of RES and BS is modeled to act as a standalone HRES MG. The first scenario considered economic cost as an optimization problem and reliability as a constraint. The PSO algorithm is applied to obtain the optimal units of HRES components. TAC and COE for the fittest solution, are \$119991.2 /yr and 0.104 \$/kWh, respectively. The second scenario included the GHG emissions, converting CO_2 emissions from each component to cost values. Multiple optimization techniques are implemented and compared. MRFO algorithm is found to deliver the optimal results in lesser time. The optimal solution has

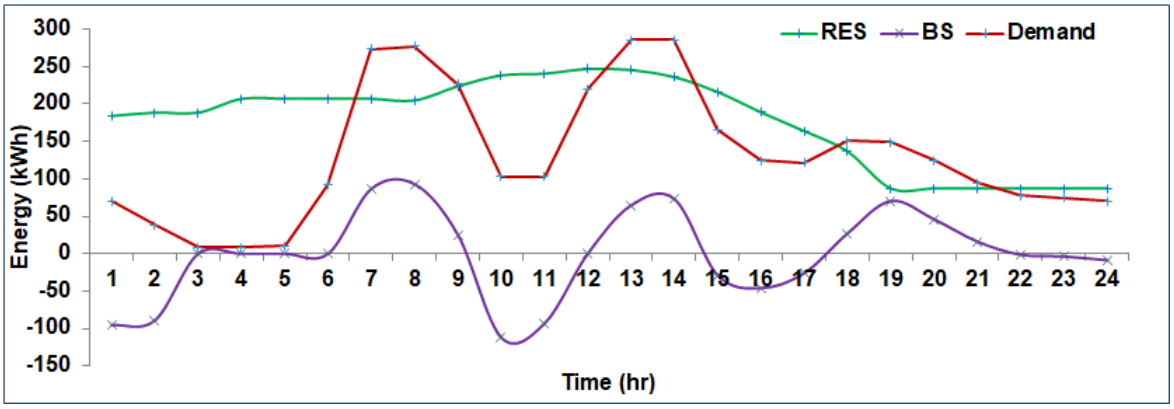

Figure 4.15: Daily Power Supply and Demand for Optimal HRES MG

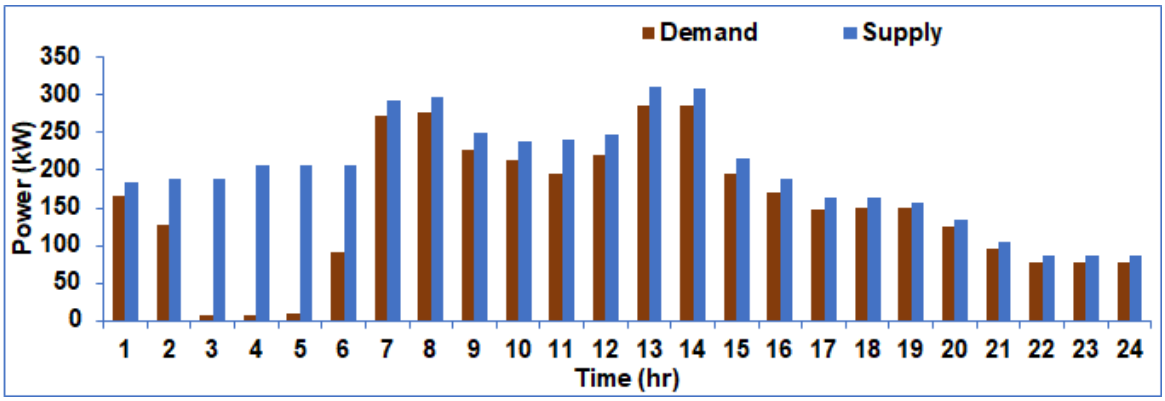

Figure 4.16: Demand and Supply Pattern for Optimal HRES MG

TAC and COE as $134275.8 /kWh and 0.116 $/kWh, respectively. The application of HRES to form a standalone MG provides reliability, reduces economic costs and lowers GHG emissions of the system.

Chapter 5

Grid Performance Improvement with HRES

This chapter discusses the use of HRES as DG to reduce power loss and improve the voltage profile of power systems. The economic benefits of implementing HRES as DG are investigated. The impact of subsidies on the economic benefit of grid-connected HRES MG is also assessed.

5.1 Power System Performance Assessment with DG Integration

The performance of a power system network is evaluated through parameters such as power quality, economic benefits, reliability, GHG emissions etc. Introducing DG into the grid can help improve these evaluation parameters [96, 97]. The placement and sizing of DG in the grid should be performed in an optimal way to derive maximum benefits. This optimization problem can be solved through meta-heuristic algorithms, like MRFO. The combination of solar and wind is considered to operate as DG. In this case study, the primary objective is to maximize economic benefit by incorporating HRES as DG while minimizing power loss and improving the voltage profile of the system.

The methodology applied in this case study are: (i) comparing the perfor-

mance of different evolutionary optimization techniques for optimal placement and sizing of DG in the standard IEEE 33-bus system, (ii) investigate DG placement and sizing for the practical case, (iii) optimize solar and wind as constituents of DG and (iv) analyze the economic benefit of HRES integration into the power system.

The site selected in this case study is the Ethiopian Electric Power (EEP). The reason for selecting this site is poor power quality. EEP is characterized by frequent and high-duration power interruptions, as summarized in Table 5.1. The eastern region of EEP had the most power outages in comparison to other regions listed Table 5.1. The eastern region of EEP is also characterized by long

Table 5.1: Power Outages Data for EEP @2021 [98]

Region	**Substation**	**Outage duration (hr/yr)**	**Number of outages (fr/yr)**
Addis Ababa	26	1076	160
Central	24	2435	156
East	**12**	**2268**	**177**
North East	10	177	155
North West	7	1735	173
North	11	879	111
South West	11	1427	43
South	20	486	147
West	10	288	85

transmission lines, a lack of generation facilities near the load centers and large load variations. In this region, for a 230 kV transmission line, the minimum voltage rating was recorded at 210 kV, on October 23, 2020, whereas the maximum value of 241 kV was measured on September 15, 2020. The minimum and maximum measured voltages for a period of six months are plotted in Figure 5.1. The minimum voltage is 8.6% lesser than the base voltage, which is quite more than the permissible limit of 5%. The data presented in Table 5.1 and Figure 5.1

clearly indicates that the power system is having poor performance and needs to be improvised.

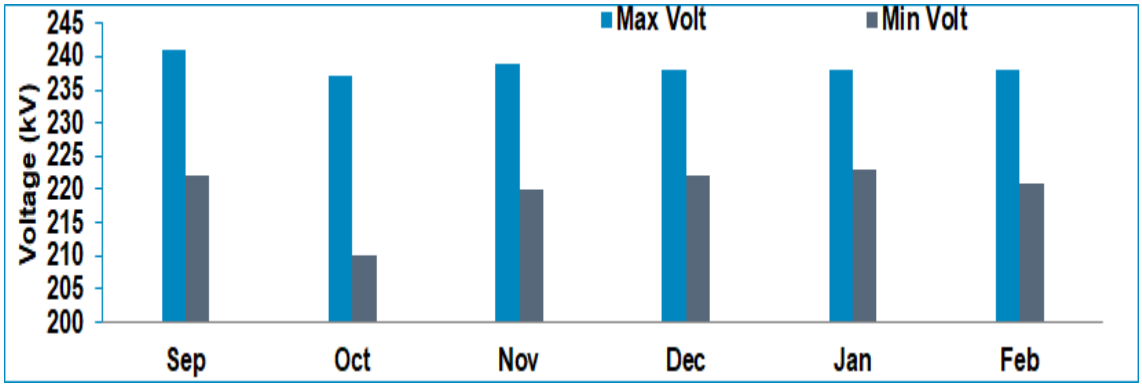

Figure 5.1: Minimum and Maximum Voltage Profile of Eastern Region of EEP [99]

5.1.1 Problem Formulation for DG Placement and Sizing

The objective of this case study is to minimize the total Power Loss (P_L) of an electric power network, using Eq. (5.1.1). The constraints considered are the bus voltage limits as given in 5.1.2.

$$F_1 = Minimize\ P_L = \sum_{j=1}^{n} P_{l(j)} \tag{5.1.1}$$

Such that

$$V_{min} \leq V_b \leq V_{max} \tag{5.1.2}$$

Where n: number of branches in the network; V_b: voltage value on bus 'b' (V); V_{min} and V_{max}: minimum and maximum permissible bus voltage (0.95 pu and 1.05 pu), respectively [100]; $P_{l(j)}$: power loss in branch 'j' which is formulated in Eq. (5.1.3)

$$P_{l(j)} = R_j \left(\frac{P_b^2 + Q_b^2}{V_b^2} \right) \tag{5.1.3}$$

Where P_b and Q_b: active (MW) and reactive power (MVAr) flow from bus 'b' into branch 'j'; R_j: resistance of branch 'j' (Ω); X_j: reactance of branch 'j' (Ω).

The improvement in power system performance with DG integration can be evaluated through the Line Loss Reduction Index (LLRI) and Voltage Profile Improvement Index (VPII). The LLRI is used to determine the power loss reduction in the network and is formulated in Eq. (5.1.4).

$$LLRI = \frac{\mathrm{P_{LW/DG}}}{\mathrm{P_{LWO/DG}}} \tag{5.1.4}$$

Where $P_{LW/D}$ and $P_{LWO/D}$: real power losses with DG and without DG (MW) integration.

The result of LLRI is interpreted as follows:

If LLRI<1, DG reduces power loss

If LLRI=1, no change

If LLRI>1, DG is not beneficial.

VPII is utilized to assess the variation in voltage profile of buses due to DG integration and is formulated in Eq. (5.1.5).

$$VPII = \frac{VP_{W/DG}}{VP_{W0/DG}} \tag{5.1.5}$$

Where $VP_{W/DG}$ and $VP_{WO/DG}$: voltage profiles with and without DG, respectively, that is calculated using Eq. (5.1.6).

$$VP = \sum_{i=1}^{N} |VP_i| \tag{5.1.6}$$

Where VP_i: Voltage deviation from 1 pu on bus 'i' and is formulated in Eq.

(5.1.7).

$$VP_i = |V_i - V_{ref}| \tag{5.1.7}$$

Where V_i: voltage values on bus 'i' (pu); V_{ref}: reference voltage of the system (1.0 pu).

The significance of variation in VPII status is presented below:

If VPII < 1, DG improves the voltage profile

If VPII = 1, DG has no impact on voltage profile

If VPII > 1, DG is not beneficial.

5.1.2 Methodology

The methodology applied for DG sizing and placement is summarized in the flowchart of Figure 5.2. The input data, related to buses, branches and generators, is compiled in the simulation software. The load flow analysis is performed through MATPOWER / MATLAB [101].

The optimization method is applied to optimally place and size the HRES components in the system. Random solutions are generated within the search space. The objective of the optimization method is the reduction of power losses. However, violation of voltage limits adds penalty to the output of a solution, thus making it undesirable.

5.1.3 Optimal DG Placement and Sizing for IEEE 33 Bus System

For DG location and size, MRFO is implemented after comparing its performance against other optimization techniques. MRFO is compared to other meta-heuristic methods for the standard IEEE 33-bus system. The performance of MRFO is compared with Multi-Objective Whale Optimization Algorithm

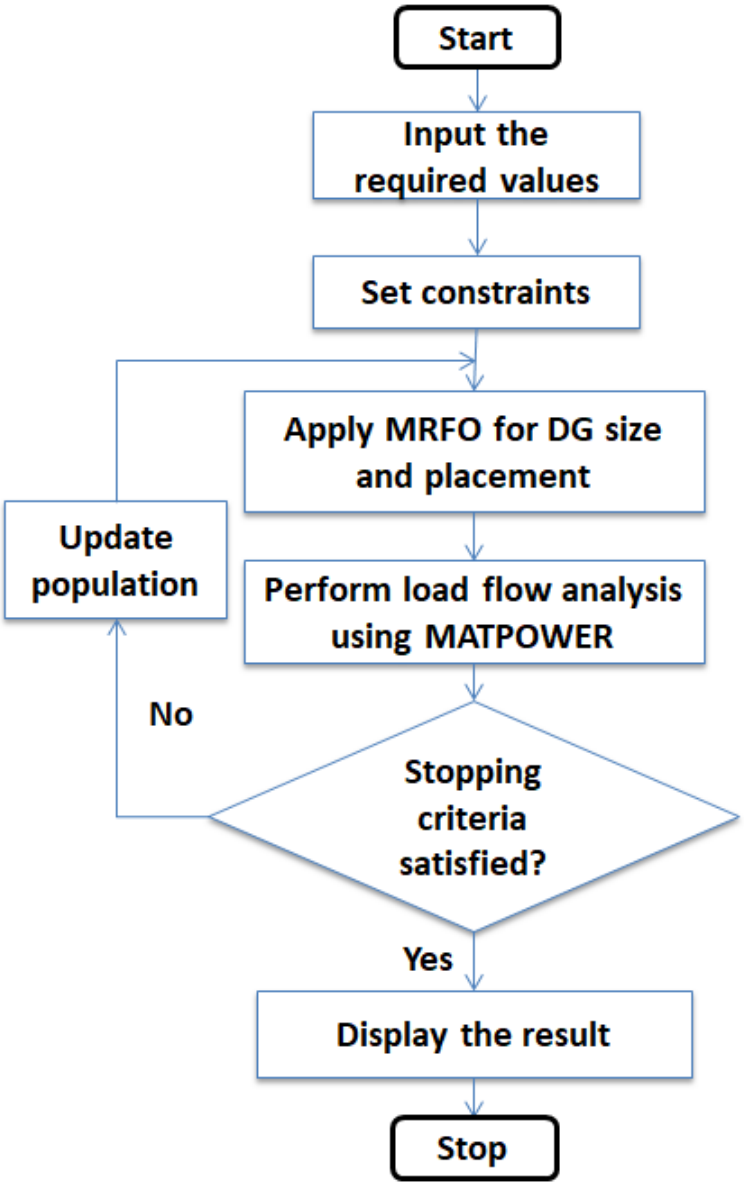

Figure 5.2: Methodology for Optimal Placement and Sizing of DG

(MOWOA), Multi-Objective Particle Swarm Optimization (MOPSO), Simulated Annealing (SA) and Krill Herding Algorithm (KHA). Power loss and voltage profile are considered when comparing these methods.

Authors in [102] have applied MOWOA and MOPSO to get the fittest solution. A power loss of 79.2 kW is recorded through MOWOA with a DG size of 1021.6 kW, 1200 kW and 1200 kW at bus numbers 14, 24 and 31, respectively. On the other hand, with MOPSO, the minimum power loss is obtained as 83.09 kW and DGs with a size of 1200 kW, 949.8 kW and 1142.7 kW are

placed on buses 12, 25 and 33, respectively. In [12] and [103], the authors recommend KHA and SA, respectively, for obtaining the optimal solution for the same problem. The power loss observed is 75.412 kW in [12] with a DG size of 810.7 kW, 836.8 kW and 841 kW on bus numbers 13, 25 and 30, respectively. In [103], the minimum power loss recorded was 82.03 kW with a DG size of 1112.4 kW, 487.4 kW and 867.9 kW at bus numbers 6, 18 and 30, respectively.

The power loss obtained by MRFO is 73.4 kW with a DG size of 1003.9 kW, 1007.4 kW and 1009.3 kW on buses 11, 24 and 29, respectively. The findings of the optimization methods investigated are summarized in Table 5.2. The optimal solution of MRFO reduces the loss by 2.6%, 8%, 10% and 12.6% when compared to KHA, MOWOA, SA and MOPSO, respectively. Since MRFO produces better results than other techniques, it is being used to solve the real-world problem of the EEP, in this case study.

5.1.4 Optimal DG Placement and Sizing for EEP

As a case study, the eastern region of EEP is proposed to evaluate the impact of DG installation on the power system network. The network has 17 buses, 20 branches and 03 generators as sketched in Figure 5.3. The power generating stations located nearest to this region are at Koka and Melka-wakena (M wek) with a capacity of 43.5 MW and 153 MW, respectively. The main grid is connected through the Kaliti bus, which is considered a slack bus during the analysis.

The data required for executing the power flow for the proposed system is arranged in a proper format and fed to MATPOWER. The data related to buses, generators and branches are summarized in Appendix I, II and III.

Before the integration of DG, the highest power losses (i.e., top three) occur on branches: 3 (Koka to Hurso), 2 (Koka to M wek) and 20 (Kaliti to Koka) as

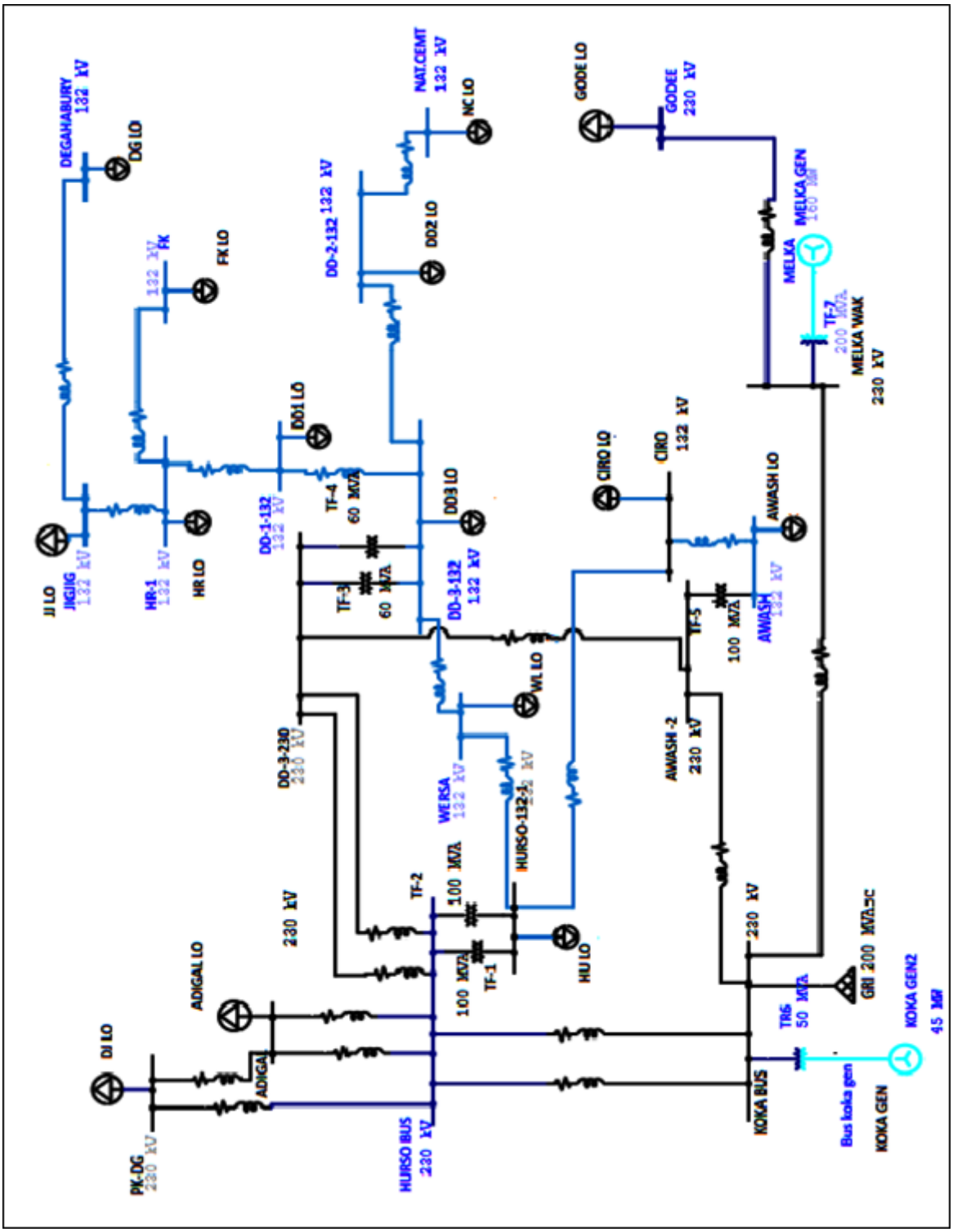

Figure 5.3: Eastern Region EEP Network Layout

Table 5.2: Comparison of Optimal DG Placement and Sizing for IEEE 33 Bus System

Technique	**DG Location**	**DG Size (kW)**	**P_L (kW)**	**Min V (pu) / bus no.**
MRFO	11 24 29	1003.9 1007.4 1009.3	73.4	0.966 / 33
MOWOA [102]	14 24 31	1021.6 1200 1200	79.72	0.984 / 30
MOPSO [102]	12 25 33	1200 949.8 1142.7	83.99	NA
KHA [12]	13 25 30	810.7 836.8 841	75.412	0.961 / 18
SA [103]	6 18 30	1112.4 487.4 867.9	82.03	0.9677 / 14

shown in Table 5.3. Lowest voltage (i.e., lowest three) is observed on bus 12 (Degahabor), bus 11 (Jigjiga) and bus 10 (Fike) as shown in Table 5.4.

During the investigation, the DG placement and sizing are applied to all buses except generator buses, Djibouti bus and Dire Dawa (DD) buses. The generator buses are located far away from the load area and hence adding DG will further increase line losses. The Djibouti bus is also located at the border of Ethiopia. The cost of land within the city of Dire Dawa is extremely high and there is insufficient space for HRES installation as well.

To explore the search space and find the optimal solution, MRFO uses 50 Manta rays (population) and 50 iterations. It is executed 30 times to obtain the optimal solution. The sample solutions generated randomly for a single itera-

Table 5.3: Network Power Loss Before DG Integration

Branch No	From Bus	To Bus	P_L (MW)
1	Koka	Awash	3.34
2	Koka	M wek	3.93
3	Koka	Hurso	10.56
4	Hurso	DD 3	0.09
5	Hurso	Adigal	0.72
6	Hurso	Djibouti	1.26
7	M wek	Gode	0.12
8	DD 3	DD 1	0.14
9	DD 3	DD 2	1.24
10	DD 2	Harar	3.14
11	Harar	Fike	0.1
12	Harar	Jigjiga	1.2
13	Jigjiga	Degehabor	0.03
14	Hurso	Warsela	0.1
15	Warsela	DD 3	0.01
16	Hurso	Ciro	0.22
17	Awash	Ciro	0.28
18	Awash	DD 3	2.49
19	Adigal	Djibouti	0.5
20	Kaliti	Koka	3.68
Total			33.2

tion is shown in Table 5.5. In this table, F means Feasible and NF means Not Feasible. The DG's can be placed on any number of buses subject to the constraint of maximum generation capacity, which is discussed later. Out of the total sample solutions the feasible solutions are only three out of twelve (i.e., 25 %). An infeasible solution, is a solution in which the minimum system voltage is less than 0.95 pu or maximum system voltage is greater than 1.05 pu.

The optimal DG placement for the system under consideration is shown in Figure 5.4. The Hurso, Adigala, Wersala, Harar, Fike, and Ciro are the proposed DG locations, with DG sizes of 39 MW, 73 MW, 81 MW, 47 MW, 13 MW, and

Table 5.4: Voltage Profile Before DG Integration

Bus No	Bus Name	Voltage (pu)	Ang (deg)
1	Koka	1	-2.14
2	Hurso	0.92	-9.32
3	Adigal	0.9	-11.02
4	Djibouti	0.88	-12.54
5	Wersala	0.92	-9.58
6	DD 3	0.92	-9.63
7	DD 2	0.91	-11.88
8	DD 1	0.92	-9.96
9	Harar	0.88	-18.98
10	Fike	0.87	-20.4
11	Jigjiga	0.86	-25.79
12	Degehabor	0.86	-26.48
13	Ciro	0.96	-7.73
14	Awash	0.96	-5.8
15	M wek	1	2.95
16	Gode	0.99	2
17	Kaliti	1	1

7 MW, respectively. The system's overall power loss is decreased by 73.5% (from 33.2 MW to 8.8 MW) at peak load. The power loss reduction on each branch after DG is introduced into the system is shown in Table 5.6. There is a significant reduction in power loss in branches 1, 3 and 10. The network's performance is also tested using LLRI and presented in Table 5.6. According to the results of LLRI, which is evaluated as 0.27, the system performance is improved. The introduction of DG enhanced the network's minimum voltage from 0.86 pu to 0.96 pu, which is within the specified voltage limits. The voltage magnitude of all buses after DG integration is shown in Table 5.7. The VPII of the system is evaluated using Eq. (5.1.5) and presented in Table 5.7. The VPII is found to be 0.25 which indicates the the voltage profile of the system has improved. The voltage magnitude at each bus before and after DG integration

Table 5.5: Sample Solutions and their Analysis for DG Sizing and Placement

Bus Number								**Objectives & Constraints**			
2	3	5	9	10	11	12	13	**P_L (MW)**	**Volt limit (pu)& Bus location**	**No. DG**	**Feasi-bility**
132	6	148	135	-	-	6	2	16.5	1.156 p.u. @ bus 12	6	NF
115	64	50	115	-	64	-	-	17.5	1.225 p.u. @ bus 12	5	NF
-	-	121	-	95	-	-	-	13.2	0.937 p.u. @ bus 4, 1.058 p.u. @ bus 10	2	NF
70	-	80	69	-	-	-	-	10.1	0.942 p.u. @ bus 4	3	NF
21	-	312	18	-	-	28	-	12.8	1.118 p.u. @ bus 12	4	NF
-	166	-	22	-	-	-	125	16	0.955 p.u. @ bus 4, 1.028 p.u. @ bus 13	3	F
104	-	147	149	-	-	-	-	15.5	1.140 p.u. @ bus 12	3	NF
-	-	-	-	18	58	32	-	18.3	0.922 p.u. @ bus 4, 1.142 p.u. @ bus 12	3	NF
27	50	27	77	50	-	50	-	14.3	1.203 p.u. @ bus 12	6	NF
71	76	-	6	-	78	4	12	10.3	1.151 p.u. @ bus 12	6	NF
175	64	160	-	-	-	-	108	24.4	0.976 p.u. @ bus 4, 1.042 p.u. @ bus 13	4	F
39	73	81	47	13	-	-	7	8.8	0.957 p.u.@ bus 4, 1.046 p.u. @ bus 12	6	F

Table 5.6: Network Power Loss after DG Integration

Branch	**From Bus**	**To bus**	**P_L** (MW)	**Change in P_L** (%)	**LLRI**
1	Koka	Awash	0.22	93.4	0.06
2	Koka	M wek	3.93	0	1
3	Koka	Hurso	0.41	96.1	0.04
4	Hurso	DD 3	0.02	77.8	0.2
5	Hurso	Adigal	0.06	91.7	0.08
6	Hurso	Djibouti	0.53	57.9	0.42
7	M wek	Gode	0.12	0	1
8	DD 3	DD 1	0.13	7.1	0.87
9	DD 3	DD 2	0.25	79.8	0.2
10	DD 2	Harar	0.55	82.5	0.18
11	Harar	Fike	0.01	90	0.1
12	Harar	Jigjiga	0.99	17.5	0.83
13	Jigjiga	Degehabor	0.03	0	0.76
14	Hurso	Warsela	0	100	0.02
15	Warsela	DD 3	0.02	-100	2.43
16	Hurso	Ciro	0.04	81.8	0.16
17	Awash	Ciro	0.03	89.3	0.11
18	Awash	DD 3	0.08	96.8	0.03
19	Adigal	Djibouti	0.78	-56	1.56
20	Kaliti	Koka	0.6	83.7	0.16
Total			8.8	73.4	0.27

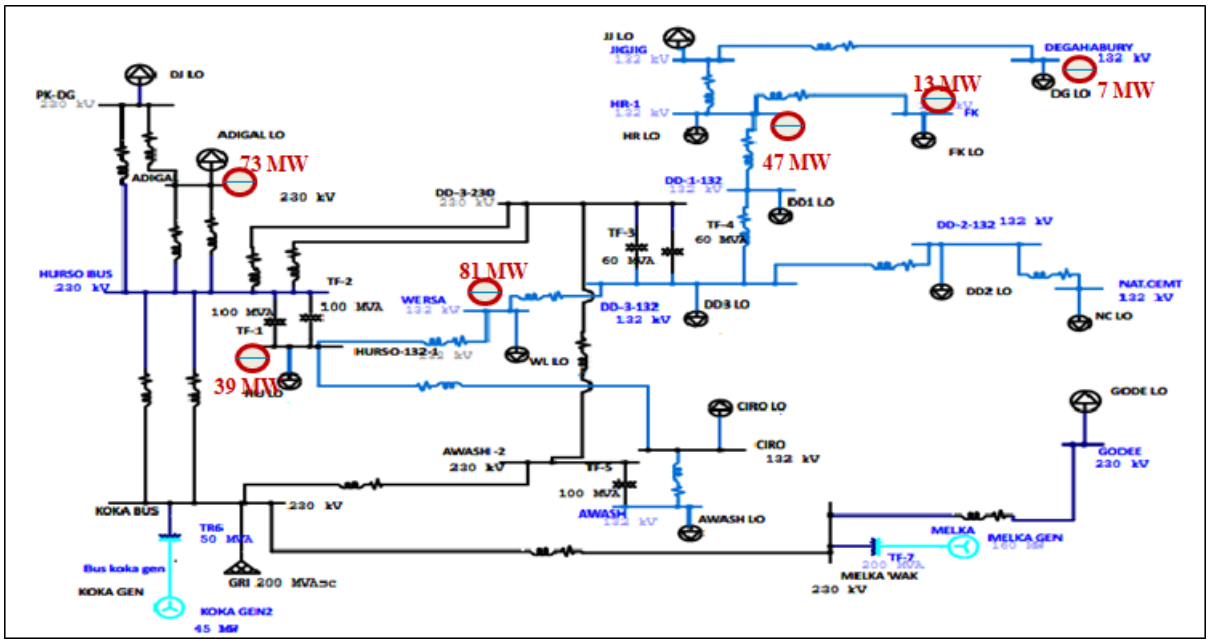

Figure 5.4: Optimal DG Integration in Eastern Region of EEP Network

is shown in Figure 5.5.

5.1.5 Determination of HRES Constituent Ratings

Solar and wind resources are abundant in the EEP's eastern region and are proposed as constituents of DG. The optimal combination of solar PV and WT is analyzed considering the daily load curve. The objective of the study is to obtain the optimal combination of HRES components, used as DG. This objective is represented through the Load Fill Factor (LFF), which is required to be maximized. The LFF is used to calculate the percentage contribution of HRES in supplying the load within the given time frame and is formulated in Eq. (5.1.8). The constraints to be satisfied for this problem are presented through Eqs. (5.1.11) to (5.1.16).

$$F = Maximize \quad LFF = 1 - \frac{\sum_{t=1}^{24}(P_{d(t)} - P_{HRES(t)})}{\sum_{t=1}^{24} P_{d(t)}} \tag{5.1.8}$$

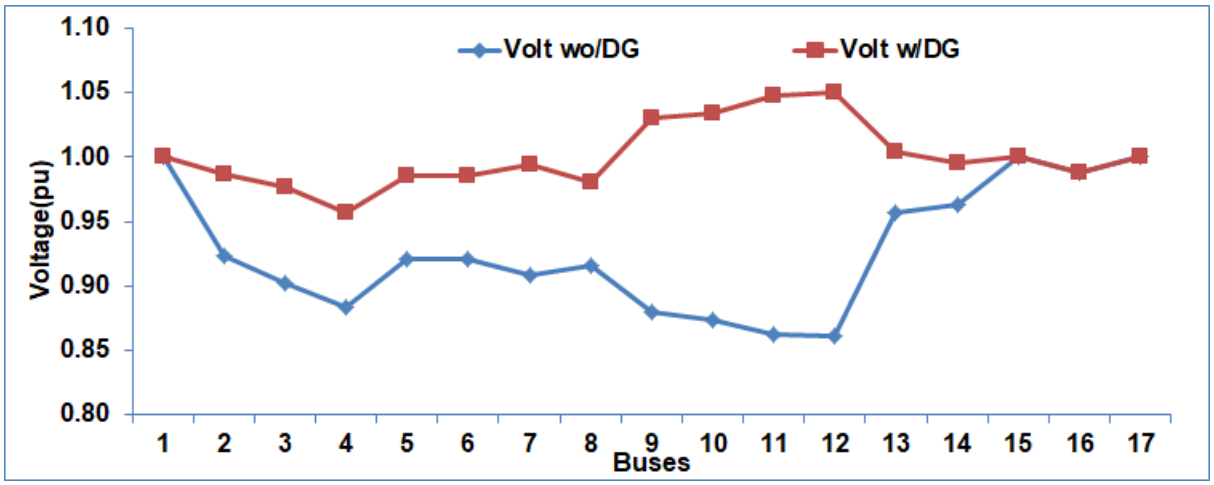

Figure 5.5: Voltage Magnitude Variation due to DG Integration

Where $P_{d(t)}$: demand at time 't'; $P_{HRES(t)}$: RES generation at time 't', which is calculated using Eq. (5.1.9).

$$P_{HRES(t)} = P_{WT(t)'} + P_{PV(t)'} \tag{5.1.9}$$

$$P_{WT(t)'} = N_{WT} P_{WT} \quad and \quad P_{PV(t)'} = N_{PV} P_{PV} \tag{5.1.10}$$

$$P_{HRES(t)} < P_d(t) \tag{5.1.11}$$

$$0 < N_{WT} P_{WT}, N_{PV} P_{PV} \leq DG_{max} \tag{5.1.12}$$

Where DG_{max}: DG size (MW);

The constraints given by Eqs. (5.1.11) and (5.1.12), are used to set the limits for HRES component size.

$$N_{prt} \geq 0 \tag{5.1.13}$$

Where N_{prt}: annual net profit ($/yr). The constraint given by Eq. (5.1.13) signifies that the integration of DG into the power system should result in a profit

Table 5.7: Voltage Profile After DG Integration

Bus No.	**Bus Name**	**Voltage (pu)**	**Ang (deg)**	**Change in V_p (%)**	**VPII**
1	Koka	1	2.27	0	0
2	Hurso	0.99	0.84	7.1	0.17
3	Adigal	0.98	0.98	8.2	0.23
4	Djibouti	0.96	-0.9	8.3	0.37
5	Wersala	0.99	0.8	7.1	0.18
6	DD 3	0.99	0.7	7.1	0.18
7	DD 2	1	-0.15	9	0.05
8	DD 1	0.98	0.41	6.1	0.23
9	Harar	1.03	-1.97	14.6	0.25
10	Fike	1.03	-2.32	15.5	0.27
11	Jigjiga	1.05	-7.15	18.1	0.35
12	Degahabor	1.05	-7.64	18.1	0.36
13	Ciro	1	0.82	4	0.09
14	Awash	1	1.24	4	0.11
15	M wek	1	7.36	0	0
16	Gode	0.99	6.41	0	1
17	Kaliti	1	1.000*	0	0
					0.25

for the utility. The system net profit (N_{prt}) is calculated using Eq. (5.1.14).

$$N_{prt} = Sp - TAC \tag{5.1.14}$$

Where Sp: the annual profit due to power loss reduction ($/yr) that is calculated in Eq. (5.1.15).

$$Sp = (E_{gWO/DG} - E_{gW/DG}) \times C_{tf} \tag{5.1.15}$$

Where $E_{gWO/DG}$ and $E_{gW/DG}$: annual energy supplied from the grid before and after DG installation (MWh/yr), respectively; C_{tf}: grid tariff ($/MWh);

$$COE < C_{tf} \tag{5.1.16}$$

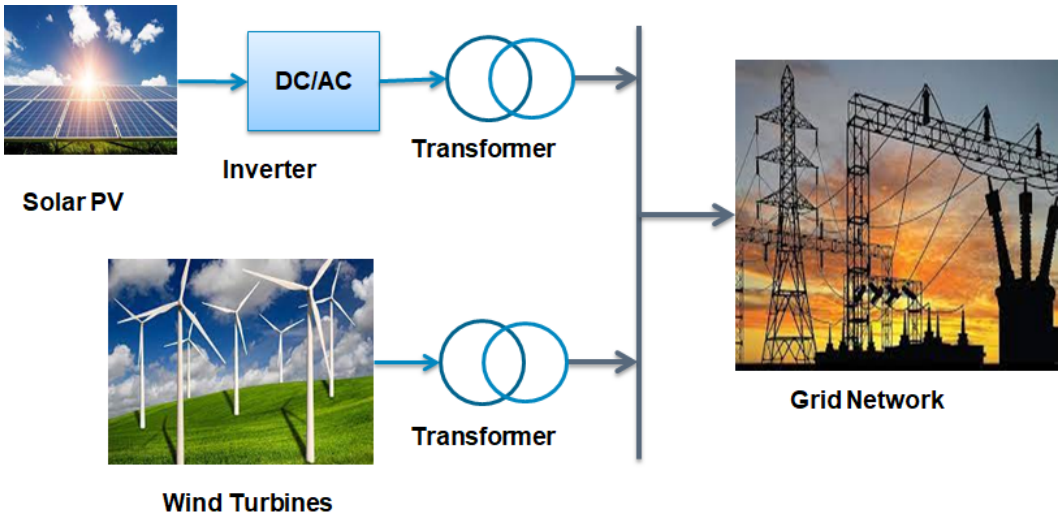

Figure 5.6: Proposed RES Model for Eastern Region of EEP

The above constraint Eq. (5.1.16) is applied to make sure that the Cost of Energy from HRES is less than the grid tariff.

The RES system model proposed as DG is shown in Figure 5.6.

In the eastern part of Ethiopia, a daily average solar radiation of 5.88 kWh/m^2 with a potential power of 489 W/m^2 is available. The daily average wind speed is 6.94 m/s @ 50 m hub height, with a power potential of 342 W/m^2. The daily power that can be generated from a single unit of RES is shown in Figure 5.7. The costs of solar PV and WT per unit with their accessories are summarized in Table 5.8.

The optimization of RES components sizing is determined through MRFO. The optimal solar PV and WT combination is found to be 475 and 288 units, respectively. The efficiency and availability of the resources are considered while optimizing the solar PV and WT combination, which can vary during the day and can be observed through Figure 5.7. The daily energy generation with the optimal component size of RES is sketched in Figure 5.8.

The daily power supply from HRES and grid, along with the load is presented in Figure 5.9. For the eastern region of EEP, the daily energy required from the

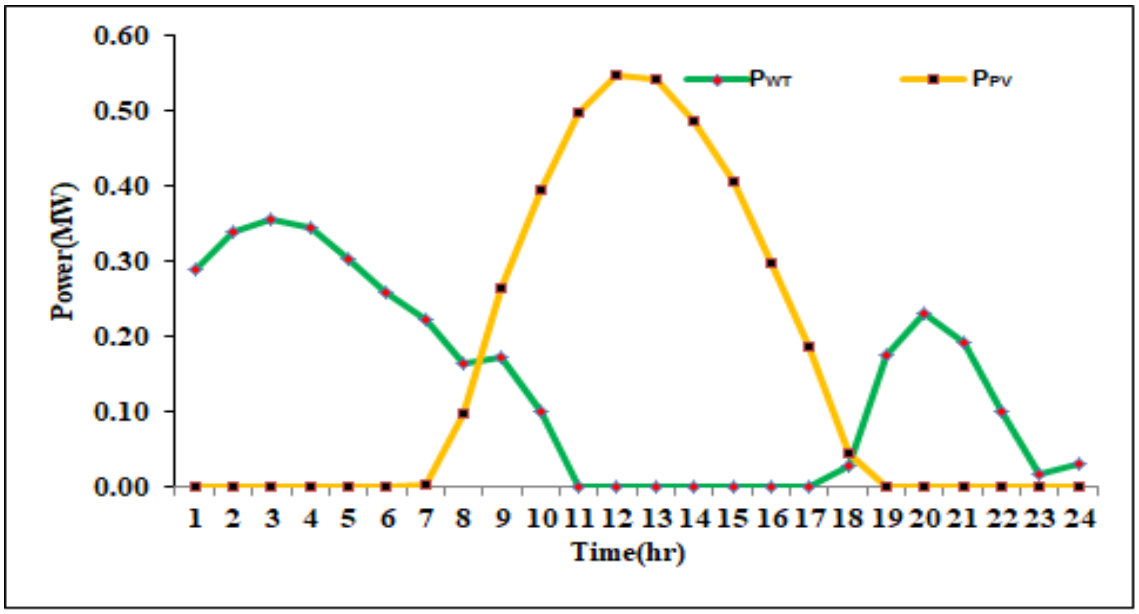

Figure 5.7: Daily Power Generation per unit of Wind and Solar: Eastern Region EEP

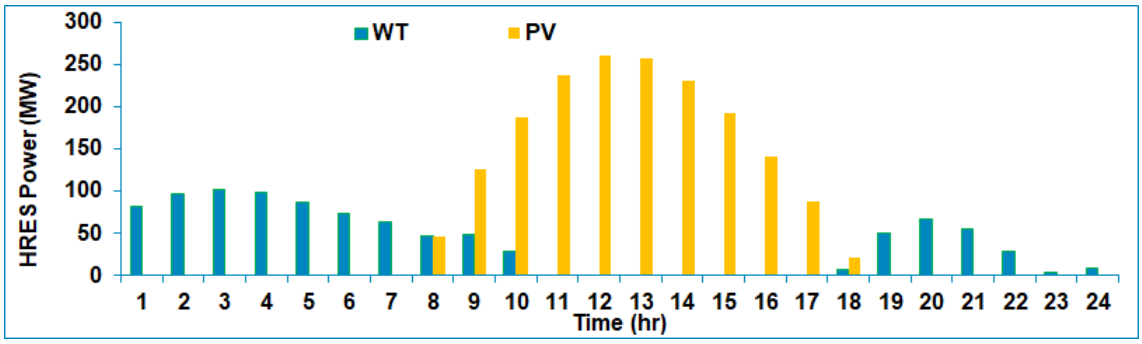

Figure 5.8: Daily Energy Profile for Optimal Combination of RES

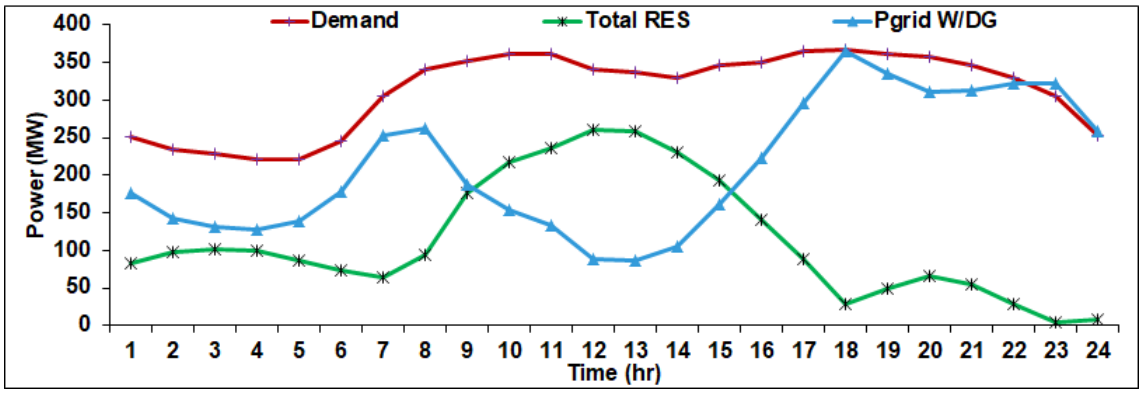

Figure 5.9: Daily Power Supply and Demand for Eastern Region of EEP

grid is 8100 MWh to supply the daily demand of 7517 MWh with a 583 MWh energy loss. The integration of solar PV and WT as DG into the system results in

Table 5.8: Component Costs of Renewable Energy Sources

Components	**C_c ($/MW)**	**C_{OM} ($/MW/yr)**	**Life Span (yr)**
Solar PV with accessory [104]	1000000	10000	25
WT with accessory [105]	1200000	42000	25

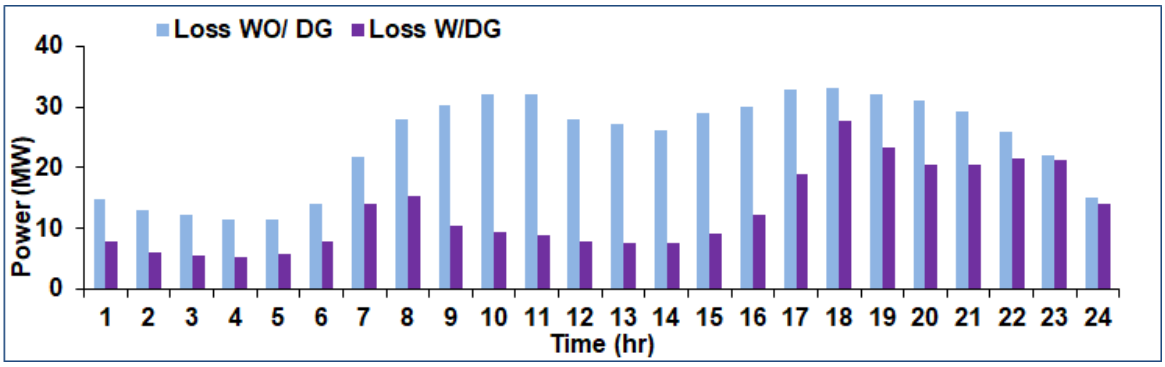

Figure 5.10: Daily Power Losses Before and After HRES Integration

a daily energy harvest of 2747 MWh. The utility will be able to save 3022 MWh after installing HRES DG on the recommended buses. The daily total energy loss is reduced by 275 MWh (i.e., 47.2%) (from 583 MWh to 308 MWh).

The daily power loss pattern before and after HRES DG integration is shown in Figure 5.10. The daily energy flow of the eastern region of EEP is summarized in Table 5.9.

Table 5.9: Summary of Energy Distribution before and after HRES Integration

Status	**Grid (MWh)**	**Load (MWh)**	**E_{Loss} (MWh)**	**DG (MWh)**
WO/DG	8100	7517	583	
W/ DG	5078	7517	308	2747
Difference	3022		275	

5.1.6 Economic Benefit of HRES Integration to Grid

The COE and payback period are used to assess the economic benefits of DG sizing and placement in the network. The COE of HRES DG should be less than the utility tariff to realise profits as mentioned in Eq. (5.1.16). The payback cost (annual profit) is calculated as the product of the grid tariff and change in power losses due to DG integration, as is formulated in Eq. (5.1.15). The payback period (PT) is calculated as the ratio of DG installation cost (DG_{cost}) to payback cost as formulated in Eq. (5.1.17.

$$P_T = \frac{DG_{cost}}{S_P} \tag{5.1.17}$$

Considering the objectives and other constraints, the COE for the optimal combination of HRES is obtained as 89.99 $/MWh. The present average grid tariff of Ethiopia is 90 $/MWh in 2022 [106]. Accordingly, the EEP can save an amount of $99274641.43 /yr as per Eq. (5.1.15), due to power loss reduction. On the other hand, the TAC incurred for DG installation is about $90228190.82 /yr according to Eq. (3.2.3), i.e., EEP can realize a net profit of $9046450.618 /yr as calculated through Eq. (5.1.14). The utility will get payback for DG installation cost within a period of 10 yrs according to Eq. (5.1.15) and (5.1.17). The economic cost parameters results are summarized in Table 5.10.

Thus, the integration of HRES as DG into the system provides economic benefits in addition to lowering power loss and improving voltage profile.

Table 5.10: Results of Economic Cost Analysis for HRES Integration to Grid

Parameters	**Value**
Number of WT	288
Number of PV Modules	475
Total annualized cost of DG	$90,228,190.80 /yr
Total annual saving	$99,274,641.40 /yr
Annual net profit	$9,046,450.62 /yr
Energy loss reduction	47.2%
Payback period	10 yrs
COE	89.99 $/MWh
Grid tariff	90 $/MWh

5.2 Analysis of Subsidy on HRES MG

HRES MG is a small power system used to improve reliability and stability and diversify the existing power supply, lower GHG emissions and reduce operating costs [8]. The analysis of this study is carried out on the clustered villages of Baheya, Ulatu and Karmadhippa, Jharkhand, India. The power supply in these villages is unreliable and supplied from conventional sources. To mitigate these problems, a grid-connected HRES MG is proposed, to have a self-reliant supply, lower economic cost and increase supply from RES. Solar, biomass and hydro resources are abundant in these villages and can be exploited to supply local demand partly or totally. Government subsidies for RES installation are proposed to improve the economic performance of the power system. The economic cost of the grid-connected MG without and with subsidy are compared.

5.2.1 Problem Formulation

The objective function of this study is to minimize COE as formulated in Eq. (5.2.1) considering the constraints listed in Eq. (5.2.2) to (5.2.5).

$$F = Minimize \quad (COE) \tag{5.2.1}$$

$$E_{(gen)}(t) = E_{pv}(t) + E_{bg}(t) + E_h(t) \pm E_{grid}(t) \tag{5.2.2}$$

$$0 \leq P_{PV} \leq P_{PV}max \tag{5.2.3}$$

$$0 \leq P_h \leq P_h max \tag{5.2.4}$$

$$0 \leq P_{bg} \leq P_{bg}max \tag{5.2.5}$$

Where $E_{(gen)}(t)$: total energy generated at time 't'; E_{pv}(t), $E_{bg}(t)$, $E_h(t)$ and E_{grid}(t): energy contributed from PV, WT, biogas and grid at time 't', respectively; P_{PV}max, $P_h$max and P_{bg}max: maximum generation limit for solar PV, hydro and biogas, respectively.

5.2.2 Load Profile and Resource Potential for Clustered Indian Villages

The proposed MG system for analysis is shown in Figure 5.11. It consists of loads and power supply from HRES and grid system.

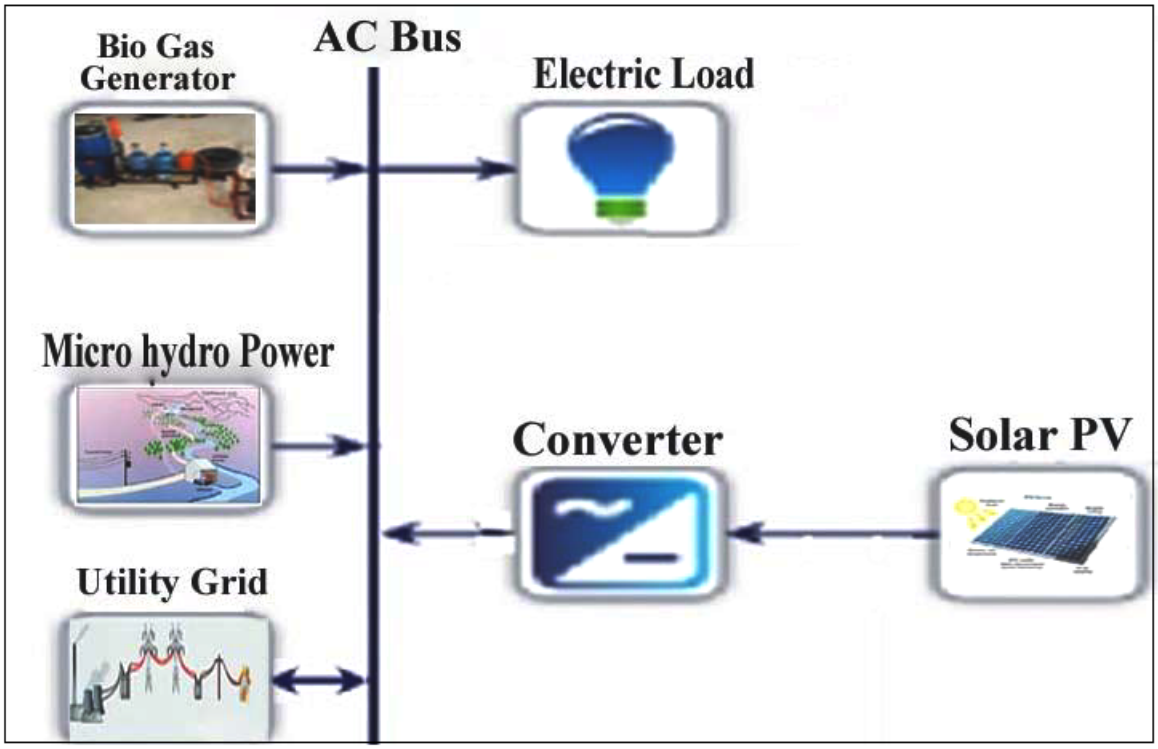

Figure 5.11: HRES MG Model for Grid Connected System

Load Profile

For analysis, three villages, Baheya (23.36^0N, 85.48^0E), Ulatu (23.38^0N, 85.46^0E) and Karmadhippa (23.37^0N, 85.47^0E), Jharkhand, India, were selected. The detailed location of villages is presented in Figure 5.12. The clustered villages have about 335 households. The load types for the villages are bulbs, fans, TVs, refrigerators, flour mills and street lights. The site load varies seasonally due to temperature fluctuations, consuming more power in summer. The total load curves for summer and winter are presented in Figure 5.13. Summer and winter daily average loads are 66.35 kW and 55.09 kW, respectively. The daily energy consumption is estimated to be 1598 kWh/day for summer and 1395 kWh/day for winter seasons.

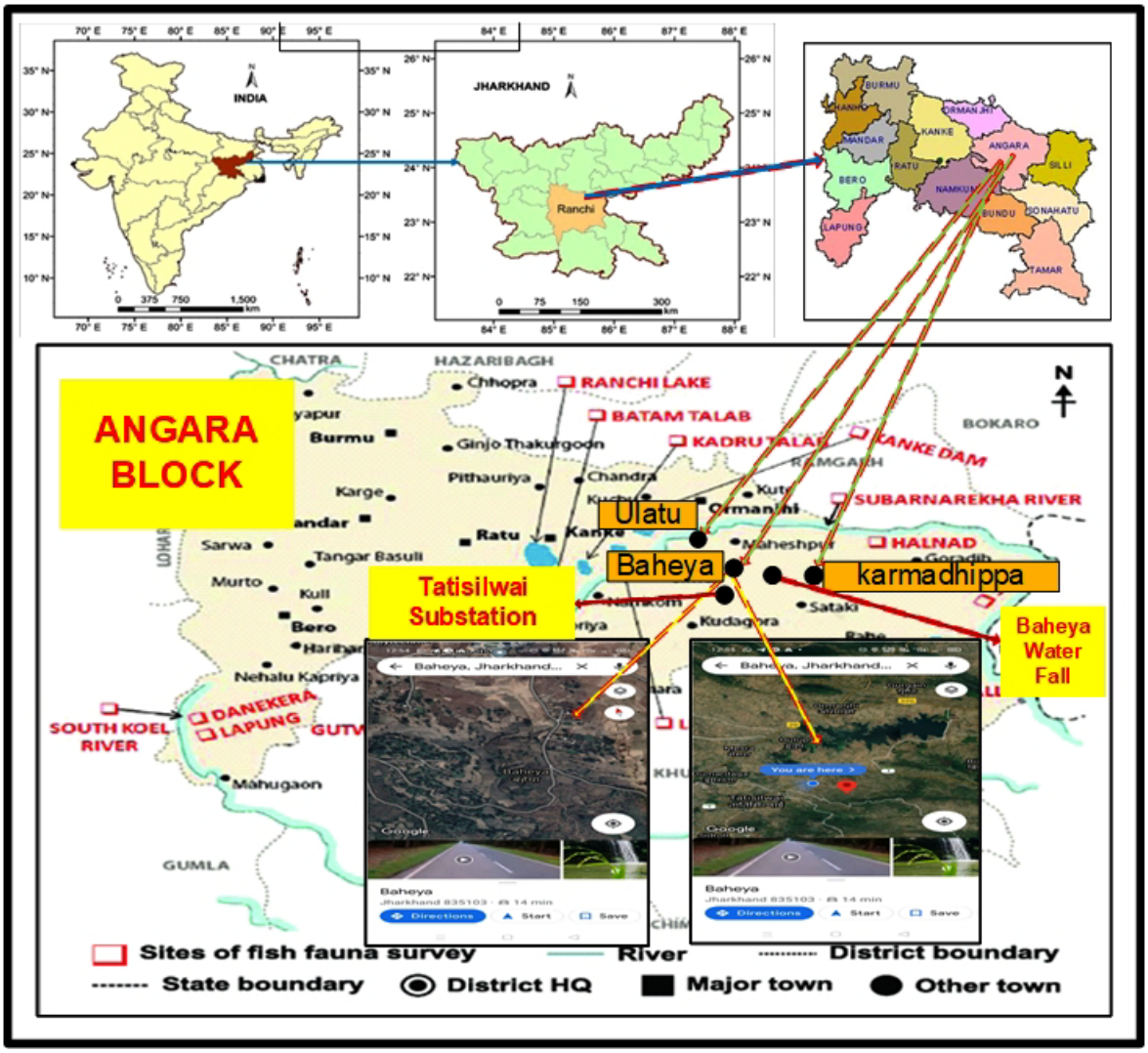

Figure 5.12: Geographical Location of Clustered Indian Villages

RES Potential at Clustered Villages

The RES at the clustered villages consists of solar, biomass and small hydropower. The cluster of three villages is in the vicinity of one another. Hence, the annual solar irradiation is considered similar for all villages. The daily average solar irradiation for each month is plotted in Figure 5.14. The solar PV panel and converter specification used for modelling grid-connected MG is summarized in Tables 5.11 and 5.12, respectively. The water stream near Baheya village is considered for power generation by establishing a Micro Hydro Power (MHP) plant, that has an average water discharge rate (Q) of 0.045 m^3/s and a

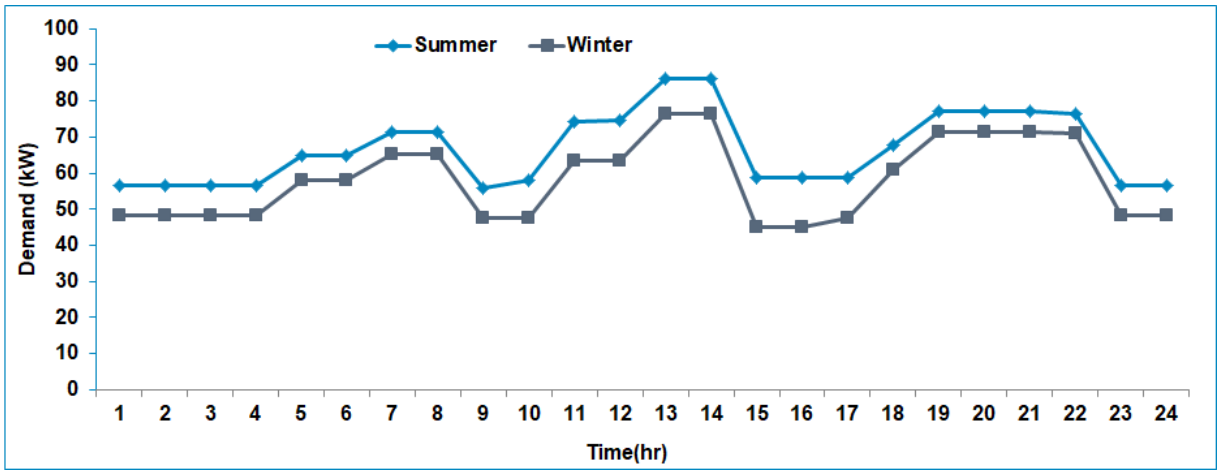

Figure 5.13: Seasonal Load Variation of Clustered Indian Villages

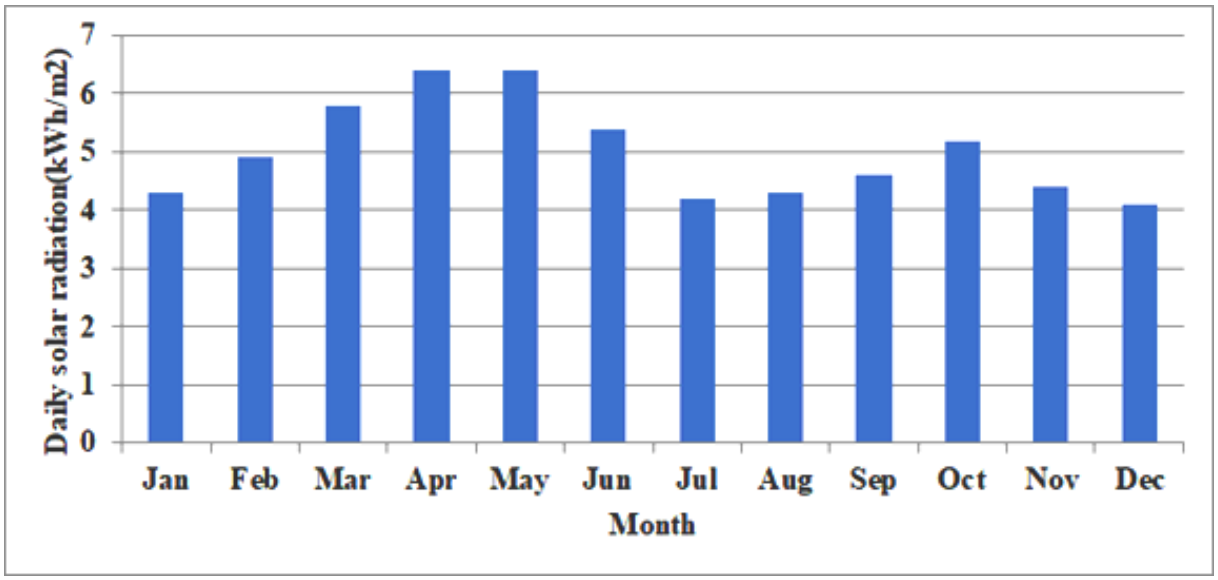

Figure 5.14: Monthly Average Solar Energy of Clustered Indian Villages [93]

net head of 20 m. Table 5.13 summarizes the MHP Specification.

Biogas resource material is collected in the form of cattle dung. The cattle present in these villages are cows, buffaloes and goats. The availability of cattle dung resources in these villages is summarized in Table 5.14. The biogas plant specifications are shown in Table 5.15.

Table 5.11: Specifications of Solar PV Panels

Parameters	Unit	Value
Rated capacity of Solar PV	W	220
Short circuit current, I_{sc}	A	7.24
Open circuit voltage, V_{oc}	V	39.4
Current at maximum power, I_{max}	A	6.71
Voltage at maximum power, V_{max}	V	32.2
Lifetime	yr	25
Initial cost of solar PV	$/kW	400
O & M cost	$/kW/yr	53

Table 5.12: Specifications of Converter

Parameters	Unit	Value
Converter rating	kW	65
Converter efficiency	%	95
Lifetime	yr	15
Capital cost	$/kW	70

5.2.3 Result and Discussion

The proposed study investigates the economic viability of installing an optimal combination of RES and the effect of subsidy. The economic cost is investigated in two scenarios: without and with subsidy. Ministry of New and Renewable Energy (MNRE), India, offers subsidies for RES as: 30% for solar PV, 10% for biogas plants and 17% for hydropower [108, 109]. This policy helps to encourage RES installation in the power system.

HOMER software is applied to determine the cost-effective combination of HRES. The optimal results found from the assessment are : 60 kW of solar PV, 7.5 kW of hydro and 3 kW of biogas plants should be installed. The annual energy generated from RES is approximated to 152955 kWh as summarized in Table 5.16. If this energy is procured from the grid at a rate of 0.0833 $/kWh i.e., grid tariff ([110] @ 2020), a cost of $12746.3 will be required. Considering the

Table 5.13: Specifications of Micro Hydro Power Plant

Parameters	**Unit**	**Value**
Rated capacity	kW	7.5
Rated discharge	m^3/s	0.045
Net head	m	20
Efficiency of the MHP	%	80
Capital Cost	$/kW	10000
O & M Cost	$/kW/yr	330
Lifetime of component	yr	25

Table 5.14: Biogas Potential of Clustered Indian Villages [107]

Animals	**Cattle Count**	**Cattle Dung (kg/cattle/day)**	**Total Dung (kg/day)**	**Biogas Yield (m^3/kg)**	**Total (m^3/day)**
Goat	230	2	460	0.0185	8.5
Buffalo	420	14	5880	0.04	235.0
Cow	465	10	4650	0.038	176.5
Total	1115	—	10645	—	420

optimal combination of the MG components, the total capital cost is $129128.12, without subsidy. The COE of MG is 0.0709 $/kWh after RES integration. The HRES MG tariff is lesser than the grid tariff by 14.88%, without subsidy.

After subsidies are introduced to the HRES components, the capital cost is reduced to $103510.28. The COE of HRES MG declines from 0.0709 $/kWh to 0.0656 $/kWh, i.e., a reduction of 21.24 % from the grid tariff and 7.47 % from RES MG without subsidy.

The payback period is also considered as an economic index in this study. The payback period for HRES MG is found to be 9.4 yrs without subsidy whereas it is 7.2 yrs with subsidy. The economic performance comparison of grid-connected MG with and without subsidy is summarized in Table 5.17.

Table 5.15: Specifications of Biogas Plant

Parameters	**Unit**	**Value**
Rated capacity of the Biogas system	kW	3
Conversion efficiency	%	50
Lifetime of civil work	Year	25
Lifetime of engine generator	h	20,000
Capital Cost of engine	$/kW	200
O & M Cost	$/kW/yr	195

Table 5.16: Total Energy Generation per unit of RES.

Renewable Energy Source	**Operation per day**	**Generation (kWh/day)**	**Generation (kWh/yr)**
60kW PV	5 hrs	300	99000
7.5kW Hydro	24 hrs	180	44100
3kW Biogas	8 to 10/day	27	9855
Annual Generation		507	152955

Table 5.17: Economic Analysis Without and With Subsidy

Status	**PV (kW)**	**Bio (kW)**	**Hydro (kW)**	**Conv (kW)**	**COE ($/kWh)**	**Total Capital cost ($)**	**Payback period (yrs)**
Without Subsidy	60.0	3.0	7.5	65	0.0709	129,128.12	9.4
With subsidy	60.0	3.0	7.5	65	0.0656	103,510.28	7.2

5.3 Summary

The integration of HRES into the grid system reduces power loss and improves the voltage profile. The HRES DG improves system reliability by providing alternative renewable energy sources. It promotes the use of RE technologies that has lower GHG emissions. The HRES has the economic advantage that they are operated at a low cost. To improve economic performance, the subsidy is proposed as another method.

Chapter 6

Conclusions and Future Scopes

6.1 Conclusions

This research work focuses on the application of HRES to electrify remote areas or improve the existing power system performance. Economic cost, reliability, GHG emissions and power quality such as power loss and voltage profile are considered as power system performance parameters and discussed in different scenarios.

The economic feasibility of grid extension or deploying standalone HRES for Jarre village, Ethiopia, has been evaluated. Due to its distance from the grid and lower load level, the standalone MG is found to be more economical. To supply power to the village, RES like solar PV and WT, which are available in abundance is proposed. To improve the reliability further, BS is included in HRES MG. Performance evaluation parameters such as reliability, economic cost and GHG emission (CO_2) are considered as the objective functions to determine the HRES components' optimal combination. The economic cost (TAC and COE) is considered as the objective of the case study while the reliability index, LPSP is considered as a constraint. PSO is used to evaluate the optimal solution in the this case study. The optimal number of units of PV, WT and BS are 247, 46 and 250, respectively, for the optimized output. The economic cost analysis gives a

TAC of $119992.2 /yr and COE of 0.104 $/kWh. In the second scenario for Jarre Village, GHG emission (CO_2) is included in the objective problem in terms of costs. The meta-heuristic optimization techniques of PSO, DE, MRFO, SFLA, RSA and RUN are compared to obtain optimal HRES components. The investigation has shown that the solution provided by MRFO is the best among the optimization methods considered. The optimal component units obtained from the analysis are 247 PV panels, 46 WT and 249 of BS packs. The economic cost parameters are TAC of $134275.85 /yr and COE of 0.116 $/kWh. TAC and COE of the second scenario are increased due to GHG emission consideration in the analysis.

The integration of HRES as DG to improve power system performance is the other objective of the study. The analysis is performed on the eastern region of Ethiopia's Electric Power network. The objective of this case study is to minimize the power loss and improve the voltage profile of the network. The optimal size and location of DG are obtained using MRFO with MATPOWER in MATLAB. The optimal solution has a total DG size of 260 MW. DG is located at six different buses in the eastern region of EEP. Due to DG introduction to the network, total power loss is reduced from 33.2 MW to 8.8 MW and the minimum voltage limit is improved from 0.86 pu to 0.96 pu at the peak load. The optimal size of HRES components are determined using MRFO. With the optimal combination of solar PV panels and WT, the daily energy loss was reduced by 275 MWh from 583 MWh to 308 MWh. The utility will save up to $9,046,450.6 /yr at the selected site.

The effect of the subsidy on MG's economic performance is analyzed at grid-connected clustered villages (Baheya, Ulatu and Karmadhippa), in India. The economic cost is evaluated with and without subsidy for the optimal combina-

tion of MG components (solar PV, WT, biogas and hydro). The introduction of subsidies improves the COE of the MG by 21% compared to the grid tariff and the payback period is also shortened from 9.4 yrs to 7.2 yrs. The analysis of case studies used in various aspects revealed that incorporating HRES into the power system improved reliability, reduced costs, reduced GHG emissions and improved power quality.

6.2 Future Scope

The issues that were not considered during this research work but need attention in future works are:

- The present research work can be extended to different RES and storage systems for optimal combinations of the components.
- The load and energy resources are considered for a day (24 hours). Using long-term load and energy resource data may lead to better solutions for the objectives.
- Effect of Energy Management System (EMS) on analysis of HRES components optimization is not considered in this research work.
- The introduction of HRES MG into the grid, to improve power loss and voltage profile is investigated. More research is needed to examine the effects of RES integration into the grid network.
- To get the optimal solution of the HRES MG combination, meta-heuristic algorithms are applied. Comparing the performance of those techniques with other methods is recommended for future work.

Appendix

Appendix I: Bus Parameters for Eastern Region EEP

Bus	**Bus Type**	**P**$_d$	**Q**$_d$	**V**$_m$	**V**$_a$	**Base kV**	**V**$_{max}$	**V**$_{min}$
Koka	2	10	6	1	0	230	1.1	0.9
Hurso	1	12.56	7.53	1	0	132	1.1	0.9
Adigala	1	12.65	7.59	1	0	230	1.1	0.9
Djibuti	1	95	61.34	1	0	230	1.1	0.9
Wersala	1	30	11.62	1	0	132	1.1	0.9
DD 3	1	20	9.91	1	0	230	1.1	0.9
DD 2	1	15	7.58	1	0	132	1.1	0.9
DD 1	1	50	25.06	1	0	132	1.1	0.9
Harar	1	31.95	19.17	1	0	132	1.1	0.9
Fike	1	12.08	6.71	1	0	132	1.1	0.9
Jigjiga	1	24.1	13.14	1	0	132	1.1	0.9
Degehabor	1	6.254	3.75	1	0	132	1.1	0.9
Ciro	1	12.62	7.57	1	0	132	1.1	0.9
Awash	1	16.76	10.39	1	0	230	1.1	0.9
M wek	2	0	0	1	0	230	1.1	0.9
Gode	1	18.47	11.08	1	0	230	1.1	0.9
Kaliti	3	0	0	1	0	230	1.1	0.9

Bus type: 1 - load bus, 2 - generator bus and 3 - slack bus

Appendix II: Generation Plants Data for Eastern Region EEP

Bus	**P**$_g$ **(MW)**	**Q**$_g$ **(MVAr)**	**Q**$_{max}$ **(MVAr)**	**Q**$_{min}$ **(MVAr)**	**S**$_{Base}$ **(MVA)**	**P**$_{max}$ **(MW)**	**P**$_{min}$ **(MW)**
Kaliti	0	0	200	-200	100	400	0
Koka	43.5	0	36	-36	100	43.5	0
M wek	153	0	130	-130	100	180	0

Appendix III: Branch Parameters for Eastern Region EEP

From Bus	To Bus	R (pu)	X (pu)	B (pu)
Koka	Awash	0.0158	0.0474	0.0569
Koka	M wek	0.0201	0.0603	0.0724
Koka	Hurso	0.0193	0.0578	0.0693
Hurso	DD 3	0.0035	0.0105	0.0126
Hurso	Adigal	0.0164	0.0493	0.0592
Hurso	Djibuti	0.0333	0.1000	0.1201
M wek	Gode	0.0327	0.0980	0.1176
DD 3	DD 1	0.0039	0.0116	0.0140
DD 3	DD 2	0.0116	0.0349	0.0419
DD 2	Harar	0.0417	0.1250	0.1500
Harar	Fike	0.0520	0.1561	0.1873
Harar	Jigjiga	0.0920	0.2761	0.3313
Jigjiga	Degehabor	0.0589	0.1266	0.1520
Hurso	Warsela	0.0025	0.0074	0.0088
Warsela	DD 3	0.0009	0.0026	0.0031
Hurso	Ciro	0.0829	0.2488	0.2985
Awash	Ciro	0.0388	0.1163	0.1395
Awash	DD 3	0.0231	0.0693	0.0831
Adigal	Djibuti	0.0183	0.0548	0.0657
Kaliti	Koka	0.0081	0.0244	0.0293

Bibliography

[1] IRENA. (2018) Global energy transformation. [Online]. Available: https://www.irena.org/-/media/Files/IRENA/Agency/Publication/2018/Apr/IRENA_Report_GET_2018.pdf

[2] P. IEA. (2021,) Global energy review 2020. [Online]. Available: https://www.iea.org/reports/global-energy-review-2020

[3] S. T. Series. (2020,) overview on latest global trends in renewable energy costs. [Online]. Available: https://www.irena.org/Statistics/View-Data-by-Topic/Costs/Global-Trends

[4] L. N. Thomas B Johansson, Kes McCormick and W. Turkenburg. The potentials of renewable energy. [Online]. Available: https://ren21.net/Portals/0/documents/irecs/renew2004/

[5] IRENA. (11 April 2022,) Renewable capacity highlights. [Online]. Available: https://irena.org/publications/2022/Apr/Renewable-Capacity-Statistics-2022

[6] M. S. Javed, T. Ma, J. Jurasz, S. Ahmed, and J. Mikulik, "Performance comparison of heuristic algorithms for optimization of hybrid off-grid renewable energy systems," *Energy*, vol. 210, p. 118599, 2020.

[7] B. B. Adetokun, C. M. Muriithi, and J. O. Ojo, "Voltage stability assessment and enhancement of power grid with increasing wind energy penetration," *International Journal of Electrical Power & Energy Systems*, vol. 120, p. 105988, 2020.

[8] C. Ghenai, T. Salameh, and A. Merabet, "Technico-economic analysis of off grid solar pv/fuel cell energy system for residential community in desert region," *International Journal of Hydrogen Energy*, vol. 45, no. 20, pp. 11 460–11 470, 2020.

[9] H. Husin, M. Zaki *et al.*, "A critical review of the integration of renewable energy sources with various technologies," *Protection and Control of Modern Power Systems*, vol. 6, no. 1, pp. 1–18, 2021.

[10] A. Desta, "Energy supply and demand side management in industrial microgrid context," Ph.D. dissertation, Université Paris-Est, 2017.

[11] P. Li, J. Ji, H. Ji, J. Jian, F. Ding, J. Wu, and C. Wang, "Mpc-based local voltage control strategy of dgs in active distribution networks," *IEEE Transactions on Sustainable Energy*, vol. 11, no. 4, pp. 2911–2921, 2020.

[12] S. Sultana and P. K. Roy, "Krill herd algorithm for optimal location of distributed generator in radial distribution system," *Applied Soft Computing*, vol. 40, pp. 391–404, 2016.

[13] R. Aljendy, R. R. Nasyrov, A. Y. Abdelaziz, and A. A. Z. Diab, "Enhancement of power quality with hybrid distributed generation and facts device," *IETE Journal of Research*, pp. 1–12, 2019.

[14] G. Wang, Q. Wang, Z. Qiao, J. Wang, and S. Anderson, "Optimal planning of multi-micro grids based-on networks reliability," *Energy Reports*, vol. 6, pp. 1233–1249, 2020.

[15] S. Raza, T. ur Rahman, M. Saeed, and S. Jameel, "Performance analysis of power system parameters for islanding detection using mathematical

morphology," *Ain Shams Engineering Journal*, vol. 12, no. 1, pp. 517–527, 2021.

[16] D. Emad, M. El-Hameed, M. Yousef, and A. El-Fergany, "Computational methods for optimal planning of hybrid renewable microgrids: a comprehensive review and challenges," *Archives of Computational Methods in Engineering*, vol. 27, no. 4, pp. 1297–1319, 2020.

[17] B. K. Das, R. Hassan, M. S. H. Tushar, F. Zaman, M. Hasan, and P. Das, "Techno-economic and environmental assessment of a hybrid renewable energy system using multi-objective genetic algorithm: A case study for remote island in bangladesh," *Energy Conversion and Management*, vol. 230, p. 113823, 2021.

[18] J. Li, P. Liu, and Z. Li, "Optimal design of a hybrid renewable energy system with grid connection and comparison of techno-economic performances with an off-grid system: A case study of west china," *Computers & Chemical Engineering*, vol. 159, p. 107657, 2022.

[19] J. M. Aberilla, A. Gallego-Schmid, L. Stamford, and A. Azapagic, "Design and environmental sustainability assessment of small-scale off-grid energy systems for remote rural communities," *Applied Energy*, vol. 258, p. 114004, 2020.

[20] H. M. Farh, A. A. Al-Shamma'a, A. M. Al-Shaalan, A. Alkuhayli, A. M. Noman, and T. Kandil, "Technical and economic evaluation for off-grid hybrid renewable energy system using novel bonobo optimizer," *Sustainability*, vol. 14, no. 3, p. 1533, 2022.

[21] H. Andrei, C. A. Badea, P. Andrei, and F. Spertino, "Energetic-environmental-economic feasibility and impact assessment of grid-connected photovoltaic system in wastewater treatment plant: Case study," *Energies*, vol. 14, no. 1, p. 100, 2021.

[22] A. Ghaffari and A. Askarzadeh, "Design optimization of a hybrid system subject to reliability level and renewable energy penetration," *Energy*, vol. 193, p. 116754, 2020.

[23] M. R. Naseh and E. Behdani, "Feasibility study for size optimisation of a geothermal/pv/wind/diesel hybrid power plant using the harmony search algorithm," *International Journal of Sustainable Energy*, pp. 1–18, 2020.

[24] M. Samy, M. I. Mosaad, and S. Barakat, "Optimal economic study of hybrid pv-wind-fuel cell system integrated to unreliable electric utility using hybrid search optimization technique," *International Journal of Hydrogen Energy*, vol. 46, no. 20, pp. 11 217–11 231, 2021.

[25] T. Ma and M. S. Javed, "Integrated sizing of hybrid pv-wind-battery system for remote island considering the saturation of each renewable energy resource," *Energy conversion and management*, vol. 182, pp. 178–190, 2019.

[26] B. Lu, A. Blakers, M. Stocks, C. Cheng, and A. Nadolny, "A zero-carbon, reliable and affordable energy future in australia," *Energy*, vol. 220, p. 119678, 2021.

[27] A. Abazari, M. M. Soleymani, I. Kamwa, M. Babaei, M. Ghafouri, S. Muyeen, and A. M. Foley, "A reliable and cost-effective planning

framework of rural area hybrid system considering intelligent weather forecasting," *Energy Reports*, vol. 7, pp. 5647–5666, 2021.

[28] T. Adefarati and R. Bansal, "Reliability, economic and environmental analysis of a microgrid system in the presence of renewable energy resources," *Applied Energy*, vol. 236, pp. 1089–1114, 2019.

[29] M. T. Castro, J. D. A. Pascasio, L. L. Delina, P. H. M. Balite, and J. D. Ocon, "Techno-economic and financial analyses of hybrid renewable energy system microgrids in 634 philippine off-grid islands: policy implications on public subsidies and private investments," *Energy*, vol. 257, p. 124599, 2022.

[30] N. M. Kumar, S. S. Chopra, A. A. Chand, R. M. Elavarasan, and G. Shafiullah, "Hybrid renewable energy microgrid for a residential community: A techno-economic and environmental perspective in the context of the sdg7," *Sustainability*, vol. 12, no. 10, p. 3944, 2020.

[31] M. Ravanbakhshian and A. Amindoust, "Developing a mathematical model of location decision optimization for solar cells using genetic algorithm," *Energy Sources, Part A: Recovery, Utilization, and Environmental Effects*, pp. 1–15, 2019.

[32] N. D. Nordin and H. A. Rahman, "Comparison of optimum design, sizing, and economic analysis of standalone photovoltaic/battery without and with hydrogen production systems," *Renewable Energy*, vol. 141, pp. 107–123, 2019.

[33] S. Kumar, K. K. Mandal, and N. Chakraborty, "A novel opposition-based tuned-chaotic differential evolution technique for techno-economic anal-

ysis by optimal placement of distributed generation," *Engineering Optimization*, pp. 1–22, 2019.

[34] L. A. Wong, V. K. Ramachandaramurthy, S. L. Walker, P. Taylor, and M. J. Sanjari, "Optimal placement and sizing of battery energy storage system for losses reduction using whale optimization algorithm," *Journal of Energy Storage*, vol. 26, p. 100892, 2019.

[35] S. S. Tanwar and D. Khatod, "Techno-economic and environmental approach for optimal placement and sizing of renewable dgs in distribution system," *Energy*, vol. 127, pp. 52–67, 2017.

[36] H. HassanzadehFard and A. Jalilian, "Optimal sizing and location of renewable energy based dg units in distribution systems considering load growth," *International Journal of Electrical Power & Energy Systems*, vol. 101, pp. 356–370, 2018.

[37] M. Jamil and A. S. Anees, "Optimal sizing and location of spv (solar photovoltaic) based mldg (multiple location distributed generator) in distribution system for loss reduction, voltage profile improvement with economical benefits," *Energy*, vol. 103, pp. 231–239, 2016.

[38] A. Arasteh, P. Alemi, and M. Beiraghi, "Optimal allocation of photovoltaic/wind energy system in distribution network using meta-heuristic algorithm," *Applied Soft Computing*, vol. 109, p. 107594, 2021.

[39] B. Khaki and P. Das, "Sizing and placement of battery energy storage systems and wind turbines by minimizing costs and system losses," *arXiv preprint arXiv:1903.12029*, 2019.

[40] W. Haider, S. Hassan, A. Mehdi, A. Hussain, G. O. M. Adjayeng, and C.-H. Kim, "Voltage profile enhancement and loss minimization using optimal placement and sizing of distributed generation in reconfigured network," *Machines*, vol. 9, no. 1, p. 20, 2021.

[41] K. Cherukupalli and V. Anand N, "Optimal sizing and location of distributed generators for power flow analysis in smart grid using ias-mvpa strategy," *International Journal of Computational Intelligence and Applications*, vol. 20, no. 04, p. 2150027, 2021.

[42] Z. Ding, H. Hou, G. Yu, E. Hu, L. Duan, and J. Zhao, "Performance analysis of a wind-solar hybrid power generation system," *Energy conversion and management*, vol. 181, pp. 223–234, 2019.

[43] A. Nekkache, B. Bouzidi, A. Kaabeche, and Y. Bakelli, "Hybrid pv-wind based water pumping system optimum sizing: a pso-llp-lpsp optimization and cost analysis," in *2018 International Conference on Electrical Sciences and Technologies in Maghreb (CISTEM)*. IEEE, 2018, pp. 1–6.

[44] P. Nagapurkar and J. D. Smith, "Techno-economic optimization and environmental life cycle assessment (lca) of microgrids located in the us using genetic algorithm," *Energy conversion and management*, vol. 181, pp. 272–291, 2019.

[45] N. Ghorbani, A. Kasaeian, A. Toopshekan, L. Bahrami, and A. Maghami, "Optimizing a hybrid wind-pv-battery system using ga-pso and mopso for reducing cost and increasing reliability," *Energy*, vol. 154, pp. 581–591, 2018.

[46] Y. Yang, S. Guo, D. Liu, R. Li, and Y. Chu, "Operation optimization strategy for wind-concentrated solar power hybrid power generation system," *Energy conversion and management*, vol. 160, pp. 243–250, 2018.

[47] M. H. Moghaddam, A. Kalam, J. Shi, M. Miveh, and P. Peidaee, "Supplying the load by the optimization of a stand-alone hybrid power system using firefly algorithm considering reliability indices," in *2017 Australasian Universities Power Engineering Conference (AUPEC)*. IEEE, 2017, pp. 1–5.

[48] A. A. Bashir, M. Pourakbari-Kasmaei, J. Contreras, and M. Lehtonen, "A novel energy scheduling framework for reliable and economic operation of islanded and grid-connected microgrids," *Electric Power Systems Research*, vol. 171, pp. 85–96, 2019.

[49] D. Yu, H. Zhu, W. Han, and D. Holburn, "Dynamic multi agent-based management and load frequency control of pv/fuel cell/wind turbine/chp in autonomous microgrid system," *Energy*, vol. 173, pp. 554–568, 2019.

[50] M. Subramaniyan, S. Subramaniyan, M. Veeraswamy, and V. R. Jawalkar, "Optimal reconfiguration/distributed generation integration in distribution system using adaptive weighted improved discrete particle swarm optimization," *COMPEL-The international journal for computation and mathematics in electrical and electronic engineering*, vol. 38, no. 1, pp. 247–262, 2019.

[51] W. M. Amutha and V. Rajini, "Cost benefit and technical analysis of rural electrification alternatives in southern india using homer," *Renewable and Sustainable Energy Reviews*, vol. 62, pp. 236–246, 2016.

[52] A. Maleki, M. Ameri, and F. Keynia, "Scrutiny of multifarious particle swarm optimization for finding the optimal size of a pv/wind/battery hybrid system," *Renewable Energy*, vol. 80, pp. 552–563, 2015.

[53] E. F. Camacho, T. Samad, M. Garcia-Sanz, and I. Hiskens, "Control for renewable energy and smart grids," *The Impact of Control Technology, Control Systems Society*, vol. 4, no. 8, pp. 69–88, 2011.

[54] N. Alamir, S. Kamel, T. F. Megahed, M. Hori, and S. M. Abdelkader, "Developing hybrid demand response technique for energy management in microgrid based on pelican optimization algorithm," *Electric Power Systems Research*, vol. 214, p. 108905, 2023.

[55] P. Breeze, *Power generation technologies*. Newnes, 2019.

[56] C. S. Kaunda, C. Z. Kimambo, and T. K. Nielsen, "Hydropower in the context of sustainable energy supply: a review of technologies and challenges," *International Scholarly Research Notices*, vol. 2012, 2012.

[57] S. Sansaniwal, M. Rosen, and S. Tyagi, "Global challenges in the sustainable development of biomass gasification: An overview," *Renewable and Sustainable Energy Reviews*, vol. 80, pp. 23–43, 2017.

[58] C. A. Murphy, A. Schleifer, and K. Eurek, "A taxonomy of systems that combine utility-scale renewable energy and energy storage technologies," *Renewable and Sustainable Energy Reviews*, vol. 139, p. 110711, 2021.

[59] F. A. Alturki and E. M. Awwad, "Sizing and cost minimization of standalone hybrid wt/pv/biomass/pump-hydro storage-based energy systems," *Energies*, vol. 14, no. 2, p. 489, 2021.

[60] T. M. Gür, "Review of electrical energy storage technologies, materials and systems: challenges and prospects for large-scale grid storage," *Energy & Environmental Science*, vol. 11, no. 10, pp. 2696–2767, 2018.

[61] A. Lorestani and M. Ardehali, "Optimization of autonomous combined heat and power system including pvt, wt, storages, and electric heat utilizing novel evolutionary particle swarm optimization algorithm," *Renewable Energy*, vol. 119, pp. 490–503, 2018.

[62] I. Qamber, "Novel modeling of forced outage rate effect on the lolp and lole," *International Journal of Computing and Digital Systems*, vol. 9, no. 2, pp. 229–237, 2020.

[63] F. A. Khan, N. Pal, and S. H. Saeed, "Review of solar photovoltaic and wind hybrid energy systems for sizing strategies optimization techniques and cost analysis methodologies," *Renewable and Sustainable Energy Reviews*, vol. 92, pp. 937–947, 2018.

[64] R. M. Moharil and P. S. Kulkarni, "Evaluation of generation system reliability indices using rbfnn method," *Journal of Research in Engineering and Applied Sciences*, 2021.

[65] M. Esen, G. Bayrak, O. Çakmak, S. Çelikdemir, and M. Özdemir, "A consistent power management system design for solar and wind energy-based residential applications," in *2019 1st Global Power, Energy and Communication Conference (GPECOM)*. IEEE, 2019, pp. 358–363.

[66] S. Raja, B. Arguello, and B. J. Pierre, "Dynamic programming method to optimally select power distribution system reliability upgrades," *IEEE Open Access Journal of Power and Energy*, vol. 8, pp. 118–127, 2021.

[67] Y. Moumouni and M. Pouye, "Analysis of power distribution system reliability indices, niamey, niger," in *2020 3rd International Conference on Power and Energy Applications (ICPEA)*. IEEE, 2020, pp. 131–135.

[68] A. Ezeala, D. Idoniboyeobu, and S. Braide, "Analysis of 11kv, obi-wali, rumuigbo distribution network for improved performance using predictive reliability assessment method," *American Journal of Engineering Research*, vol. 9, pp. 132–145, 2020.

[69] L. Ali, S. Muyeen, H. Bizhani, and A. Ghosh, "A peer-to-peer energy trading for a clustered microgrid–game theoretical approach," *International Journal of Electrical Power & Energy Systems*, vol. 133, p. 107307, 2021.

[70] F. A. Khan, N. Pal, and S. H. Saeed, "Review of solar photovoltaic and wind hybrid energy systems for sizing strategies optimization techniques and cost analysis methodologies," *Renewable and Sustainable Energy Reviews*, vol. 92, pp. 937–947, 2018.

[71] L.-N. Xing, H.-L. Xu, A. K. Sani, M. A. Hossain, and S. Muyeen, "Techno-economic and environmental assessment of the hybrid energy system considering electric and thermal loads," *Electronics*, vol. 10, no. 24, p. 3136, 2021.

[72] W. Kessler, "Comparing energy payback and simple payback period for solar photovoltaic systems," in *E3S Web of Conferences*, vol. 22. EDP Sciences, 2017, p. 00080.

[73] A. Abazari, M. M. Soleymani, I. Kamwa, M. Babaei, M. Ghafouri, S. Muyeen, and A. M. Foley, "A reliable and cost-effective planning

framework of rural area hybrid system considering intelligent weather forecasting," *Energy Reports*, vol. 7, pp. 5647–5666, 2021.

[74] C. Trust, "Guide to pas 2050: how to assess the carbon footprint of goods and services," 2008.

[75] A. Dhar, M. A. Naeth, P. D. Jennings, and M. G. El-Din, "Perspectives on environmental impacts and a land reclamation strategy for solar and wind energy systems," *Science of The Total Environment*, vol. 718, p. 134602, 2020.

[76] A. Akella, R. Saini, and M. P. Sharma, "Social, economical and environmental impacts of renewable energy systems," *Renewable Energy*, vol. 34, no. 2, pp. 390–396, 2009.

[77] M. D. Al-Falahi, S. Jayasinghe, and H. Enshaei, "A review on recent size optimization methodologies for standalone solar and wind hybrid renewable energy system," *Energy Conversion and Management*, vol. 143, pp. 252–274, 2017.

[78] S. Kumar, T. Kaur, S. Upadhyay, V. Sharma, and D. Vatsal, "Optimal sizing of stand alone hybrid renewable energy system with load shifting," *Energy Sources, Part A: Recovery, Utilization, and Environmental Effects*, pp. 1–20, 2020.

[79] I. F. Monitor, "How to mitigate climate change," *International Monetary Fund (IMF): Washington, DC, USA*, 2019.

[80] M. J. Hadidian-Moghaddam, S. Arabi-Nowdeh, M. Bigdeli, and D. Azizian, "A multi-objective optimal sizing and siting of distributed genera-

tion using ant lion optimization technique," *Ain shams engineering journal*, vol. 9, no. 4, pp. 2101–2109, 2018.

[81] N. Gunantara, "A review of multi-objective optimization: Methods and its applications," *Cogent Engineering*, vol. 5, no. 1, p. 1502242, 2018.

[82] A. Kumar, A. R. Singh, Y. Deng, X. He, P. Kumar, and R. C. Bansal, "Integrated assessment of a sustainable microgrid for a remote village in hilly region," *Energy conversion and management*, vol. 180, pp. 442–472, 2019.

[83] J. Kennedy and R. Eberhart, "Particle swarm optimization," in *Proceedings of ICNN'95-International Conference on Neural Networks*, vol. 4. IEEE, 1995, pp. 1942–1948.

[84] R. Storn and K. Price, "Differential evolution–a simple and efficient heuristic for global optimization over continuous spaces," *Journal of global optimization*, vol. 11, no. 4, pp. 341–359, 1997.

[85] E. H. Houssein, I. E. Ibrahim, N. Neggaz, M. Hassaballah, and Y. M. Wazery, "An efficient ecg arrhythmia classification method based on manta ray foraging optimization," *Expert Systems with Applications*, vol. 181, p. 115131, 2021.

[86] M. M. Eusuff and K. E. Lansey, "Optimization of water distribution network design using the shuffled frog leaping algorithm," *Journal of Water Resources planning and management*, vol. 129, no. 3, pp. 210–225, 2003.

[87] L. Abualigah, M. Abd Elaziz, P. Sumari, Z. W. Geem, and A. H. Gandomi, "Reptile search algorithm (rsa): A nature-inspired meta-heuristic optimizer," *Expert Systems with Applications*, p. 116158, 2021.

[88] I. Ahmadianfar, A. A. Heidari, A. H. Gandomi, X. Chu, and H. Chen, "Run beyond the metaphor: An efficient optimization algorithm based on runge kutta method," *Expert Systems with Applications*, vol. 181, p. 115079, 2021.

[89] C. L. Azimoh, P. Klintenberg, F. Wallin, B. Karlsson, and C. Mbohwa, "Electricity for development: Mini-grid solution for rural electrification in south africa," *Energy Conversion and Management*, vol. 110, pp. 268–277, 2016.

[90] O. Longe, N. Rao, F. Omowole, A. Oluwalami, and O. Oni, "A case study on off-grid microgrid for universal electricity access in the eastern cape of south africa," *International Journal of Energy Engineering*, vol. 7, no. 2, pp. 55–63, 2017.

[91] *Medium Voltage line construction cost break down*, Ethiopia Electric utility, Eastern region, 2021, manual Data sheet.

[92] M. Walker. Why we created homer grid: Understanding the differences between homer grid and homer pro. [Online]. Available: https://microgridnews.com/homer-grid-vs-homer-pro

[93] . Power data access viewer. [Online]. Available: https://power.larc.nasa.gov/data-access-viewer/

[94] A. Kadiyala, R. Kommalapati, and Z. Huque, "Evaluation of the life cycle greenhouse gas emissions from hydroelectricity generation systems," *Sustainability*, vol. 8, no. 6, p. 539, 2016.

[95] HUAWEI, "Zertifikat-product-carbon-footprint-report-für-huawei-sun2000-6ktl-l," 2020.

[96] M. W. Khan, J. Wang, M. Ma, L. Xiong, P. Li, and F. Wu, "Optimal energy management and control aspects of distributed microgrid using multi-agent systems," *Sustainable Cities and Society*, vol. 44, pp. 855–870, 2019.

[97] F. Bandeiras, M. Gomes, P. Coelho, and J. Fernandes, "Towards net zero energy in industrial and commercial buildings in portugal," *Renewable and Sustainable Energy Reviews*, vol. 119, p. 109580, 2020.

[98] *Power Outage within different Region and System Layout*, Ethiopia Electric Power, 2021, manual Data Sheet.

[99] *Maximum and Minimum Voltages on Dire Dawa substation 3 for six month*, Ethiopia Electric Power, Eastern region, 2020, manual Data sheet.

[100] H. V. Padullaparti, P. Chirapongsananurak, and S. Santoso, "Grid-edge voltage control in utility distribution circuits," *Power Engineering: Advances and Challenges Part B: Electrical Power*, p. 251, 2018.

[101] R. D. Zimmerman, C. E. Murillo-Sanchez, and D. Gan, "Matpower," *PSERC.[Online]. Software Available at: http://www. pserc. cornell. edu/matpower*, 1997.

[102] S. Kamel, A. Selim, F. Jurado, J. Yu, K. Xie, and C. Yu, "Multi-objective whale optimization algorithm for optimal integration of multiple dgs into distribution systems," in *2019 IEEE Innovative Smart Grid Technologies-Asia (ISGT Asia)*. IEEE, 2019, pp. 1312–1317.

[103] S. Kumar and N. Kumar, "A novel approach to identify optimal access point and capacity of multiple dgs in a small, medium and large scale

radial distribution systems," *Int. J. Electr. Power Energy Syst*, vol. 45, pp. 142–151, 2013.

[104] K. Solar Pvt. Ltd. 1 mw solar power plant: Types, models, price and complete details in india 2022. [Online]. Available: https://kenbrooksolar.com/solar-power-plants/mw-solar-power-grid#:~:text=The%20estimated%20cost%20of%201,4%20crore.

[105] D. Blewett. Wind turbine cost: How much? are they worth it in 2022? [Online]. Available: https://weatherguardwind.com/how-much-does-wind-turbine-cost-worth-it/

[106] A. D. Beyene. (2022,) Impacts and drivers of policies for electricity access, micro- and macro-economic analysis of ethiopia's tariff reform. [Online]. Available: https://www.energyeconomicgrowth.org/node/236

[107] M. U. Khan, M. Ahmad, M. Sultan, I. Sohoo, P. C. Ghimire, A. Zahid, A. Sarwar, M. Farooq, U. Sajjad, P. Abdeshahian *et al.*, "Biogas production potential from livestock manure in pakistan," *Sustainability*, vol. 13, no. 12, p. 6751, 2021.

[108] "Final report, evaluation of small hydro power (shp) programme of ministry of new and renewable energy, india (mnre)." [Online]. Available: https://mnre.gov.in/img/documents/uploads/7b691718d9194ab68b7d9638bb901a74.pdf

[109] Jharkhand renewable energy development agency, state govt. agency under department of energy. [Online]. Available: https://www.jreda.com/

[110] “Jharkhand state electricity regulatory commission, true-up for fy 2016-17 & fy 2017-18, apr for fy 2018-19 and arr & tariff for fy 2019-20,” 2020.

Publications

International Journals (Published / Accepted)

[1] **Negasa Muleta and Altaf Q H Badar**, ”Techno-economic Analysis and Design of Hybrid Renewable Energy Micro-grid for Rural Electrification ,” ***Energy Harvesting and Systems*** , vol. 9, no. 1, 2022, pp. 39-51. DOI:10.1515/ehs-2021-0013 **(Scopus)**

[2] **Negasa Muleta and Altaf Q. H. Badar, ”A comprehensive review on different optimisation components for hybrid renewable energy sources,”*Int. J. of Engineering Systems Modeling and Simulation***, 2022, DOI:10.1504/IJESMS.2022.10048772 **(Scopus / ESCI)**

[3] **Negasa Muleta, Altaf Q. H. Badar and Naiyer Mumtaz**, ”Moving Towards Self Reliant Micro-grids in Indian Scenario ,” ***Distributed Generation & Alternative Energy Journal***, Vol 37 Iss 4, 2022, 1191-1214. DOI:10.13052/dg 3306.37412 **(Scopus)**

International conferences (Published / Accepted)

[1] **Negasa Muleta and Altaf Q. H. Badar**, ”Study of Energy Management System and IOT Integration in Smart Grid ,” ***1st International Conference on Power Electronics and Energy (ICPEE-2021)*** , KIIT, Bhubaneswar, India , 2-3 Jan. 2021 , pp. 1-5. DOI: 10.1109/ ICPEE 50452.2021.9358769

[2] **Negasa Muleta and Altaf Q. H. Badar**, ”Study of Renewable Energy

Resources Distribution and Its Challenges in the case of Ethiopia," ***1st International Conference on Smart Technologies for Power and Green Energy (STPGE-2022)***, KIIT, Bhubaneswar, India, 12–13 Feb. 2022, https://doi.org/10.1007/978-981-19-2764-5_9.

International Journals (Under Review)

[1] **Negasa Muleta and Altaf Q. H. Badar**, "Designing of an Optimal Standalone Hybrid Renewable Energy Micro-grid Model through Different Algorithms," ***Journal of Engineering Research***, 2022. **(Scopus / SCIE)**

[2] **Negasa Muleta and Altaf Q. H. Badar**, "Economic Analysis of HRES based Distributed Generation for Mitigation of Power Loss and Voltage Profile Problem ," ***International Journal of Electrical Power & Energy Systems, 2022. (Scopus).***